

Master's thesis

2021

Master's thesis

YUN LIU

NTNU
Norwegian University of
Science and Technology
Faculty of Natural Sciences
Department of Chemical Engineering

YUN LIU

Low temperature carbon dioxide capture by PEI-modified mesoporous silica: synthesis and adsorption performance analysis

June 2021



Norwegian University of
Science and Technology

Low temperature carbon dioxide capture by PEI-modified mesoporous silica: synthesis and adsorption performance analysis

YUN LIU

Chemical Engineering

Submission date: June 2021

Supervisor: Professor De Chen, IKP

Co-supervisor: Dr. Kumar Ranjan Rout, IKP

Norwegian University of Science and Technology
Department of Chemical Engineering

PREFACE

This master thesis has been conducted during the spring semester in 2021 at the Norwegian University of Science and Technology. This project is supported by SINTEF - the largest research organization in Europe

Due to personal health reasons and the effects due to COVID-19 pandemic, the research of this thesis is faced with huge difficulties and challenges. Therefore, I do feel grateful on receiving plentiful help from my supervisor professor De Chen. Without his encouragement and support, it would not be possible to achieve such good results of this thesis research.

In addition, I would like to thank my supervisor professor De Chen, co-supervisor Dr. Kumar Ranjan Rout, for their academical guidance during this thesis research. Also, I would like to sincerely thank Dumitrita Spinu (PhD candidate) and Jørgen Lausund Grinna (M.Sc in Chemical engineering) for valuable guidance and experimental supports.

Moreover, I would like to thank Estelle Marie Vanhaecke, Anne Hoff, Karin Wiggen Dragsten, Christopher Sørmoand and Amin Hossein Zavieh (nano lab) for the technical support on my laboratory work.

Hereby, I declare that this is an independent work according to the exam regulations of the Norwegian university of science and technology (NTNU)

Trondheim, 04 June 2021

Yun Liu

ABSTRACT

Mesoporous silica sorbents were prepared at different synthesis conditions by conventional sol-gel methods. The rigid spherical silica sorbents of high surface area and high porosity in narrow distribution were tuned by varying initial gel composition and operation condition and studied. Physical properties and morphology studies were carried out by nitrogen adsorption / desorption and SEM techniques. The surface area, pore volume and pore size of synthesis silica sorbents in this study were up to $700 \text{ m}^2/\text{g}$, $1.5 \text{ cm}^3/\text{g}$ and 7 nm , respectively. These mesoporous silica particles had a size in range of 4 to $10 \text{ }\mu\text{m}$.

CO_2 adsorption and desorption performance of synthesized sorbents were studied via TGA after amine modification at different loading concentrations. Both equilibrium and working CO_2 capacity of PEI-modified mesoporous silica were discussed in this work. As per unit amine mass, the optimum and practical CO_2 of solid sorbents were up to 6.02 and 5 mmol/g , respectively within a $5 \text{ vol.}\%$ of CO_2 inlet gas condition at $75 \text{ }^\circ\text{C}$ adsorption temperature. The cycle stability of solid sorbent in a pure N_2 regeneration environment obtained an outstanding result as 99.1% and 95.4% under mild and harsh condition, respectively.

In addition, studies of amine loading check and comparison with previous master student's work were also discussed in this thesis research.

Contents

PREFACE	iii
ABSTRACT	v
LIST OF FIGURES	vii
LIST OF TABLES	ix
LIST OF ABBREVIATIONS	xi
1. INTRODUCTION	1
2. LITERATURE REVIEW	3
2.1. Outlines of carbon capture processes	3
2.1.1. Post-combustion CO ₂ capture (CO ₂ /N ₂ at low pressure)	3
2.1.2. Pre-combustion CO ₂ capture (CO ₂ /H ₂ at high pressure)	4
2.1.3. Oxy-fuel combustion (O ₂ /N ₂ at low pressure)	4
2.1.4. Post-combustion CO ₂ capture technology chosen for this thesis research	5
2.2. Promising adsorbents for post-combustion CO ₂ capture.....	5
2.3. Solid adsorbents selection for physical adsorption CO ₂ capture.....	8
2.4. Different types of solid adsorbents	10
2.4.1. Carbonaceous adsorbents.....	10
2.4.2. Non-Carbonaceous adsorbents.....	13
2.4.3. Comparison of various physical solid adsorbents for carbon dioxide adsorption .	15
2.5. Amine functionalization on mesoporous solid adsorbent for CO ₂ capture	16
2.6. PEI-modified mesoporous silica materials chosen for post-combustion CO ₂ capture studied further in this thesis research.....	20
3. THEORY	21
3.1. Synthesis mechanism for mesoporous silica materials.....	21
3.2. Polyethylenimine (PEI) impregnation to Mesoporous silica materials	22
3.3. CO ₂ capture by PEI-modified Mesoporous silica materials	23
3.4. Characterization.....	24
3.4.1. Nitrogen adsorption and desorption.....	24
3.4.2. Scanning Electron Microscope	25

CONTENTS

3.4.3. Thermal Gravimetric Analysis.....	25
4. EXPERIMENTS	27
4.1. Synthesis of mesoporous silica nanoparticles	27
4.2. Amine-impregnation of synthesized mesoporous silica samples	27
4.3. Characterization.....	28
4.3.1. Nitrogen adsorption and desorption.....	28
4.3.2. Scanning electron microscope	28
4.3.3. Thermo gravimetric analysis.....	28
5. RESULT AND DISCUSSION	31
5.1. Synthesis of mesoporous silica supports	31
5.1.1. Tuning procedure for targeted adsorbent synthesis	32
5.1.2. Morphology studies	36
5.1.3. Targeted samples chosen for CO ₂ adsorption performance tests.....	37
5.2. CO ₂ adsorption performance of PEI-modified mesoporous silica samples	38
5.2.1. CO ₂ uptake and stability of PEI_Vp1.2 silica samples.....	38
5.2.2. CO ₂ uptake and stability of PEI_Vp1.5 silica samples.....	50
5.2.3. CO ₂ uptake and stability of PEI_Vp1.5 silica samples in harsh condition	59
5.3. CO ₂ uptake correction as per actual PEI loading	63
5.3.1. Physical properties and Morphology of PEI-modified mesoporous silica	63
5.3.2. Amine decomposition and remove at high temperature	65
5.4. CO ₂ capture performances comparison between different samples	67
5.4.1. CO ₂ adsorption performance of PEI_SiO ₂ samples with different mesoporous structure.....	67
5.4.2. CO ₂ adsorption performance of 40PEI_SiO ₂ samples compared with previous master study work	69
6. CONCLUSION.....	73
7. FUTURE WORK.....	75
BIBLIOGRAPHY	77
APPENDIX	A1

LIST OF FIGURES

FIGURE 1: SCHEMATIC REPRESENTATION OF THREE DIFFERENT CO ₂ CAPTURE TECHNOLOGIES ...	3
FIGURE 2: PERCENTAGE OF TOTAL AMOUNT OF ANNUAL CO ₂ EMISSIONS FROM DIFFERENT INDUSTRIES (DE CONINCK ET AL., 2009)	5
FIGURE 3: SCHEMATIC REPRESENTATION FOR FLUE GAS CO ₂ CAPTURE FROM COAL-FIRED POWER PLANT (WALTERS ET AL., 2016)	6
FIGURE 4: GRAPHICAL DIAGRAM OF AQUEOUS AMINE SCRUBBING TECHNOLOGY (BEN-MANSOUR ET AL., 2016)	6
FIGURE 5: GRAPHICAL DIAGRAM OF CARBON DIOXIDE CAPTURE BY SOLID ADSORBENTS (BEN-MANSOUR ET AL., 2016)	7
FIGURE 6: SCHEMATIC DIFFERENCES BETWEEN CONVENTIONAL ADSORBENT AND POROUS ADSORBENT DURING THE ADSORPTION PROCESS	8
FIGURE 7: PHYSICAL SOLID ADSORBENTS FOR CARBON DIOXIDE ADSORPTION	10
FIGURE 8: COMPARISON OF CARBON DIOXIDE UPTAKES OF ARRIVED CARBON AND CARBON NANOTUBES ADSORBENT (CINKE ET AL., 2003)	12
FIGURE 9: GRAPHICAL DIAGRAM OF PRODUCING MOFs MATERIALS (ABD ET AL., 2020)	14
FIGURE 10: SCHEMATIC REPRESENTATION OF THE FORMATION OF SEVERAL AMINE-FUNCTIONALIZED MESOPOROUS SILICA	17
FIGURE 11: ILLUSTRATION OF WATER IMPACTS ON CO ₂ ADSORPTION CAPACITY	19
FIGURE 12: SCHEME OF THE FORMATION OF MESOPOROUS SILICA MATERIALS WITH AND WITHOUT CTAB WITH TEOS AS SILICON PRECURSOR	22
FIGURE 13: PHYSICAL IMPREGNATION ILLUSTRATION	23
FIGURE 14: SCHEMATIC OF FUNCTIONALIZATION OF POROUS MATERIALS WITH POLYMERIC AMINES AND THEIR CO ₂ CAPTURE ACTION (VARGHESE AND KARANIKOLOS, 2020)	24
FIGURE 15: SCHEMATIC OF AN SEM	25
FIGURE 16: SCHEMATIC DIAGRAM OF THE TGA SET-UP	26
FIGURE 17: SAMPLE NAMING RULE	32
FIGURE 18: MECHANISM FOR THE SYNTHESIS OF MESOPOROUS SILICA USING P123 AND CTAB AS TEMPLATE AND CO-TEMPLATE, RESPECTIVELY	32
FIGURE 19: ISOTHERM LINEAR PLOT AND BJH DESORPTION dV/dLOG(w) PORE VOLUME OF SILICA SAMPLES SYNTHESIZED WITH DIFFERENT SOLUTIONS AND TEMPERATURE	36
FIGURE 20: SEM IMAGES OF SILICA SAMPLES SYNTHESIZED WITH DIFFERENT SOLUTIONS AND TEMPERATURE	37

LIST OF FIGURES

FIGURE 21: CO ₂ CAPTURE PERFORMANCE ANALYSIS OF PEI_SiO ₂ _Vp1.2 UNDER MILD CONDITIONS.....	39
FIGURE 22: CO ₂ UPTAKE OF THE FIRST (LEFT) AND SECOND (RIGHT) CYCLE DURING 100 MIN CONTACT TIME OF PEI_SiO ₂ _Vp1.2.....	44
FIGURE 23: CO ₂ UPTAKE OF THE FIRST (TOP) AND SECOND (BOTTOM) CYCLE DURING 10 MIN CONTACT TIME OF PEI_SiO ₂ _Vp1.2.....	45
FIGURE 24: CO ₂ UPTAKE PER GRAM SORBENTS (TOP) AND PER GRAM PEI (BOTTOM) FROM FIRST TWO CYCLES IN DIFFERENT CONTACT TIME OF PEI_SiO ₂ _Vp1.2.....	47
FIGURE 25: ADSORPTION PERFORMANCE OF PEI_SiO ₂ _Vp1.2 WITH OPTIMUM AND PRACTICAL CO ₂ CAPACITIES PER GRAM SORBENTS (TOP) AND PER GRAM PEI (BOTTOM)	48
FIGURE 26: COMPARISON OF THE CO ₂ ADSORPTION CAPACITY OF DIFFERENT PEI_SiO ₂ _Vp1.2 SAMPLES UNDER MILD OPERATION CONDITIONS	49
FIGURE 27: COMPARISON OF THE STABILITY OF DIFFERENT PEI_SiO ₂ _Vp1.2 SAMPLES UNDER MILD OPERATION CONDITIONS	49
FIGURE 28: CO ₂ CAPTURE PERFORMANCE ANALYSIS OF PEI_SiO ₂ _Vp1.5 UNDER MILD CONDITIONS.....	50
FIGURE 29: CO ₂ UPTAKE OF THE FIRST (LEFT) AND SECOND (RIGHT) CYCLE DURING 100 MIN CONTACT TIME OF PEI_SiO ₂ _Vp1.5.....	54
FIGURE 30: CO ₂ UPTAKE OF THE FIRST (TOP) AND SECOND (BOTTOM) CYCLE DURING 10 MIN CONTACT TIME OF PEI_SiO ₂ _Vp1.5.....	55
FIGURE 31: CO ₂ UPTAKE PER GRAM SORBENTS (TOP) AND PER GRAM PEI (BOTTOM) FROM FIRST TWO CYCLES IN DIFFERENT CONTACT TIME OF PEI_SiO ₂ _Vp1.2.....	56
FIGURE 32: ADSORPTION PERFORMANCE OF PEI_SiO ₂ _Vp1.5 WITH OPTIMUM AND PRACTICAL CO ₂ CAPACITIES PER GRAM SORBENTS (TOP) AND PER GRAM PEI (BOTTOM)	57
FIGURE 33: COMPARISON OF THE CO ₂ ADSORPTION CAPACITY OF DIFFERENT PEI_SiO ₂ _Vp1.5 SAMPLES UNDER MILD OPERATION CONDITIONS	58
FIGURE 34: COMPARISON OF THE STABILITY OF DIFFERENT PEI_SiO ₂ _Vp1.5 SAMPLES UNDER MILD OPERATION CONDITIONS	58
FIGURE 35: CO ₂ CAPTURE PERFORMANCE ANALYSIS OF PEI_SiO ₂ _Vp1.5 UNDER HARSH CONDITIONS.....	60
FIGURE 36: COMPARISON OF THE STABILITY OF DIFFERENT PEI_SiO ₂ _Vp1.5 SAMPLES UNDER HARSH OPERATION CONDITIONS	63
FIGURE 37: AN EXAMPLE OF SEM IMAGES OF SILICA SORBENTS IN DIFFERENT STAGE.....	65
FIGURE 38: PEI DECOMPOSITION EXPERIMENTS CARRIED ON DIFFERENT PEI-MODIFIED SiO ₂ SAMPLES.....	66
FIGURE 39: CO ₂ OPTIMUM ADSORPTION CAPACITY OF PEI_SiO ₂ SAMPLES UNDER DIFFERENT OPERATING CONDITIONS.....	68
FIGURE 40: CO ₂ PRACTICAL ADSORPTION CAPACITY AND CYCLE STABILITY OF PEI_SiO ₂ SAMPLES WITH DIFFERENT POROSITY UNDER MILD CONDITIONS.....	69
FIGURE 41: COMPARISON OF THE STABILITY OF 40PEI_SiO ₂ SAMPLES WITH PREVIOUS THESIS STUDY	71

LIST OF TABLES

TABLE 1: COMPARISON OF PRO AND CONS AMONG CARBON-BASED ADSORBENT, ZEOLITES, AND MOFs FOR CARBON DIOXIDE ADSORPTION.....	16
TABLE 2: SUMMARY OF N-LOADING METHODS ONTO ADSORBENTS AND THEIR CHARACTERISTICS (HU ET AL., 2020).....	17
TABLE 3 - DETAILS OF POLYMERIC AMINES REPORTED FOR CO ₂ CAPTURE APPLICATIONS (VARGHESE AND KARANIKOLOS, 2020)	18
TABLE 4: EXPERIMENTAL PARAMETERS OF MESOPOROUS SILICA SAMPLES FOR PORE REGULATION	31
TABLE 5: PHYSICAL PROPERTIES OF SYNTHESIZED MESOPOROUS SILICA SAMPLES	34
TABLE 6: CO ₂ ADSORPTION / DESORPTION CONDITIONS TEST VIA TGA	38
TABLE 7: CO ₂ UPTAKE AND STABILITY OF 30PEI_Vp1.2 IN MILD ADSORPTION / DESORPTION CONDITION	40
TABLE 8: CO ₂ UPTAKE AND STABILITY OF 40PEI_Vp1.2 IN MILD ADSORPTION / DESORPTION CONDITION	41
TABLE 9: CO ₂ UPTAKE AND STABILITY OF 50PEI_Vp1.2 IN MILD ADSORPTION / DESORPTION CONDITION	42
TABLE 10: CO ₂ UPTAKE AND STABILITY OF 60PEI_Vp1.2 IN MILD ADSORPTION / DESORPTION CONDITION	43
TABLE 11: CO ₂ UPTAKE AND STABILITY OF 30PEI_Vp1.5 IN MILD ADSORPTION / DESORPTION CONDITION	51
TABLE 12: CO ₂ UPTAKE AND STABILITY OF 40PEI_Vp1.5 IN MILD ADSORPTION / DESORPTION CONDITION	52
TABLE 13: CO ₂ UPTAKE AND STABILITY OF 50PEI_Vp1.5 IN MILD ADSORPTION / DESORPTION CONDITION	53
TABLE 14: SUMMARY OF THE CO ₂ CAPTURE PRACTICAL PERFORMANCE WITH DIFFERENT PEI_SiO ₂ SORBENTS UNDER MILD OPERATION CONDITIONS IN THIS THESIS STUDIES	59
TABLE 15: CO ₂ UPTAKE AND STABILITY OF 30PEI_Vp1.5 IN HASH ADSORPTION / DESORPTION CONDITION	60
TABLE 16: CO ₂ UPTAKE AND STABILITY OF 40PEI_Vp1.5 IN HASH ADSORPTION / DESORPTION CONDITION	61
TABLE 17: CO ₂ UPTAKE AND STABILITY OF 50PEI_Vp1.5 IN HASH ADSORPTION / DESORPTION CONDITION	61
TABLE 18: SUMMARY OF THE CO ₂ CAPTURE OPTIMUM PERFORMANCE WITH DIFFERENT PEI_SiO ₂ SORBENTS UNDER HARSH OPERATION CONDITIONS IN THIS THESIS STUDIES	62
TABLE 19: PHYSICAL PROPERTIES OF PEI-MODIFIED MESOPOROUS SILICA SAMPLES.....	64

LIST OF TABLES

TABLE 20: SUMMARY OF AMINE LOADING CORRECTION TO PEI-MODIFIED SiO₂ SAMPLES 66

TABLE 21: UPDATED CO₂ OPTIMUM CAPACITIES OF PEI-MODIFIED SiO₂ SAMPLES..... 67

TABLE 22: UPDATED CO₂ PRACTICAL CAPACITIES OF PEI-MODIFIED SiO₂ SAMPLES 67

TABLE 23: CO₂ CAPTURE PERFORMANCE COMPARED WITH OTHER STUDY FOR 40PEI_SiO₂ ADSORBENTS 70

TABLE 24: SUMMARY OF THE CO₂ CAPTURE OPTIMUM PERFORMANCE BETWEEN 40PEI_SiO₂ SORBENTS FROM THIS THESIS STUDIES AND PREVIOUS MASTER STUDY 71

TABLE 25: PHYSICAL PROPERTIES OF TWO 40 WT.% LOADED SILICA MATERIALS..... 72

LIST OF ABBREVIATIONS

Abbreviation:

<i>Ads.</i>	Adsorption
<i>BET</i>	Brunauer-Emmet-Teller
<i>BJH</i>	Barrett-Joyner-Halenda
<i>CTAB</i>	Cetyltrimethylammonium bromide
<i>CCS</i>	Carbon dioxide capture and storage
<i>CO₂</i>	Carbon dioxide
<i>Des.</i>	Desorption
<i>EtOH</i>	Ethanol
<i>HCl</i>	Hydrochloride acid
<i>H₂O</i>	Water
<i>PEI</i>	Polyethylenimine
<i>PEI_SiO₂</i>	Mesoporous silica impregnated with polyethylenimine
<i>P123</i>	Poly(ethylene oxide)–block–poly(propylene oxide)– block–poly(ethylene oxide)
<i>SEM</i>	Scanning Electron Microscope
<i>Temp.</i>	Temperature
<i>TEOS</i>	Tetraethyl orthosilicate
<i>TGA</i>	Thermogravimetric analysis
<i>V_p</i>	Pore volume

1. INTRODUCTION

It is well known that the CO₂, as the greenhouse gas, mainly contribute to the global warming and climate change (Association, 2015). Reduction on the emission of CO₂ to the atmosphere has become as a common mission in the world and CO₂ capture and storage (CCS) has been researching for several years (Association, 2015). 80% of CO₂ in the world are emitted from the flue gas exhausted after extensive combustion of fossil fuels in the coal-fired power plants (De Coninck et al., 2009). Post-combustion flue gas is typically composed of 70% of N₂ and 15% of CO₂ with moisture and other impurities at ambient pressures (1 bar) and temperatures (298 K), but the CO₂ volume percentage could be even lower to 5% after desulfurization (Hu et al., 2015).

Therefore, efficient post-combustion CO₂ adsorbents fitted for power plant flue gas condition is interesting to be developed (Hu et al., 2015). Due to several withdraws of the amine liquid absorption process, like amine degradation, a high energy penalty, corrosion of setup and secondary environmental pollution (Kim et al., 2017). Nano-porous solid sorbents have been widely investigated for the application of CCS in terms of its high CO₂ adsorption capacity and low energy input for sorbents' regeneration (Fisher and Gray, 2015, Verdegaal et al., 2016). Amongst them, mesoporous silica materials feature high surface area, thermal stability as well as large pore volume, which allow for amines group immobilisation in turn to an outstanding performance on CO₂ capture at low temperatures (Sanz-Pérez et al., 2016a, Lee and Yavuz, 2016). The most common methods used for mesoporous silica adsorbents are derived from alkoxide based precursors such as Tetraethylorthosilicate (TEOS) by sol-gel process (Minju et al., 2017).

According to the literature review and previous work done by other students in IKP group, solid sorbents synthesis to expected properties with high surface area and large pore volume

1. INTRODUCTION

with narrow distribution is still employing aim to optimum CO₂ capture performance of high adsorption capacity as well as good thermal stability during long-term CO₂ adsorption and desorption runs. Therefore, this research work focused mainly on the two aspects: developing silica adsorbents with stable pore structures as mentioned above; and evaluating CO₂ adsorption performances of various silica composites with amine impregnations as per the simulation of flue gas condition from post-combustion.

2. LITERATURE REVIEW

2.1. Outlines of carbon capture processes

According to different industrial conditions and the purpose of reduction anthropogenic carbon dioxide emission, several CO₂ capture process routs has been developed as cost/effective and scalable techniques and adopted practically in various industrial applications: 1) post-combustion capture; b) pre-combustion capture and c) oxy-fuel combustion. The separation of each type of process has been shown in an outline sketch, given in Figure 1 (Modak and Jana, 2019).

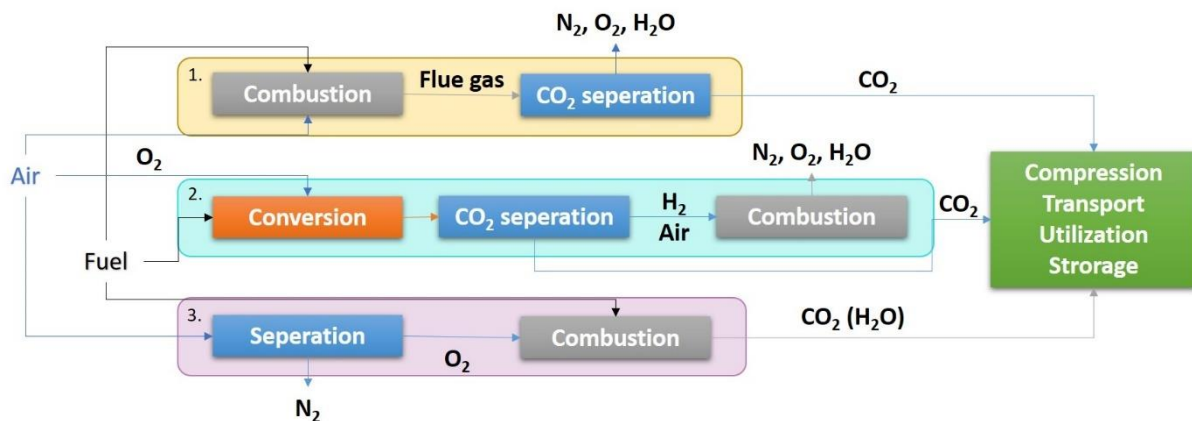


Figure 1: Schematic representation of three different CO₂ capture technologies

2.1.1. Post-combustion CO₂ capture (CO₂ /N₂ at low pressure)

For most applications of the post/combustion CO₂ capture process, N₂ separation is a must when tail gas emits the atmosphere after combustion of fossil fuels. In common, the flue gas produced by fossil fuels combustion, which consists of generally 15% CO₂, 70% N₂ along with other minor components (H₂O, CO, NO_x, and SO_x) with total pressure of 1 bar and the temperature

between 40 and 60 °C (Demessence et al., 2009). CO₂ can be captured and separated by passing through a suitable adsorbent, and then the adsorbed CO₂ is compressed for transportation and storage or further utilization. To be noticed, the high purity of captured CO₂ is benefit for its compression, transportation and storing underground from cost-effective perspective consideration. However, researches indicated that the CO₂ concentration, normally, is around 4 vol% after desulfurization which increases the difficulty of adsorption, it is quite inevitable to explore high-effective adsorbents (Demessence et al., 2009).

2.1.2. Pre-combustion CO₂ capture (CO₂ /H₂ at high pressure)

In the pre-combustion technology, fuel reacts with air/O₂ to produce synthesis gas which is a mixture of CO and H₂. With further converter reaction, the CO reacted with steam to produce CO₂ (25%–35%, by volume) and additional H₂ (30%–50%, by volume) at high pressure (5–40 bar) in the catalytic reactor, then the pre-combustion capture process is applied to separate CO₂ from H₂ at elevated pressures (~30 bar) and temperatures (~40 °C) with an adsorbent bed (Change, 2005). Application of pre-combustion capture process is a part of purification of natural gas and/or syngas, it provides, meanwhile, suitable feeds regarding energy generation, CO₂ separation, steam reforming process and gasification of coke or oil residues (Demessence et al., 2009). By decreasing pressure, the adsorbents can be recycled. Compared with the post-combustion technology, the availability of ~15% CO₂ makes CO₂ separation convenience in this process, whereas severe problem could be occurred due to high reaction temperature and H₂-rich turbine fuel (Change, 2005).

2.1.3. Oxy-fuel combustion (O₂/N₂ at low pressure)

As shown in above sketch, the combustion of fossil fuel, in the conventional oxy-fuel combustion line, is carried out under nearly pure O₂ atmosphere in purpose of minimizing NO_x generation. O₂ is fed into the power generator and diluted to a partial pressure of 0.21 bar with CO₂ in the combustion process, and the emitted gaseous products are mainly composed of CO₂ (55%–65%, by volume) and H₂O (25%–35%, by volume) (Passé-Coutrin et al., 2005). Compared with post-/pre-combustion capture technologies, CO₂ captured by oxy-fuel combustion process can be directly subjected to sequestration after dehydration, and it is easily implanted into industry regarding to its simplicity in the separation of flue gas and high purity

of CO₂ adsorbed, whereas the rigorous requirement for nearly pure O₂ combustion chamber is both technical and economical challenge of implementation of oxy-fuel combustion process.

2.1.4. Post-combustion CO₂ capture technology chosen for this thesis research

Fossil fuel-fired power plants are the main contributors to the world energy resources at the moment and it is increasing in future as illustrated in Figure 2. Since this demand will mainly be satisfied producing power from fossil fuels, the emissions of greenhouse gases will continue to increase, to solving this problem, among several CO₂ capture technologies introduces above, the post-combustion carbon capture processes technique with secure energy supply, as the only option for the retrofitting of existing power plants, can be ensured from fossil fuels reducing the emission of CO₂ to atmosphere and mitigating the global warming effect.

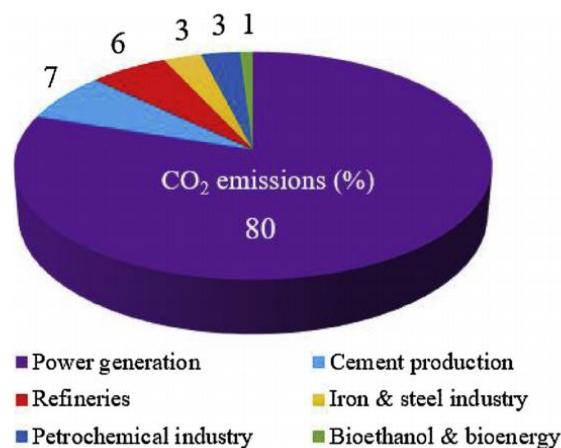


Figure 2: Percentage of total amount of annual CO₂ emissions from different industries (De Coninck et al., 2009)

2.2. Promising adsorbents for post-combustion CO₂ capture

Many different technologies of post-combustion CO₂ capture has been proposed and some of them have commercial demonstration and application for several years, such as absorption, membranes, cryogenic carbon dioxide, and adsorption. The most commonly implemented in industry is chemical absorption technology and the absorbents it deployed from single amines like MDEA, DEA, MEA, and TEA to mixed amines like PZ/MDEA, MEA/MDEA, SULFOLANE/MDEA, etc. to absorber carbon dioxide from other gases (Ooi et al., 2020, Abd and Naji, 2020, Naji and Abd, 2019). In Figure 3, it presents a pictorial representation of

2. LITERATURE REVIEW

aqueous amine-based coal-fired power plant for CO₂ adsorption and separation from acidic gas mixtures to enhance oil recovery operation.

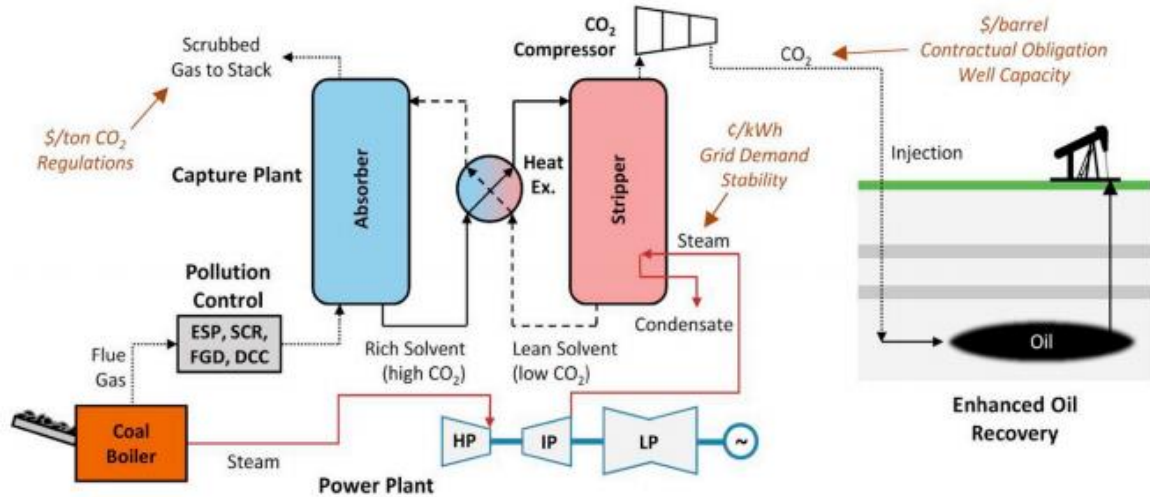


Figure 3: Schematic representation for flue gas CO₂ capture from coal-fired power plant (Walters et al., 2016)

Although the amine-based absorption technology is the state-of-art of post-combustion CO₂ capture process, it has several serious drawbacks, in which the main drawbacks of employing absorption technology are the extensive energy demand especially in the regeneration stage. Take the most widely used absorbent at present, MEA as an example, its regeneration energy consumption is between 3.2~5.5 GJ/ton CO₂. It is an attempt to reduce the energy consumption of absorbent regeneration to 2.0 GJ/ton CO₂ (Abd and Naji, 2020). Steam is main heat source used for absorbents regeneration as shown in Figure 4.

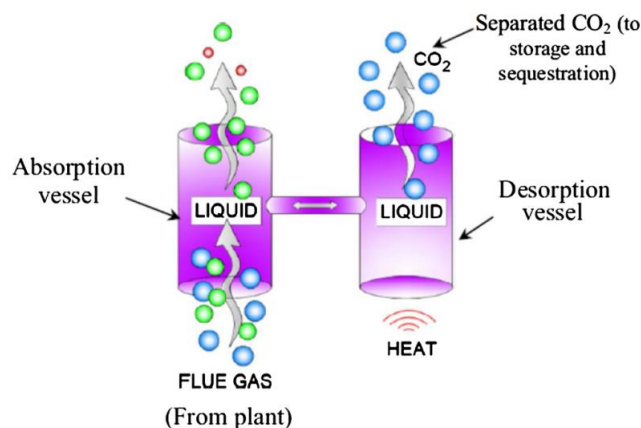
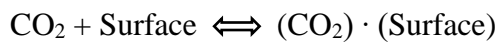


Figure 4: Graphical diagram of aqueous amine scrubbing technology (Ben-Mansour et al., 2016)

Besides the energy consumption issue, due to the corrosive nature and degradation of absorbents, as well as secondary environmental pollution caused by discharging of absorbent, use of aqueous amines as CO₂ absorbent in the existing power plants caused the corrosion issues of the plant facilities, accompanying with the requirement of costly design and high longevity of the system in order to keep them for safe running (Sanz-Pérez et al., 2016b).

As the chemical absorption method still has unresolved problems, in recent years research has also been carried out in the direction of solid adsorption. The mechanism of carbon dioxide removal on the adsorbent surface can be envisaged as (Ben-Mansour et al., 2016):



Because of van der Waals attraction of carbon dioxide molecules and the adsorbent surface, as well as, via pole/ion and pole/pole interactions between the quadrupole of carbon dioxide and the ionic and polar sites of the solid adsorbent surface, selection for carbon dioxide is obtained (see Figure 5). Advantages of carbon dioxide removal using solid adsorbents are included but not least: high carbon dioxide uptake, high recovery and stability materials, efficient under humid conditions, and low cost in contradiction to absorption processes (Satyapal et al., 2001, Kapdi et al., 2005).

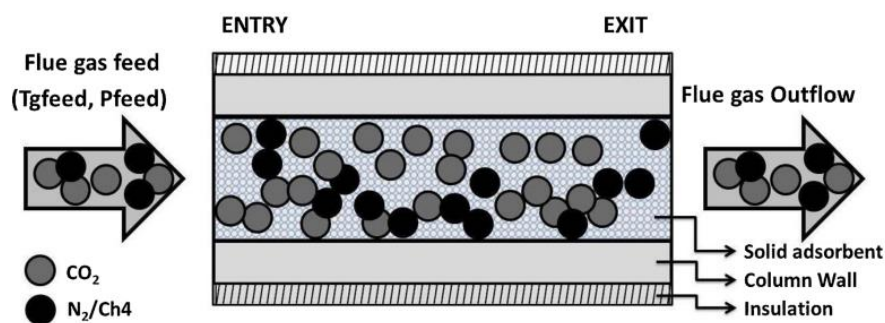


Figure 5: Graphical diagram of carbon dioxide capture by solid adsorbents (Ben-Mansour et al., 2016)

2.3. Solid adsorbents selection for physical adsorption CO₂ capture

For convenience and cost-effective adsorption and desorption of CO₂, porous solid adsorbents (see Figure 6) are much better candidates as: a) they can support facilitates better adsorption sites; b) they have high accessibility for CO₂ molecules; and 3) they can be easily recycled many times (Abd et al., 2020).

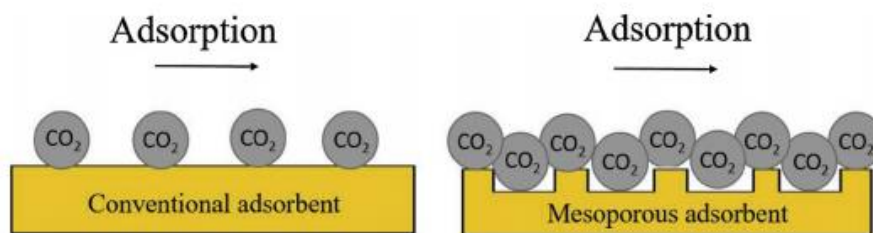


Figure 6: Schematic differences between conventional adsorbent and porous adsorbent during the adsorption process

The International Union of Pure and Applied Chemistry defined porous solid adsorbent by three types based on the pore size as:

- Micropores, < 2 nm
- Mesopores, in-between 2 and 50 nm, and
- Macropores, > 50 nm

Besides the pore size, a lot of factors impact on the adsorption capacity, for instance, the shape of pores like silts, cylinders and/or other cross-linked shapes is valuable to manage the adsorption performance (Derouane, 1998). Thus, the adsorbent material should meet some necessary criteria to be satisfied in both economical and operational for carbon dioxide capture as summarized by several researches:

- CO₂ uptake

The most critical factor for adsorbent is its adsorption performance to the capital cost of the adsorption process. The CO₂ adsorption capacity determines the required amount of adsorbent which turns in the sizing of relevant adsorption column. Higher uptake of carbon dioxide minimizes both adsorbent amount and setup size (Gray et al., 2008).

- CO₂ selectivity

The ratio of CO₂ capacity to N₂ capacity which has a direct impact on the entrapped carbon dioxide in post-combustion capture process. Efficient adsorbent should show high carbon dioxide selectivity, as well as the adsorbents must offer high capacity for CO₂ in humid conditions (Gray et al., 2008).

- Adsorption/desorption kinetics

Fast adsorption/desorption kinetics for carbon dioxide produce a sharp carbon dioxide breakthrough curve and key to control the cycle time to enhance the efficiency of adsorbents accordingly. The carbon dioxide adsorption kinetics on the porous adsorbents influenced by the reaction kinetics of carbon dioxide with the functional group on the adsorbent surface, besides the mass transfer through the adsorbent surface(Gray et al., 2008).

- Mechanical strength

The high kinetics can be maintained by better mechanical strength of adsorbents. Besides, adequate mechanical strength leads less adsorbent consumption and results in achieving a cost-effective CO₂ capture process (Gray et al., 2008).

- Adsorption heat

Low energy required for adsorbents regeneration is an essential factor to judge the competitive of CO₂ capture technology. Recommended value given by some studies indicated that for physisorption cases, the heat of adsorption is ranging between -25 to -50 kJ/mol, whereas it is much low than absorption technologies with amine solvents (Samanta et al., 2012).

- Adsorbent cost

A baseline of 10\$ per kg of the adsorbent is resulted from a sensitivity economic analysis conducted for reference over two dozen years ago for amine modified adsorbents (Tarka Jr et al., 2006). Till now, lots of researches are still carrying out on reducing adsorbent costs while maintaining satisfied CO₂ capture capacity.

2.4. Different types of solid adsorbents

As shown in the Figure 7, solid sorbents developed nowadays can be categorized in two big parts based on original materials chosen: 1) carbonaceous adsorbents and 2) non-carbonaceous adsorbents.

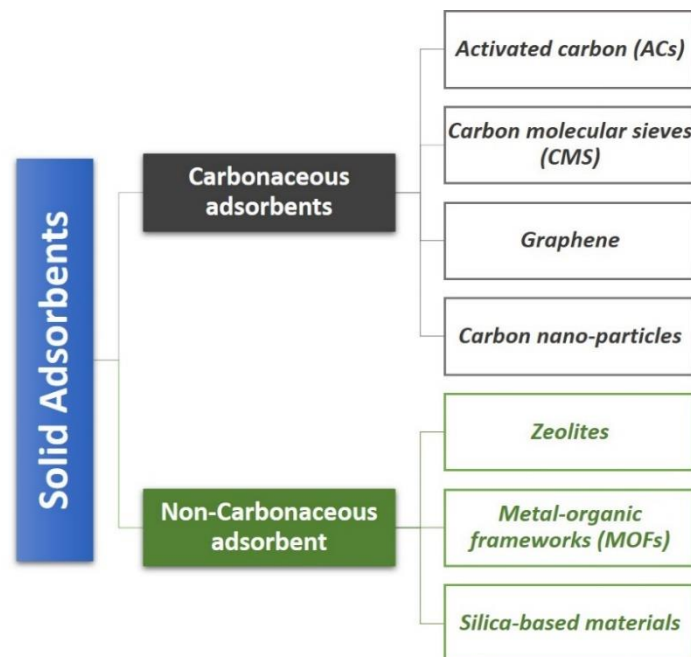


Figure 7: Physical solid adsorbents for carbon dioxide adsorption

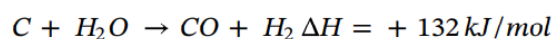
2.4.1. Carbonaceous adsorbents

Carbonaceous adsorbents are usually consisting of carbon and other associated material, many types used for CO₂ capture research are studied such as porous activated carbons, molecular carbon sieve, carbon nanoparticles, and graphene. Due to their advantages of cheap, easily consisted of natural sources, high specific surface area, large pore volume, and lightweight, those types of solid adsorbents generally are considered as excellent sorbents with properties of eco-affinity, thermal and chemical stability, heat and electrical conductivity, or high strength (Lozano-Castelló et al., 2002, Bilalis et al., 2014).

▪ **Activated carbon materials (ACs)**

Activated carbons synthesize from carbonaceous materials via pyrolysis at elevated temperature and specific pressure through the activation furnace where high surface area and

complex pore structure are formed. The carbonization stage employs inert gas like nitrogen or argon to remove the volatile matters and/or impurities and produce enriched carbon samples. After purified by inert gas like N₂ and Ar, the carbonized sample will react with CO₂ to complete the physical activation process under high temperature (up to 1273 K) as illustrated in below equations (Xu et al., 2018):



The chemical activation process involves impregnation of raw materials with a dehydrating agent before the carbonization/activation process is used broadly to overcome the main drawbacks of the physical activation of energy requirements and low carbon yield to match the industrial specifications scale (20–40 wt.%) (Xu et al., 2018).

Activated carbons are low-cost adsorbents with a fast adsorption process and low desorption energy penalty as well as high thermal stability (Seo and Park, 2010). However, they have several disadvantage under post-combustion capture conditions, like 1) the activated carbons are highly sensitive for moisture that water negatively affected the carbon dioxide adsorption at low pressure; 2) low CO₂ selectivity with negative impacts of the presence of impurities (Wang et al., 2008, Tong et al., 2017); and 3) poor mechanical strength that may cause high attrition in the bed and more adsorbents replacement from negative impacts on cost perspective consideration (Wang et al., 2014).

▪ **Carbon molecular sieves adsorbents (CMS)**

CMSs are microporous carbon adsorbents with molecule-sized pores by synthesized through four steps 1) carbonization of raw material, 2) surface activation, 3) deposition usually via chemical vapor, and 4) subsequent carbonization of aromatic molecules (Abd et al., 2020). Its property of narrow pore size distribution which leads to a high adsorption performance and selectivity on carbon dioxide adsorption (Foley, 1995). Although the carbon dioxide uptake decreased as the temperature increased, CMSs was still reported that they have equivalent adsorption capacity with other carbon-based adsorbents or even better (Silvestre-Albero et al., 2011).

▪ Graphene

It is basically a flat single layer of sp² hybridized carbon atoms, densely packed into an ordered two-dimensional honeycomb network (Abd et al., 2020). Since 2012, many literature researches have been carried out to investigate the employing of graphene/graphite as carbon dioxide adsorbent owing to the large active surface area and low preparation cost. Results showed that graphite has a low affinity for carbon dioxide to some extent and low surface area in comparison to other carbon-based adsorbents (Zhang et al., 2011). Besides, the CO₂ uptake reduces as the temperature increases due to the exothermic nature of the adsorption process, low selectivity and recyclability are challenge for this material as well (Chowdhury and Balasubramanian, 2016).

▪ Carbon nanotubes

Carbon nanotubes are generally considered as efficient adsorbent for carbon dioxide separation. Research on comparison the performance of purified single walled carbon nanotubes adsorbent to activated carbon adsorbent (See Figure 8) to demonstrate that the nanotube adsorbent exhibited double carbon dioxide adsorption capacity than activated carbon (Cinke et al., 2003). But the CO₂ uptake decreases as temperature increases from study reported (Su et al., 2011).

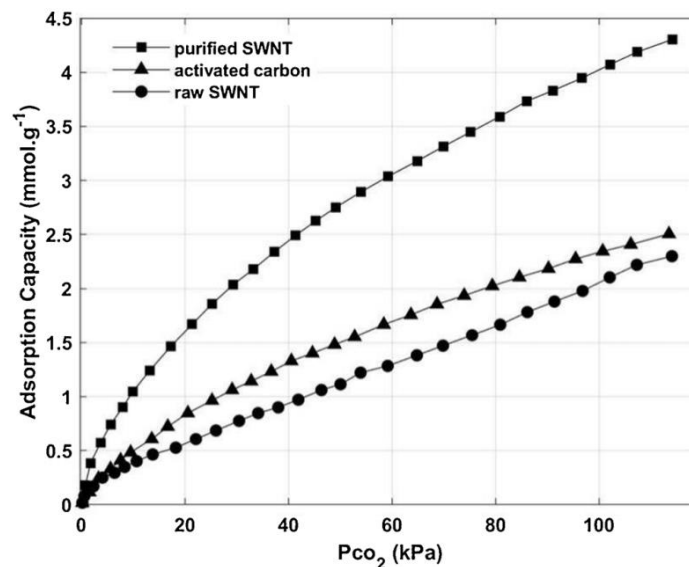


Figure 8: Comparison of carbon dioxide uptakes of arrived carbon and carbon nanotubes adsorbent (Cinke et al., 2003)

2.4.2. Non-Carbonaceous adsorbents

In addition to carbon-based adsorbents, there are many non-carbon-based materials that have been extensively studied in post-combustion carbon capture technology, such as zeolites, MOFs, silica materials, etc., which are considered to be better solid adsorbents for post-combustion carbon dioxide capture application..

- **Zeolites**

Zeolites are available naturally microporous (pore size is range from 0.5 to 1.2 nm) crystalline framework materials, which consisting of a chain of channels to capture CO₂ (Chester and Derouane, 2009). As it can also be synthesized in the research laboratory, zeolites have been broadly studied for carbon dioxide removal in the interest of their molecular sieving impact and the robust dipole–quadrupole (electrostatic) interactions between carbon dioxide and alkali metal cations in the zeolite frameworks (Zhang et al., 2008).

Common types of synthesized zeolites for carbon dioxide adsorption are well known as zeolite A, X, and Y, natural zeolite like chabazites, ferrierites, and mordenites are also applied (Siriwardane et al., 2001, Siriwardane et al., 2003). Researches on the carbon dioxide adsorption capacity and selectivity by comparing G-32H activated carbon, zeolite 13X, and 14A molecular sieves conducted that 13X performed relatively better CO₂ capacity than the ACs adsorbents, with high selectivity in the mixture gases of N₂ and H₂ (Siriwardane et al., 2001). However, zeolite adsorbents of carbon capture is typically employed at high regeneration temperature (573 K) and pressure (> 200 kPa), it turns in therefore a huge energy loss (Harlick and Sayari, 2006). Besides, small content of moisture could greatly reduce the CO₂ loading of zeolites adsorbent due to its high H₂O affinity, formed film blocked the access for carbon dioxide molecules turn in less CO₂ uptake (Chester and Derouane, 2009).

- **Metal-organic frameworks (MOFs)**

Metal-organic frameworks are solid adsorbents materials that are produced by the combination of metal ions linked by coordination bonding as shown in Figure 9. Two types are classified in the metal-organic frameworks: 1) Rigid MOFs with strong frameworks that create permanent pores similar to zeolite materials; 2) Dynamic MOFs with soft frameworks whose structures change by external impacts like pressure, temperature, and guest molecules (Li et al., 2011). Researched conducted that the high heat of adsorption in some MOFs like HKUST-1, MIL-

100/101, and the MOF-74 group can be achieved to create a bare-metal site lining the pore by liberation of a coordinating solvent (typically water) molecule (Plant et al., 2007, Llewellyn et al., 2008, Caskey et al., 2008). Generally, metalorganic frameworks possess high capacity to adsorb carbon dioxide at high pressures, whereas their adsorption capacity, at atmospheric pressures, is lower in comparison to other physical adsorbents (Abd et al., 2020).

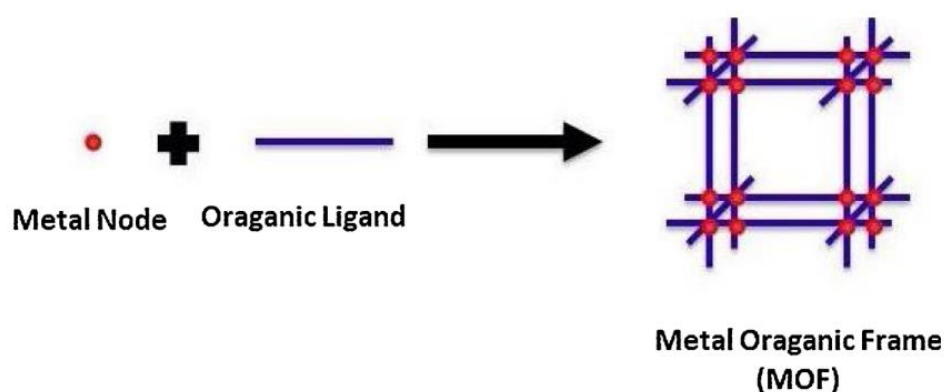


Figure 9: Graphical diagram of producing MOFs materials (Abd et al., 2020)

▪ Silica

Mesoporous silica materials commonly are considered as a thermal and chemical stable material with tunable structure, its morphological flexibility and porosity allows these nanoparticles be able to functionalize with suitable organic and inorganic groups (Kumar et al., 2017). Large micropores and mesopores on silica surfaces is one of the advantages to be utilized as an adsorbent in CO₂ capture and the adsorption can be carried out with moderate temperature at 298 K and 1 bar. Therefore, lots of studies has been employed on Mesoporous silica materials, among of them, there are two classical types widely applied as support material for post-combustion CO₂ capture technology as:

- **SBA-15** (Santa Barbara Amorphous No. 15)
An attractive mesoporous silica material having well-ordered and relatively large hexagonal pores in the range of 4.6–30 nm (Kruk et al., 2000).
- **MCM-41** (Mobil Crystalline Material No. 41)
it constitutes a structure of the class of ordered mesoporous silica materials with uniformly ordered honeycomb like pores with diameter in the range of 2–6.5 nm (Trewyn et al., 2007).

However, silica as an adsorbent without any modification is not recommended as the regeneration difficulties of silica nanoparticles with huge energy penalty during CO₂ desorption turns in undesirable economic feasibility as a distinct disadvantages, concluded by researches (Lee and Park, 2015). Therefore, most of the research efforts on silica-based adsorbents are mainly interested in modifying various types of silicas and deploying appropriate amines types. Heretofore, many studies reported the use of silica materials-based adsorbents for carbon dioxide (Abd et al., 2020).

2.4.3. Comparison of various physical solid adsorbents for carbon dioxide adsorption

It is has been concluded by many researches that the adsorption of carbon dioxide using solid adsorbents is a promising technology that can minimize the energy requirements for the regeneration process compared to the other commonly used absorption capturing technologies, and the efficient solid adsorbents used in post-combustion CO₂ capture process should offer high thermal stability, good mechanical strength, high selectivity, low synthesis cost, resistance in humid conditions (Abd et al., 2020). Pro and cons of various solid adsorbents summarized in Table 1 stated that neither carbon-based adsorbents nor non-carbonaceous (zeolites and MOFs), their features cannot fully satisfy the CO₂ capture condition from flue gas of post-combustion power plant with low CO₂ pressure after desulfurization, low temperature and humid condition, to achieve high CO₂ adsorption performance and economic efficiency (Abd et al., 2020).

2. LITERATURE REVIEW

Table 1: Comparison of pro and cons among carbon-based adsorbent, zeolites, and MOFs for carbon dioxide adsorption

Feature	Carbonaceous adsorbents	Zeolites	MOFs
Major application	High pressure CO ₂ adsorption	H ₂ enrichment	CO ₂ separation
CO ₂ selectivity	Medium	Low	High
CO ₂ capacity	Better at high pressure but reduce at low pressure	Medium	High
Stability (humid condition)	Stable	Unstable	Unstable
Materials cost	Acceptable cost	Low cost	Expensive
Advantages	<ul style="list-style-type: none"> • High conductivity • High stability • Large surface area and pore volume, • Light weight 	<ul style="list-style-type: none"> • Large micro-/mesopores • Medium CO₂ uptake at ambient conditions • Low energy penalty 	<ul style="list-style-type: none"> • Ability of tuning the pore volume • High surface area
Disadvantage	<ul style="list-style-type: none"> • Low adsorption and regeneration temperatures • Low adsorption capacity among those three type sold sorbents 	<ul style="list-style-type: none"> • High affinity with water • High energy penalty • Difficult readiness 	<ul style="list-style-type: none"> • Low CO₂ uptake at low pressures • Low economic efficiency • Difficulty on synthesis • Sensitive to humid • Morphological destroyed at high temperature

2.5. Amine functionalization on mesoporous solid adsorbent for CO₂ capture

the capability of capturing CO₂ by amino groups as well as the stable and high porosity to promote accessibility of functional groups and adsorption kinetics can be enhanced by loading or grafting amine species into or onto the inner mesopore surface of mesoporous materials (see Figure 10, as the N-containing groups can be designed and fabricated through loading or grafting linear or hyperbranched amine group into the mesopores. Amine modified adsorbents are acknowledged with high CO₂ adsorption capacity, fast adsorption kinetics, as well as easy regeneration with stable cycling performance recently (Azmi and Aziz, 2019).

According to the synthesis methods, amine-based materials are of different types, as shown in Figure 10 for instance the amine functionalization on mesoporous silica (Modak and Jana, 2019). The pros and cons of each synthesis method and their applications are summarized in Table 2.

- (i) **Class 1 (Impregnation)** materials which are prepared by impregnation of amines into the pores,

- (ii) **Class 2 (Grafting)** consisting of amines which are covalently bonded to the walls of porous materials, and
- (iii) **Class 3 (In-situ polymerization)** where amine monomers are in-situ polymerized to polyamines inside the framework.

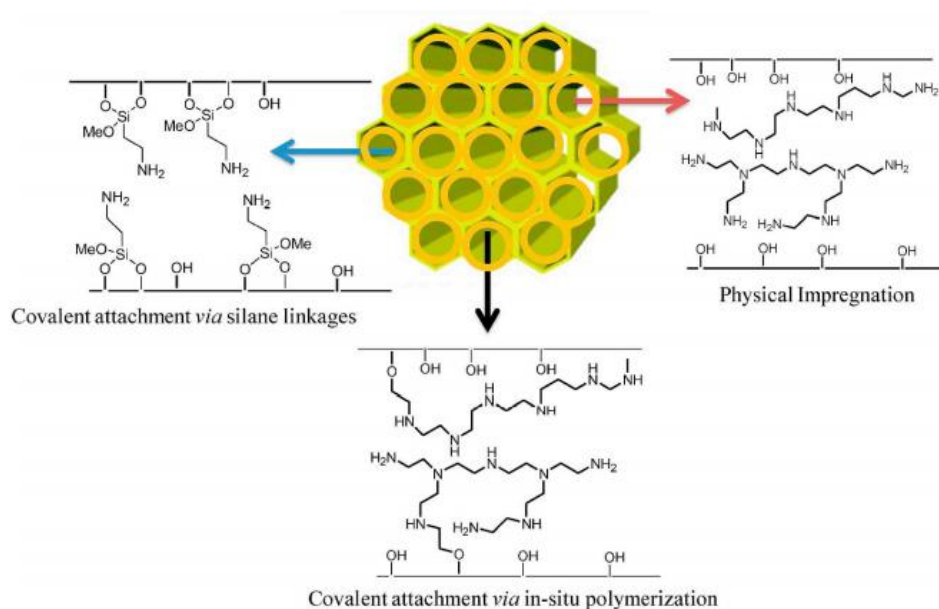


Figure 10: Schematic representation of the formation of several amine-functionalized mesoporous silica

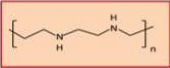
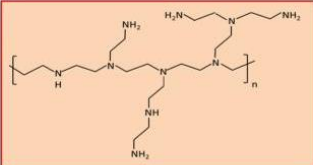
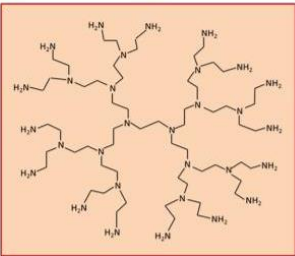
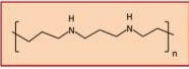
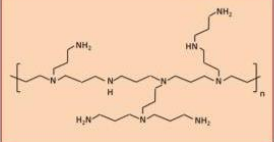
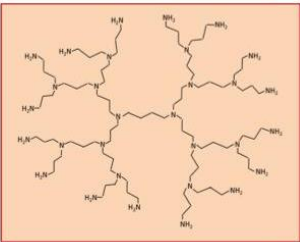
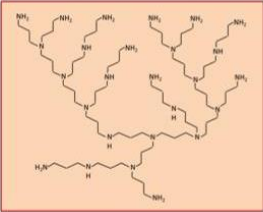
Table 2: Summary of N-loading methods onto adsorbents and their characteristics (Hu et al., 2020)

Method	N source	Advantages	Disadvantages
Impregnation	Monomeric or polymeric amine, amino acid, amino-containing ionic liquid, other amino-containing organic material except alkoxysilanes	<ul style="list-style-type: none"> • Higher amine loading than grafting • Usually higher CO₂ adsorption capacity than grafting sorbents • Repeatable synthesis method • Mild synthesis conditions 	<ul style="list-style-type: none"> • Weak connection between aminomaterial and substrate mate • Weak thermal stability • Surface amine aggregation with high amine loading
Grafting	Amine-containing alkoxysilanes	<ul style="list-style-type: none"> • Linkages between amino-material and substrate material are bonds • Stable under a higher temperature (above 200 °C) • Better amine dispersion degree • Repeatable synthesis method • Mild synthesis conditions 	<ul style="list-style-type: none"> • Amine loadings largely subject to substrate's silanol group number • Usually lower CO₂ adsorption capacity than impregnation sorbents
In-situ polymerization	N-containing precursor	<ul style="list-style-type: none"> • One-step synthesis method • Reported adsorbents usually have high adsorption performance 	No regular synthesis method

2. LITERATURE REVIEW

Modifying of mesoporous silica-based materials with amines can efficiently enhance the adsorption capacity for CO₂ by virtue of the primary and secondary amines have a high affinity for carbon dioxide and react strongly by hydroxyls on the surface as following (Lee and Park, 2015). Typical amine chosen for Mesoporous silica materials modifications are summarized as Table 3 given below.

Table 3 - Details of polymeric amines reported for CO₂ capture applications (Varghese and Karanikolos, 2020)

S.No.	Polymeric amine	Chemical structure	Remarks
1.	Polyethylenimine (or polyaziridine)		Wide availability in various structural forms and molecular weights.
1.a.	Linear polyethylenimine		Secondary amines on the back bone.
1.b.	Branched polyethylenimine		Primary, secondary, and tertiary amines at respective chain ends, back bone, and branch points.
1.c.	Polyethylenimine dendrimer		<ul style="list-style-type: none"> • Primary and tertiary amines at respective chain ends and branch points. • Regularly ordered highly branched repeating units around a central core. • Size, chemical functionality, and molecular weight can be tuned on demand. • High amine or nitrogen density.
2.	Polypropylenimine (or polyazetidine)		<ul style="list-style-type: none"> • Better oxidation stability than that of polyethylenimine. • Challenges associated to monomer synthesis and polymerization time.
2.a.	Linear polypropylenimine		Secondary amines in the back bone.
2.b.	Branched polypropylenimine		Primary, secondary, and tertiary amines at respective chain ends, back bone, and branch points.
2.c.	Polypropylenimine dendrimer		<ul style="list-style-type: none"> • Primary and tertiary amines at respective chain ends and branch points. • Regularly ordered highly branched repeating units around a central core. • Size, chemical functionality, and molecular weight can be tuned on demand. • High amine or nitrogen density.
2.d.	Hyperbranched polypropylenimine		<ul style="list-style-type: none"> • Primary, secondary, and tertiary amines at respective chain ends, back bone, and branch points. • Irregularly ordered, highly branched macromolecular structure. • High amine or nitrogen density.

3.	Polyallylamine		<ul style="list-style-type: none"> • Primary amine at the side chain. • Better thermal and oxidation stabilities. • Capable to bind strongly with other material surfaces.
4.	Polyaniline		<ul style="list-style-type: none"> • Secondary amines in the backbone. • Superior thermal stability.

Commonly, flue gas of power plant combustion consists high amount (up to 15 vol%) of water (Xu et al., 2004). For instance, silica-based adsorbent is rich with OH groups usually with water affinity during adsorption which causes the moisture content to increase, in other words, H₂O molecules will occupy the active site of silica surface and turns in reduction of the CO₂ capture performance of the silica-based adsorbent. Theoretically, by elevating the adsorption temperature, the water molecules expand and evaporates away from the support. Therefore, the accessibility of CO₂ to support surface increases, as displayed in Figure 11 (Azmi and Aziz, 2019).

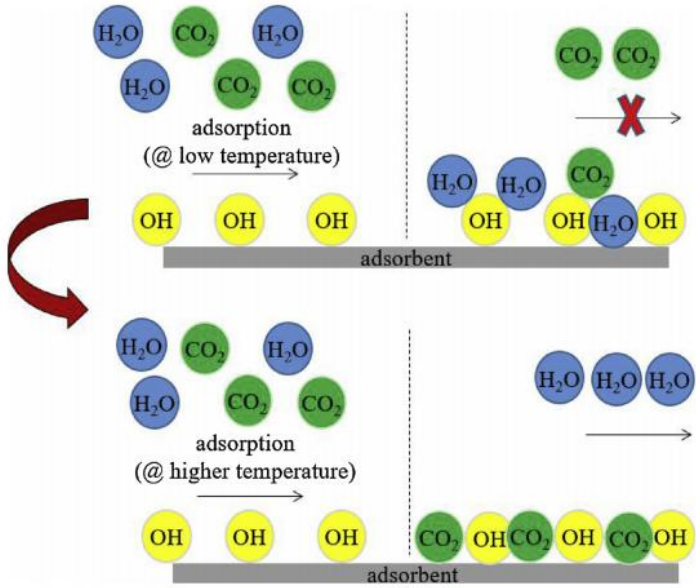


Figure 11: Illustration of water impacts on CO₂ adsorption capacity

To be noticed, the adsorption temperature tuning will impact on overall adsorbents properties and is limited by power plant flue gas condition. With amine modification on mesoporous silica adsorbents, theoretically, the water content through carbon dioxide capture should enhance the amine adsorption performance because of the formation of carbonates and bicarbonates. However, due to the competitiveness of CO₂ and water adsorb, the moisture content can turn in amine leaching (Quang et al., 2017).

2.6. PEI-modified mesoporous silica materials chosen for post-combustion CO₂ capture studied further in this thesis research

Due to the advantages of high surface area, large pore volume, tunable pore size and excellent mechanical stability, many researches on CO₂ capture by silica materials mainly on the following three aspects: 1) novel synthesizing method of amine modified silica composite materials; 2) development of new pore structures silica adsorbents; and 3) evaluation of CO₂ adsorption performances of various silica composites (Lee and Park, 2015, Choi et al., 2016). As above mentioned, silica is not recommended without modification due to huge energy requirement for its regeneration. Therefore, with modifications methods like amine functionalization and enhancing the textural properties improve the carbon dioxide adsorptive performance, mesoporous silica nanoparticles with narrow pores distribution with carbon dioxidephilic heteroatoms are compatible with carbon dioxide removal technologies, to exhibit competitive CO₂ capacity with good selectivity and stability for achieving scaled-up industrial application for realizing post-combustion carbon dioxide capture technology.

Compared with as-synthesized silica, amine-impregnated porous silica not only have higher CO₂ adsorption kinetics, but also showed advantages of high amine loading (Chen and Bhattacharjee, 2017). Besides, the CO₂ capture performance of the amine-impregnated mesoporous silica nanoparticles is also closely related to the properties of introduced amine types, which should have a high boiling point to prevent amine leaching and high N concentration to achieve a higher CO₂ capture capacity (Subagyono et al., 2011), therefore PEI becomes one of the most used for Mesoporous silica materials amine modification worldwide (N contents of ca. 33%) and high boiling point (see Table 3).

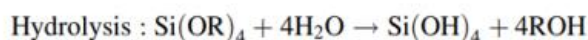
The temperature of the post-combustion CO₂ flue gas usually falls in the range of 50–75 °C (D'Alessandro et al., 2010), which is close to the optimal temperature range of CO₂ capture by PEI-modified Mesoporous silica materials at 75 °C, as researches concluded. At this adsorption temperature, the improved mobility of amine species and the facilitated diffusion of CO₂ within the pore channels lead to a high CO₂ uptake of PEI-modified Mesoporous silica materials (Subagyono et al., 2011).

3. THEORY

3.1. Synthesis mechanism for mesoporous silica materials

Mesoporous silica materials are synthesized by modified Stober's method, i.e., "sol-gel process", was widely used. Sol-gel chemistry is a mature developed process for many inorganic materials syntheses. Theoretically, reaction involves the alkoxide monomers hydrolysis and condensation into a colloidal solution (normally called as 'sol'), which would be aging to form an ordered network (normally called as 'gel') of polymer (Danks et al., 2016).

A typical sol-gel process can be accomplished in basic or acidic conditions according to the catalysts. The alkoxide group gets hydrolysed in aqueous environment first and it is experimentally proved that the hydrolysis rate of silicon precursor is faster in basic conditions compared to acidic. Subsequently condensation followed by the hydrolysis step, the schematic representation of the hydrolysis and condensation reactions are shown in follow equations (Danks et al., 2016):



Sol-gel process used in this thesis research mainly based on action of the micelle which forms organic-inorganic phase between surfactant and target production, in other words the synthesis of Mesoporous silica materials occurs wherein hydrolysis and condensation of silica on the surface of surfactant micelles takes place. The liquid silica (e.g, TEOS) transforms to solid silica. Due to the aggregation by weak intermolecular or intramolecular interaction creates a certain structure of space, as illustrated in Figure 12 (Agudelo et al., 2020).

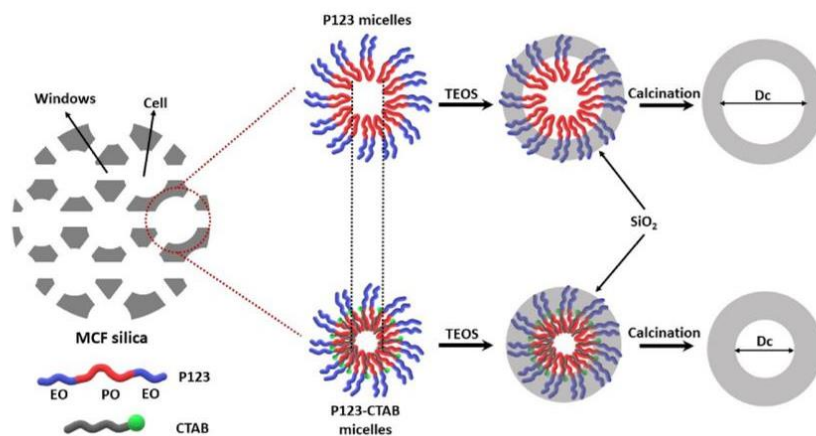


Figure 12: Scheme of the formation of Mesoporous silica materials with and without CTAB with TEOS as silicon precursor

3.2. Polyethylenimine (PEI) impregnation to Mesoporous silica materials

Due to the easy synthesis and large amount of amine introduced to the silica support, amine-modified porous silica synthesized by physical impregnation method have been the most practical adsorbents for large-scale gas separation applications in all types of amine-silica combinations (Choi et al., 2009).

After dispersing the amine into methanol evenly by stirring, a certain amount of porous is added into the amine solution continuously while stirring usually at room temperature for a certain time to help the amine molecules disperse into the pores of the support materials (Ahmed et al., 2017), as illustrated in Figure 13. The adsorption sites for capturing CO_2 are formed by the bond between amine molecules, the surface and within the pores of the support. The loading of amine on the support substrate depends on the pore volume of the support, in other words, functionalized adsorbents with higher adsorption capacities can be obtained from porous supports with large pore volumes (Chen et al., 2016). As there is no substantial chemical bond between the dispersed amines and the supports, the as-obtained adsorbents have similar thermal stabilities to the origins of the amines (Anbia et al., 2012).

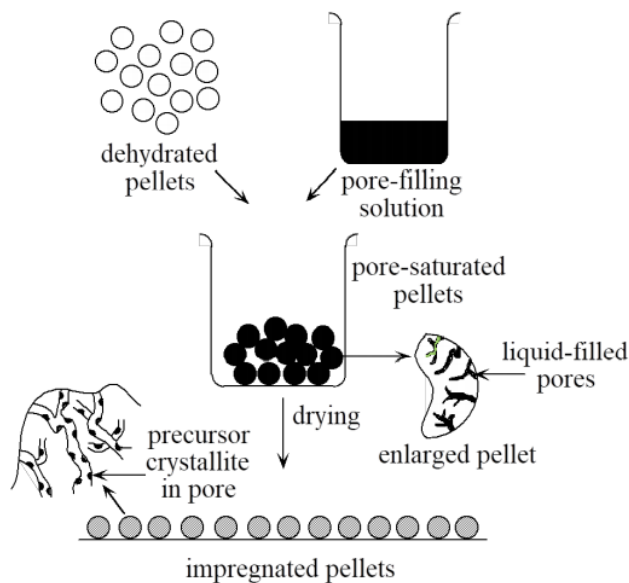


Figure 13: Physical impregnation illustration

3.3. CO₂ capture by PEI-modified Mesoporous silica materials

It is understood that the interaction mechanism of CO₂ with the amine-functionalized mesoporous silica sorbents is of paramount importance for the development of prospective adsorbents, which will turn in a reduction of emitting the anthropogenic emissions. Based on the absorption mechanism achieved by aqueous amine solutions, research on the adsorption mechanism of CO₂ over amine-based mesoporous silica and its performance of CO₂ capture were exploring over decades. Researches demonstrated that CO₂ was captured in the forms of ammonium carbamates through the two-step zwitterion mechanism in case of primary and secondary amines (Caplow, 1968). CO₂ was firstly attracted by the lone electron pair of the nitrogen atom giving rise to the formation of the zwitterionic intermediate which was then converted into an ammonium carbamate ion pair through deprotonation by a base molecule that is usually a neighbouring amine to the zwitterionic intermediate (Sartori and Savage, 1983). Carbamate could not be formed but leading to the production of bicarbonate once the amine was sterically hindered or tertiary (Davran-Candan, 2014, Yamada et al., 2011). Figure 14 indicates a schematic of functionalization of porous materials with polymeric amines and their CO₂ capture.

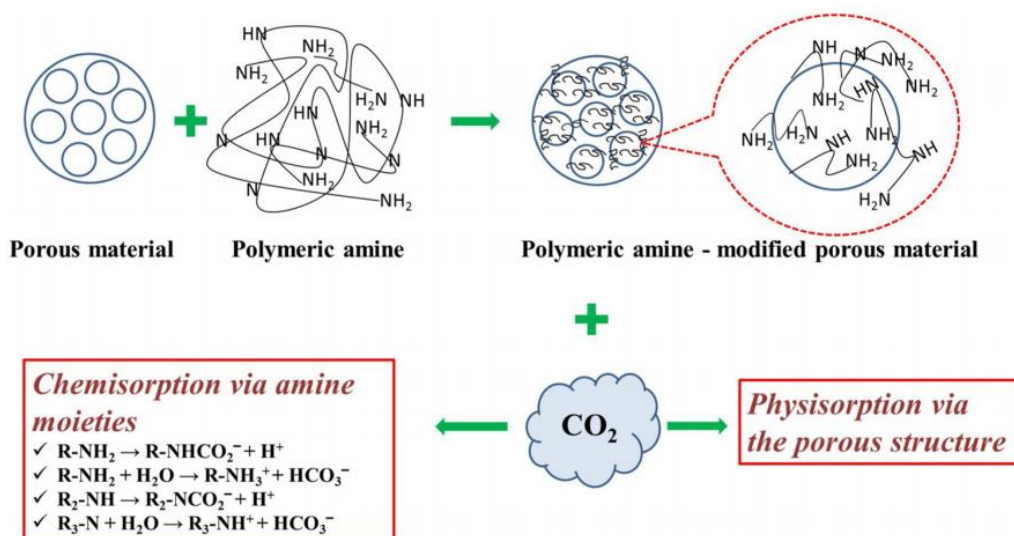


Figure 14: Schematic of functionalization of porous materials with polymeric amines and their CO₂ capture action (Varghese and Karanikolos, 2020)

3.4. Characterization

3.4.1. Nitrogen adsorption and desorption

Nitrogen adsorption and desorption is commonly understood to be applied for analysing materials' textural properties such as surface area, pore volume, pore size distribution and etc. by most using commonly the Brunauer-Emmet-Teller theory. According to the BET method, the surface area is obtained by measuring the volume of the gas adsorbed at the surface, at a constant temperature (77K liquid nitrogen), as a function of the equilibrium pressure. The pressure is demonstrated as a relative pressure: actual pressure p divided by the vapor pressure. Meanwhile, pore diameter, volume and distributions are determined by using the Barrett-Joyner-Halenda (BJH) method. Desorption data given by BJH provide a relationship between volume of adsorbed nitrogen and the monolayer coverage of adsorbed volume at a given partial pressure. Meanwhile, the Kelvin equation can be used to determine the pore size distribution in terms of the capillary condensation phenomena happened in the pores of porous material during the desorption isotherm process. (Webb and Orr, 1997)

3.4.2. Scanning Electron Microscope

Scanning Electron Microscope (SEM, shown in Figure 15), as an electron microscope, is usually applied to study the morphology and topology of the sample by obtaining an image of the objective. The high-resolution nanoscale images are achieved by scanning the sample with a high-energy beam of electrons. As the electrons interact with the sample, they produce secondary electrons, backscattered electrons, and characteristic X-rays. These signals are collected by one or more detectors to form images which are then displayed on the computer screen. When the electron beam hits the surface of the sample, it penetrates the sample to a depth of a few microns, depending on the accelerating voltage and the density of the sample. Many signals, like secondary electrons and X-rays, are produced as a result of this interaction inside the sample. (instruments, 2021)

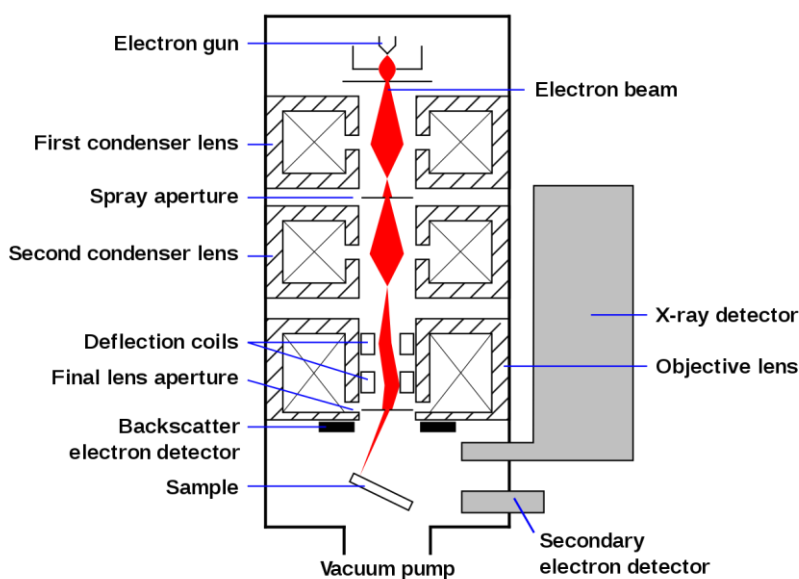


Figure 15: Schematic of an SEM

3.4.3. Thermal Gravimetric Analysis

Thermogravimetric analysis (TGA) is commonly used to characterize the CO₂ adsorption capacities and thermal stability of solid adsorbents by measuring sample weight change with temperature variation. Therefore, mass spectrometer is usually combined with TGA. Figure 16 indicates a typical configuration of TGA. CO₂ partial pressure of inlet gas could be adjusted by the mixing percentage of CO₂ and N₂ for investigating different adsorption capacities of solid

3. THEORY

adsorbent, meanwhile pure N_2 is used for regeneration purpose in this thesis research. (Zhao et al., 2018, Zhang et al., 2014)

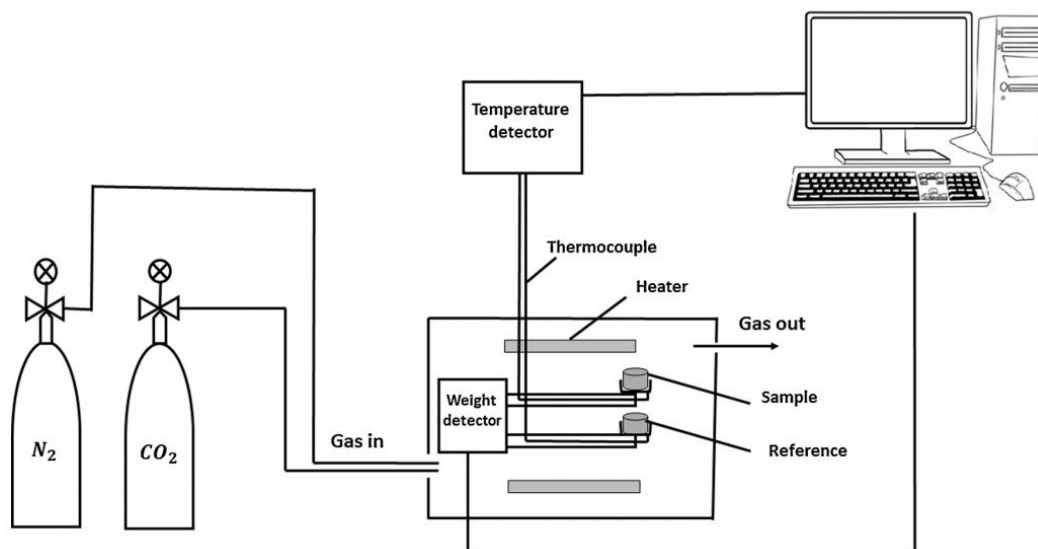


Figure 16: Schematic diagram of the TGA set-up

4. EXPERIMENTS

4.1. Synthesis of mesoporous silica nanoparticles

Synthesis of mesoporous silica materials were carried out according to two-step protocol, as previously reported (Ma et al., 2003) by using chemicals from Sigma-Aldrich which are tetraethyl orthosilicate (TEOS, 98%) as the silica source, poly(ethylene oxide)–block–poly(propylene oxide)–block–poly(ethylene oxide) (P123, Mw=2900) as the template, cetyltrimethylammonium bromide (CTAB, 99%) as the cosurfactant, and ethanol (EtOH, 96%) as the cosolvent.

A molar ratio of TEOS: 1, P123: 0.044, CTAB: 0.122, HCl: 2.67, EtOH: 9.5 and H₂O: 116 was used in the synthesis. Thus, 1.7 g of triblock copolymer P123 and 0.6 g of CTAB were dissolved in a solution formed by mixing 3 ml of HCl (37%), 26 ml H₂O and 7.5 ml EtOH to obtain a homogeneous solution. 3 ml of TEOS was added in the aqueous solution at room temperature under magnetic stirring of 30 min. In the second step, the solution was transferred into a Teflon-lined stainless-steel autoclave and heated at 80 °C for 5 h, and then kept at a higher temperature at 130 °C for 12 h. The product was cooled down to room temperature and then filtered and washed with ethanol several times and dried in oven at 90 °C for 24 h. The white powder was finally obtained after calcination in air at 550 °C for 5 h for template removal.

4.2. Amine-impregnation of synthesized mesoporous silica samples

Amino functionalisation of mesoporous silica samples was carried out by a typical wetness impregnation method described in previous chapter. Polyethylenimine (PEI, branched, Mw=600, Sigma-Aldrich) was used. The amine source was mixed with methanol and stirred during 30 min. Then, mesoporous silica samples were added to the solution with variable weight ratio of Amine/Mesoporous silica samples (30 ~ 60 wt.%) and stirred at 40 °C in a rate of 700

rpm for 2 h. The obtained amino-functionalised mesoporous silica samples were sealed and stored at room temperature for subsequent characterization.

4.3. Characterization

4.3.1. Nitrogen adsorption and desorption

Nitrogen isotherms were carried out using an automated gas adsorption analyser Tristar 3000 (Micromeritics, Instrument Co) at 77 K. Prior to the analysis, the Mesoporous silica samples and PEI-modified Mesoporous silica samples were degassed in VACPREP 061 unit at 200 °C and 60 °C overnight respectively. BET surface area was obtained from the adsorption branch in the relative pressure range between 0.05 and 0.3. Pore size distribution was calculated by BJH method.

4.3.2. Scanning electron microscope

The morphology and topology are studied using the Hitachi S-5500 in lens cold field emission scanning transmission electron microscope (S(T)EM), with a secondary electron (SE) detector. The acceleration voltage was set from 7 kv to 30 kv and beam current was set from 7 μ A to 20 μ A for different samples. All the samples were dispersed in deionized water and then dropped on a silicon wafer for test preparation.

4.3.3. Thermo gravimetric analysis

The measurements of CO₂ uptake capacity by the synthesized PEI-modified Mesoporous silica samples were carried out using the thermogravimetric analysis technique (TGA Q500 V6.7). In each run, about 10 mg of one the synthesized adsorbents were placed in an alumina oxide pan and, then, the adsorbent was degassed at 100 °C using a stream of pure N₂ gas flowing at 50 mL/min. Once the weight of the sample reached a steady value (i.e., all water is removed), the temperature was dropped to 75 °C and left to equilibrate. After the stabilization of the adsorption temperature at 75 °C after 20 min, shifted gas inlet valve to keep CO₂ partial pressure of 5 vol%, and the flow rate of CO₂ was kept constant at 50 mL/min. Then CO₂ desorption was carried out at 75 °C in pure N₂ gas flowing at 50 mL/min.

Two protocols of contact time between CO₂ and adsorbents was used in this thesis research for determine optimum and practical CO₂ uptake of synthesized adsorbents respectively. For optimum condition, the adsorption of CO₂ was monitored in time of 100 min contact until the adsorption approached equilibrium with 2 cycles. While the practical condition chosen a 10 min contact time with CO₂ but 10 cycles running to analyse the stability of adsorbents as well.

5. RESULT AND DISCUSSION

5.1. Synthesis of mesoporous silica supports

To ensure that the adsorbent could be modified or improved without damaging its original structure, the targeted adsorbent would like to be synthesized in this thesis study should be mesoporous silica supports with high surface area, high pore volume with narrow distribution as well as with rigid morphology structure. The synthesis methods chosen was conventional sol-gel process. To achieve better overall performance on CO₂ capture performance after amine impregnation, composition of solution and operation condition of synthesis was tuned to realize targeted adsorbents that could facilitate more adsorption sites for CO₂ component.

According to different composition of solutions and/or operation condition, synthesized materials list in Table 4 were denoted as naming rule shown in Figure 17.

Table 4: Experimental parameters of mesoporous silica samples for pore regulation

	TESOS (mL)	P123 (g)	CTAB (g)	EtOH (mL)	HCl (mL)	H₂O (mL)	TEOS : P123 (Molar ratio)	CTAB : P123 (Mass ratio)
40°C_SiO ₂ _1''P123_1/6CTAB	3	0.86	0.15	7.5	3	26	1:0.022	1:6
40°C_SiO ₂ _1''P123_1/3CTAB	3	0.86	0.3	7.5	3	26	1:0.022	1:3
80°C_SiO ₂ _1''P123_1/6CTAB	3	0.86	0.15	7.5	3	26	1:0.022	1:6
80°C_SiO ₂ _1''P123_1/3CTAB	3	0.86	0.3	7.5	3	26	1:0.022	1:3
80°C_SiO ₂ _2''P123_1/3CTAB	3	1.72	0.6	7.5	3	26	1:0.044	1:3
80°C_SiO ₂ _3''P123_1/3CTAB	3	2.58	0.9	7.5	3	26	1:0.066	1:3

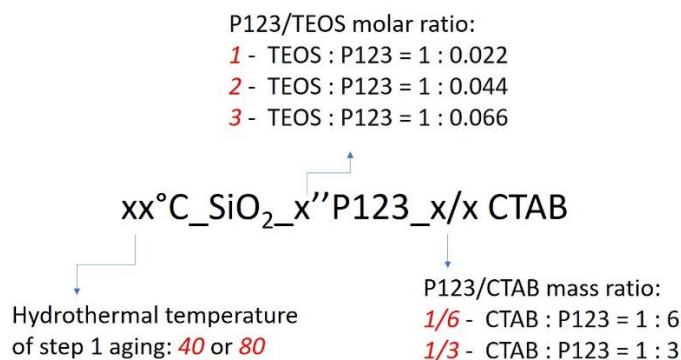


Figure 17: Sample naming rule

5.1.1. Tuning procedure for targeted adsorbent synthesis

Experiments were carried out with two heating steps: 1) 40 °C during 5 hours; 2) 130 °C during 12 hours. Total aging time was during 17 h using P123/TEOS molar ratios and P123/CTAB mass ratio of 0.022 and 6 respectively. According literature researches that the reaction mechanism firstly consists in the quick formation of ordered CTAB micelles, next P123 molecules envelop the pre-formed nucleus to form compound micelles and finally the TEOS is hydrolysed and condensed to form mesoporous silica as illustrated in Figure 18 (Liu et al., 2009). Therefore, it is necessity to add P123 to certain contents which can envelop the CTAB micelles and to carry out the co-assembly with the silicate species for the formation of silica adsorbents.

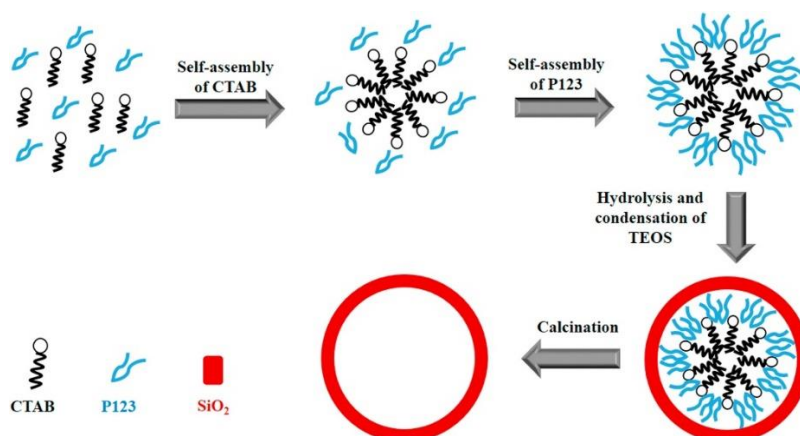


Figure 18: Mechanism for the synthesis of mesoporous silica using P123 and CTAB as template and co-template, respectively.

By identical double the amounts of CTAB while keep same operation condition, two adsorbents $40^{\circ}\text{C_SiO}_2\text{_1''P123_1/6CTAB}$ and $40^{\circ}\text{C_SiO}_2\text{_1''P123_1/3CTAB}$ was synthesized and characterized their physical properties. BET shown that double CTAB provided an enhancement of surface but no obvious improvement on pore volume at same time.

Mesoporous silica materials normally presented less structural order at low aging temperature because of P123 is a temperature-dependent surfactant and therefore the properties of the mesoporous silica can be tuned by adjusting the operation temperature (Galarneau et al., 2001). The hydrothermal temperature also demonstrated a positive impact on the morphology structure of mesoporous silica adsorbent as previous studies reported (Meléndez-Ortiz et al., 2016).

Thus, two new adsorbents were produced by different protocol, one was kept low P123/CTAB mass ratio of 1/6 as the initial solution composition but increase the first step heating temperature from 40 to 80 °C, whereas another was tuned both on double CTAB amounts together with temperature increasement. Samples obtained from them were named $80^{\circ}\text{C_SiO}_2\text{_1''P123_1/6CTAB}$ and $80^{\circ}\text{C_SiO}_2\text{_1''P123_1/3CTAB}$, respectively. BET results of those two new silica samples shown a fairly improvement on pore volume while maintain a high surface area as well, which proved that high aging temperature has a contribution on improving porosity.

The last step of the mesoporous silica synthesis was templates removal by calcination, i.e. remove P123 (main templates) and CTAB (co-templates). In order to enhance the porosity of finally silica support, a tuning on P123/TEOS molar ratio was carried out based on the synthesis composition and condition for $80^{\circ}\text{C_SiO}_2\text{_1''P123_1/3CTAB}$ by double and tribble the amount of P123, respectively. Samples synthesized finally was named $80^{\circ}\text{C_SiO}_2\text{_2''P123_1/3CTAB}$ and $80^{\circ}\text{C_SiO}_2\text{_3''P123_1/3CTAB}$. Physical properties of those two samples shown completely opposite results. The surface area, pore volume and pore size were greatly improved by double P123 composition, in contrary, with a tribble P123 input, pore volume and pore size dropped dramatically to a relevant low level. The possible explanation of this phenomenon was that excessive P123 not only did not form more micelles as expected but hindered the subsequent hydrolysis and condensation of TEOS to form mesoporous silica.

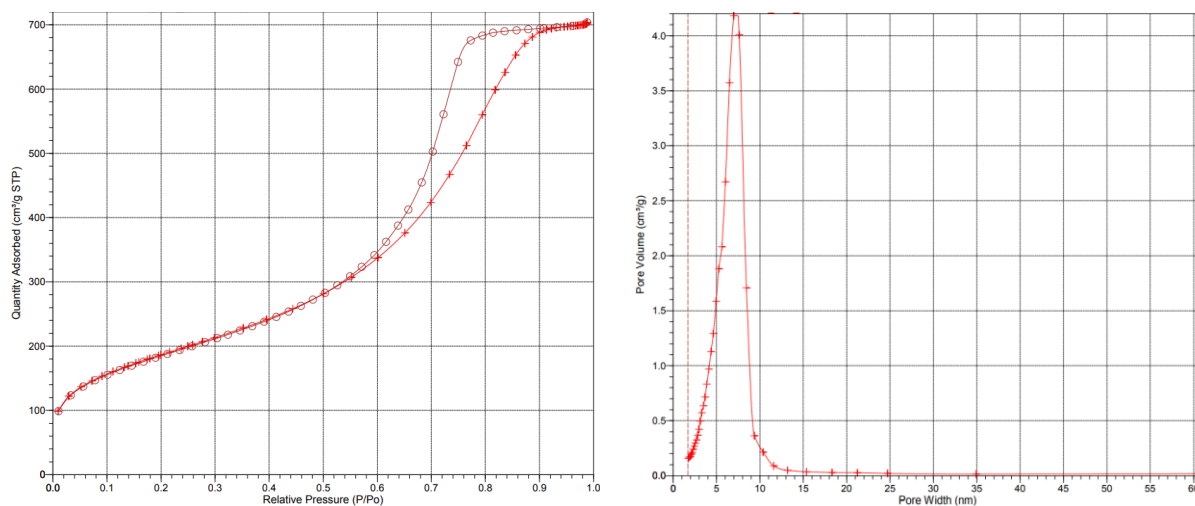
Physical properties of each silica samples were summarized in

5. RESULT AND DISCUSSION

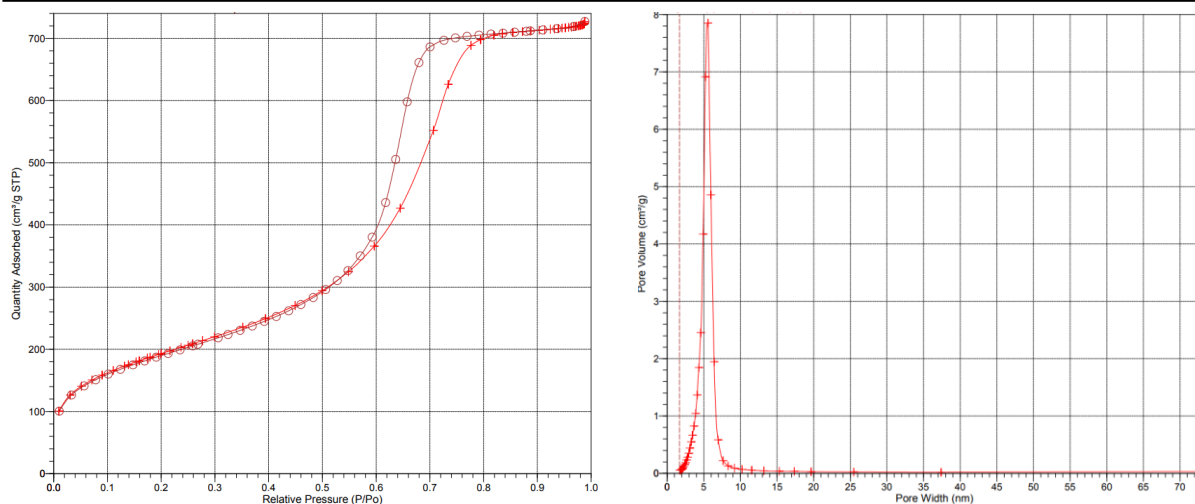
Table 5. Figure 19 shown the N₂ adsorption–desorption isotherm and pore size distribution curve demonstrated that all silica samples synthesized for structure tuning were mesoporous with a narrow pore distribution.

Table 5: Physical properties of synthesized mesoporous silica samples

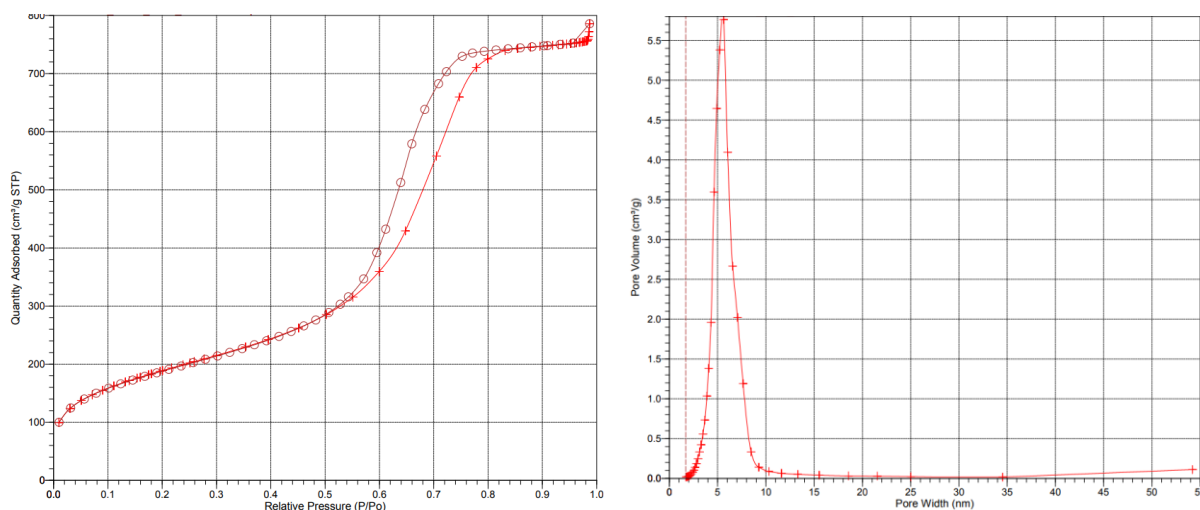
	Surface arer _{BET} (m ² /g)	Pore volume (cm ³ /g)	Pore size (nm)
40°C_SiO ₂ _1''P123_1/6CTAB	668	1.03	5.5
40°C_SiO ₂ _1''P123_1/3CTAB	690	1.09	5.1
80°C_SiO ₂ _1''P123_1/6CTAB	674	1.18	5.5
80°C_SiO ₂ _1''P123_1/3CTAB	672	1.24	5.8
80°C_SiO ₂ _2''P123_1/3CTAB	707	1.47	6.6
80°C_SiO ₂ _3''P123_1/3CTAB	703	1.02	4.7



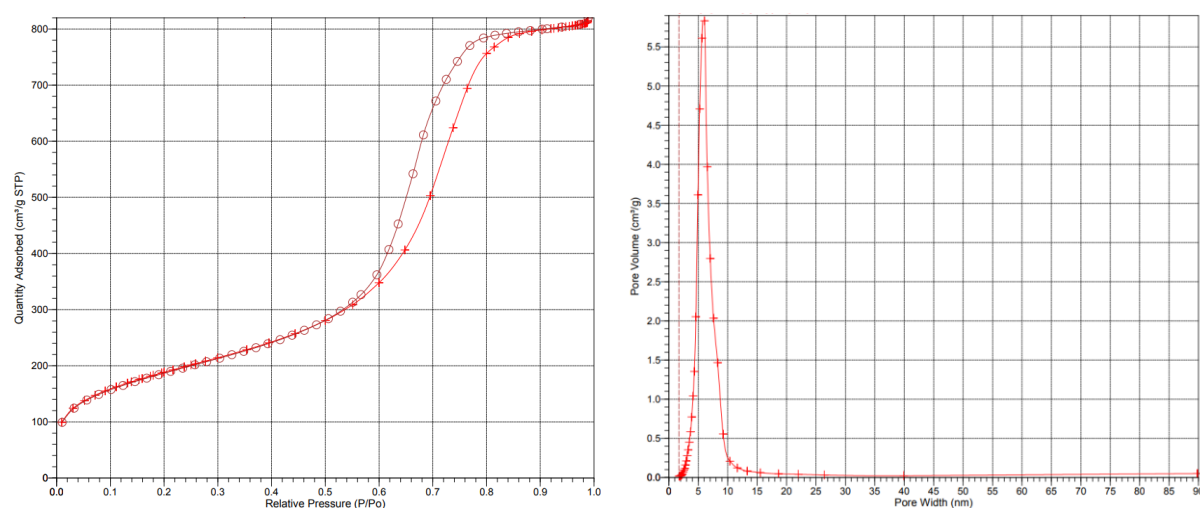
(a) 40°C_Mesoporous silica samples_1''P123_1/6CTAB



(b) 40°C_Mesoporous silica samples_1"P123_1/3CTAB

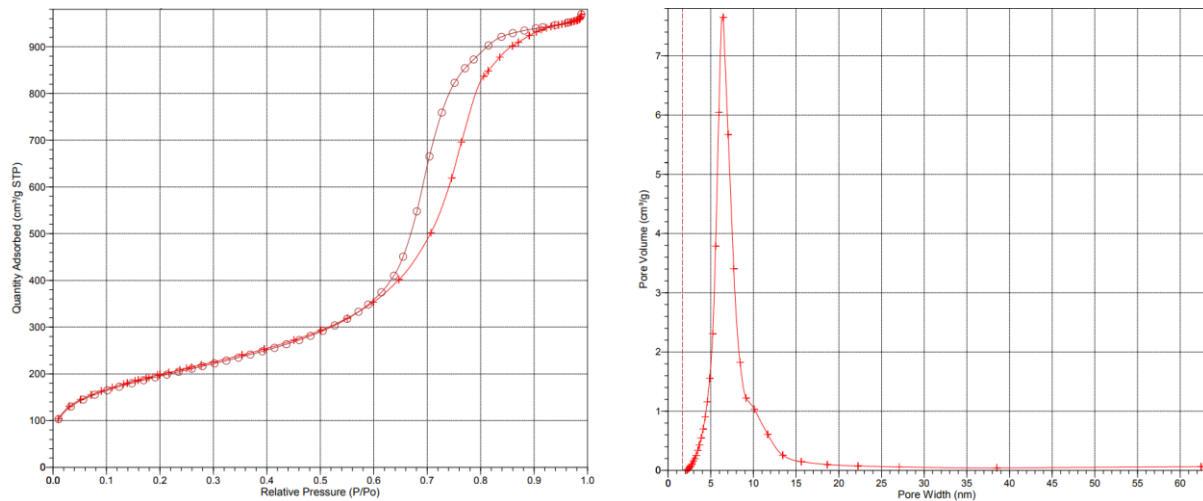


(c) 80°C_Mesoporous silica samples_1"P123_1/6CTAB

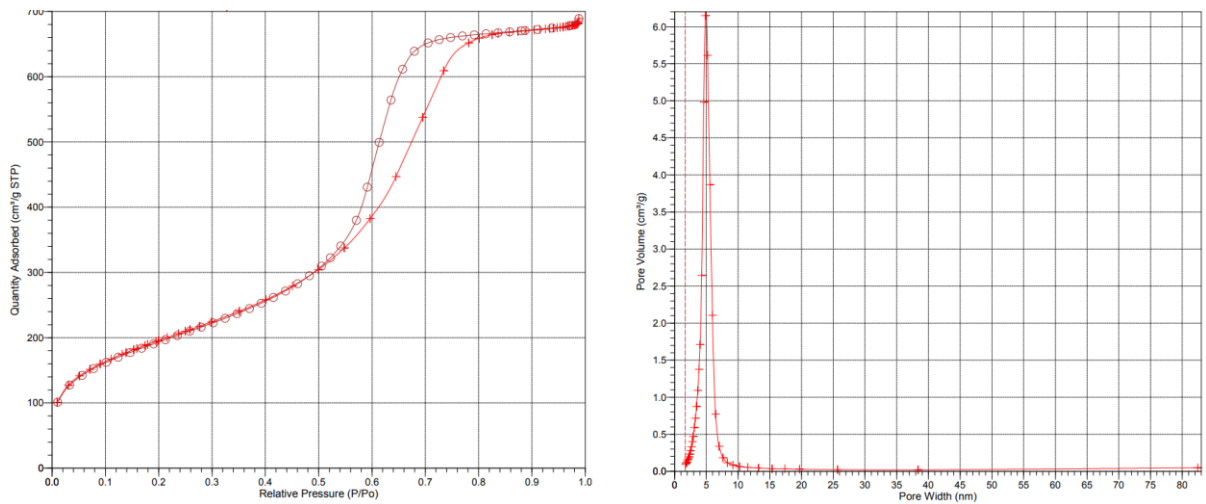


(d) 80°C_Mesoporous silica samples_1"P123_1/3CTAB

5. RESULT AND DISCUSSION



(e) 80°C_Mesoporous silica samples_2"P123_1/3CTAB



(f) 80°C_Mesoporous silica samples_3"P123_1/3CTAB

Figure 19: Isotherm Linear Plot and BJH Desorption $dV/d\log(w)$ Pore Volume of silica samples synthesized with different solutions and temperature

5.1.2. Morphology studies

Scanning electron microscopy (SEM) images of silica samples are shown in Figure 20. It can be seen that silica adsorbents presented a non-monodispersed spherical morphology with sizes from 4 to 10 μm . Aggregation existed with all samples, but it is not much critical for the synthesis of this thesis studies, as a follow-up work of this research is a pilot test run with pellets in much large sizes.

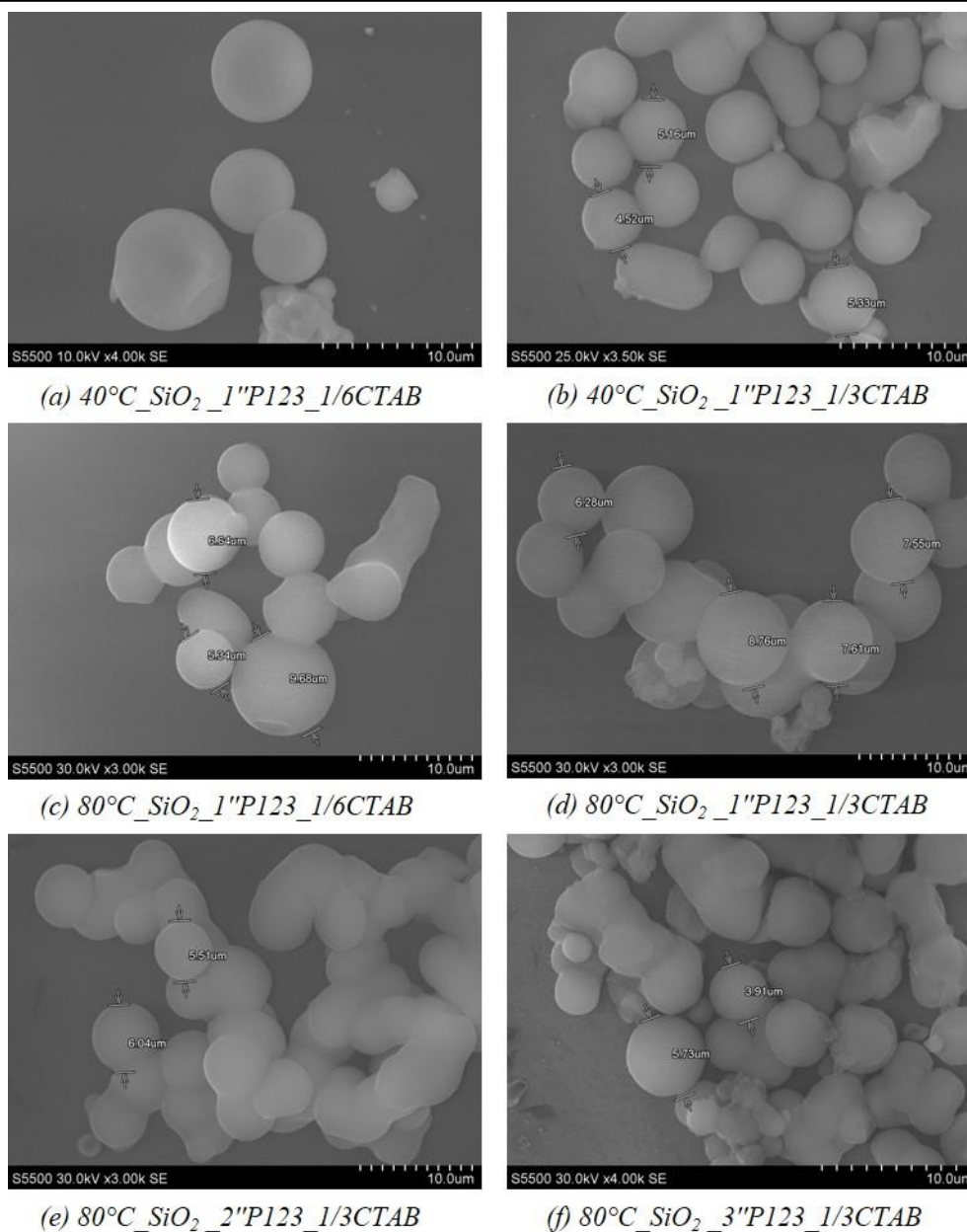


Figure 20: SEM images of silica samples synthesized with different solutions and temperature

5.1.3. Targeted samples chosen for CO₂ adsorption performance tests

As the mesoporous silica of high pore volume with narrow distribution was expected as the targeted samples chosen for followed CO₂ adsorption performance in this study, two samples chosen finally were 80°C_SiO₂_1"P123_1/3CTAB and 80°C_SiO₂_2"P123_1/3CTAB. Yield of those two mesoporous silicas was calculated as per the mass change ratio before and after calcination, which were approximately 55 % and 62%, respectively. The silica samples were denoted as PEI_SiO₂_Vp1.2 and PEI_SiO₂_Vp1.5 according to the porosity.

5.2. CO₂ adsorption performance of PEI-modified mesoporous silica samples

Once the target samples were determined, the selected mesoporous silica support materials was impregnated by PEI to preferred concentration. According to the pore volume of target support samples at 1.2 and 1.5 cm³/g, the amine weight percentage chosen for loading was set up in a range of 30 to 60 wt.% (the maximum amine contents can be added in synthesized silica support for this thesis studies).

CO₂ adsorption performance of PEI-modified SiO₂ samples were analysed by using TGA as methods described in Chapter 4.3.3. To comprehensively investigate on their CO₂ capture capability, this study adopted two different CO₂ adsorption / desorption operating conditions, namely ‘Mild conditions’ and ‘Harsh conditions’. Table 6 listed relevant parameters of the two operating conditions, respectively.

Table 6: CO₂ adsorption / desorption conditions test via TGA

	Adsorption			Desorption			Ads./ Des. Cycles
	CO ₂ (vol. %)	Temp. (°C)	Duration (min)	N ₂ (vol. %)	Temp. (°C)	Duration (min)	
Mild conditions	5	75	100	100	75	100	2
	5	75	10	100	75	10	20
Harsh conditions	5	75	100	100	120	100	10

5.2.1. CO₂ uptake and stability of PEI_Vp1.2 silica samples

The experimental curves presented in regard to the weight change with time of the PEI_Vp1.2 silica samples under mild conditions is shown in Figure 21. Experiments were carried out during 20 h in a combination of two protocols differentiated by contact time between adsorption / desorption gas and solid sorbents. Four different PEI_Vp1.2 samples modified were tested. The number given before PEI is donated as the weight percentages of PEI impregnated to silica supports, for instance 30PEI means that the amine contents in total solid sorbents is 30 wt.%.

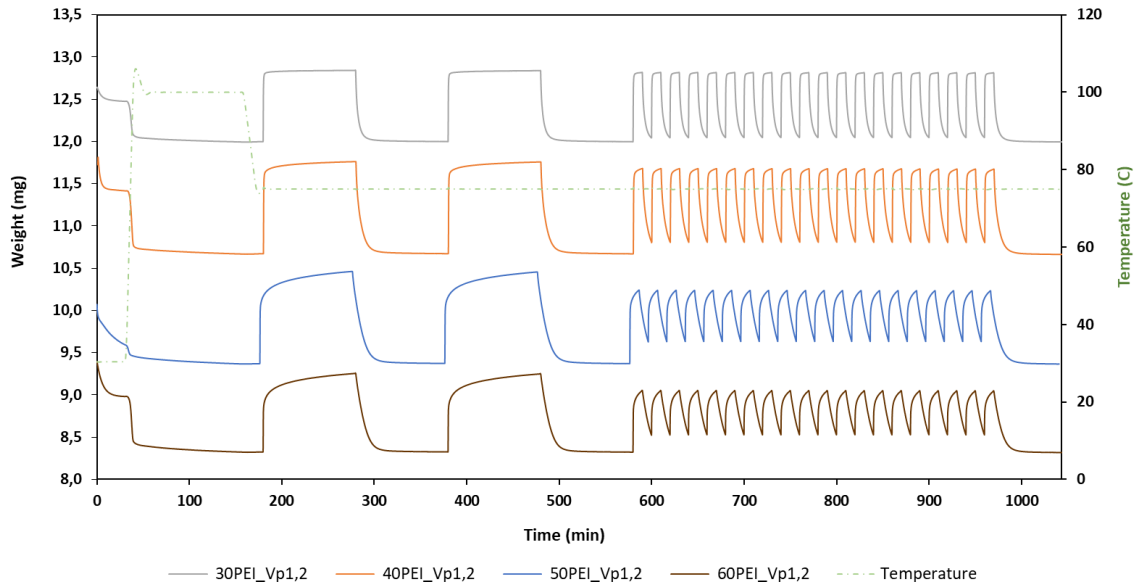


Figure 21: CO₂ capture performance analysis of PEI_SiO₂_Vp1.2 under mild conditions

The CO₂ adsorption capacities of each cycle related to varied PEI_Vp1.2 were calculated as per gram sorbent and per gram PEI, as referred to determine the optimum and practical CO₂ uptake of each PEI-modified mesoporous silica material, respectively. For details, please refer to below Table 7, Table 8, Table 9 and Table 10, Stability of each sample with 19 cycles adsorption / desorption was listed as well.

5. RESULT AND DISCUSSION

Table 7: CO₂ uptake and stability of 30PEI_Vp1.2 in mild adsorption / desorption condition

Samples: 30 wt.% PEI-modified mesoporous silica with pore volume at 1.2 cm³/g

Cycle sequence (#)	Ads./Des. Time (min)	Ads./Des. Temperature (°C)	CO ₂ adsorption capacity		Stability (%)
			mmol/g Sorbents	mmol/g PEI	
1	100 / 100	75 / 75	1.597	5.324	-
2			1.588	5.294	-
1	10 / 10	75 / 75	1.550	5.167	-
2			1.460	4.866	100.00
3			1.455	4.850	99.66
4			1.453	4.843	99.53
5			1.452	4.839	99.44
6			1.450	4.833	99.33
7			1.450	4.834	99.34
8			1.450	4.833	99.33
9			1.449	4.829	99.23
10			1.448	4.827	99.20
11			1.448	4.828	99.21
12			1.448	4.826	99.17
13			1.448	4.825	99.16
14			1.448	4.825	99.16
15			1.446	4.821	99.08
16			1.446	4.821	99.08
17			1.446	4.821	99.08
18			1.446	4.820	99.05
19			1.446	4.819	99.04
20			1.444	4.814	98.94

Table 8: CO₂ uptake and stability of 40PEI_Vp1.2 in mild adsorption / desorption condition

Samples: 40 wt.% PEI-modified mesoporous silica with pore volume at 1.2 cm³/g

Cycle sequence (#)	Ads./Des. Time (min)	Ads./Des. Temperature (°C)	CO ₂ adsorption capacity		Stability (%)
			mmol/g Sorbents	mmol/g PEI	
1	100 / 100	75 / 75	2.317	5.793	-
2			2.307	5.768	-
1	10 / 10	75 / 75	2.147	5.367	-
2			1.849	4.623	100.00
3			1.844	4.611	99.74
4			1.842	4.604	99.59
5			1.840	4.601	99.52
6			1.939	4.599	99.47
7			1.839	4.596	99.42
8			1.838	4.594	99.38
9			1.837	4.593	99.34
10			1.837	4.593	99.34
11			1.836	4.591	99.31
12			1.836	4.589	99.26
13			1.834	4.585	99.18
14			1.835	4.587	99.22
15			1.834	4.586	99.19
16			1.834	4.584	99.16
17			1.833	4.583	99.14
18			1.833	4.584	99.15
19			1.833	4.583	99.14
20			1.832	4.581	99.09

5. RESULT AND DISCUSSION

Table 9: CO₂ uptake and stability of 50PEI_Vp1.2 in mild adsorption / desorption condition

Samples: 50 wt.% PEI-modified mesoporous silica with pore volume at 1.2 cm³/g

Cycle sequence (#)	Ads./Des. Time (min)	Ads./Des. Temperature (°C)	CO ₂ adsorption capacity		Stability (%)
			mmol/g Sorbents	mmol/g PEI	
1	100 / 100	75 / 75	2.541	5.083	-
2			2.520	5.039	-
1	10 / 10	75 / 75	2.022	4.045	-
2			1.399	2.799	100.00
3			1.393	2.786	99.53
4			1.389	2.779	99.29
5			1.387	2.774	99.12
6			1.386	2.771	99.02
7			1.384	2.769	98.94
8			1.383	2.766	98.85
9			1.383	2.766	98.84
10			1.382	2.765	98.79
11			1.381	2.763	98.72
12			1.380	2.761	98.65
13			1.380	2.760	98.64
14			1.380	2.760	98.62
15			1.379	2.759	98.59
16			1.378	2.757	98.50
17			1.378	2.756	98.49
18			1.378	2.755	98.45
19			1.377	2.754	98.42
20			1.377	2.753	98.39

Table 10: CO₂ uptake and stability of 60PEI_Vp1.2 in mild adsorption / desorption condition

Samples: 60 wt.% PEI-modified mesoporous silica with pore volume at 1.2 cm³/g

Cycle sequence (#)	Ads./Des. Time (min)	Ads./Des. Temperature (°C)	CO ₂ adsorption capacity		Stability (%)
			mmol/g Sorbents	mmol/g PEI	
1	100 / 100	75 / 75	2.193	3.655	-
2			2.176	3.622	-
1	10 / 10	75 / 75	1.710	2.850	-
2			1.215	2.026	100.00
3			1.209	2.016	99.49
4			1.207	2.011	99.28
5			1.206	2.010	99.24
6			1.204	2.007	99.05
7			1.204	2.007	99.07
8			1.203	2.005	98.99
9			1.203	2.005	98.95
10			1.202	2.004	98.91
11			1.202	2.003	98.85
12			1.201	2.002	98.83
13			1.201	2.001	98.80
14			1.201	2.002	98.83
15			1.201	2.001	98.78
16			1.201	2.001	98.78
17			1.199	1.999	98.66
18			1.199	1.999	98.68
19			1.200	1.999	98.70
20			1.198	1.997	98.60

5. RESULT AND DISCUSSION

As mentioned above, under mild adsorption / desorption conditions the operation is combined by two different protocol differentiated by contact time between gas and sorbents. In principle, this was a ‘2 + 20 cycles’ CO₂ capture mode. The first two cycles operated during 100 minutes in both adsorption and desorption step. CO₂ adsorption obtained by those two cycles were used to determine the equilibrium CO₂ uptake of such PEI_SiO₂ sorbents, i.e. hereinafter referred to as ‘Optimum Capacity’.

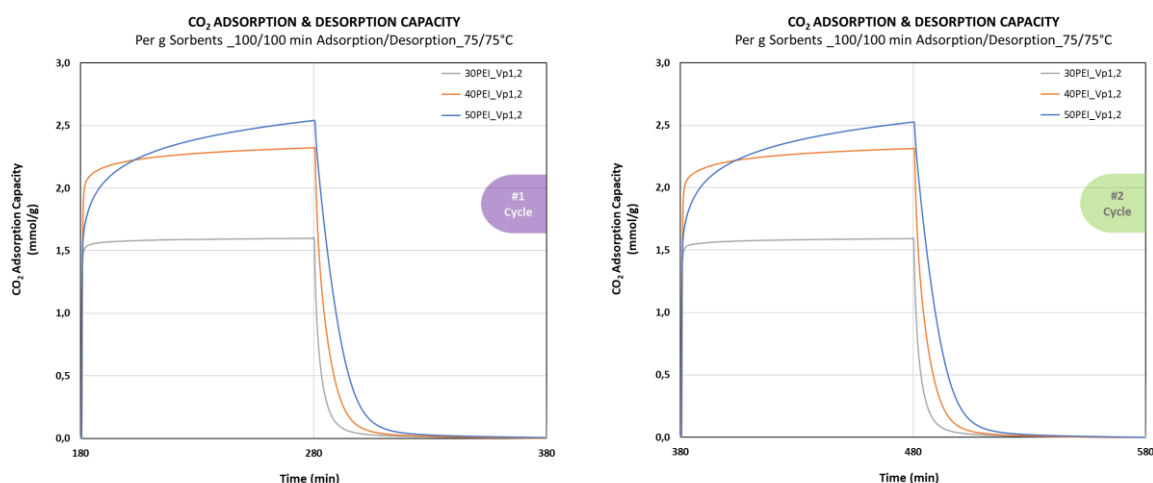


Figure 22: CO₂ uptake of the first (left) and second (right) cycle during 100 min contact time of PEI_SiO₂_Vp1.2

CO₂ adsorption and desorption uptake shown in Figure 22 demonstrated that different PEI_SiO₂_Vp1.2 samples have reached or closed to their equilibrium CO₂ adsorption capacity, meanwhile after 100 minutes desorption, samples achieved a fully regeneration that made the sorbents were free to next round CO₂ capture as shown as the second cycle above. Consideration of time-consumption to stable the machine, usually the final optimum CO₂ capacity determined for each sample was taken the value from #2 adsorption/desorption run, i.e. data in red shown in above datasheets.

Whatever in pilot instruments or actual industrial application, the contact time between gases and catalysts is too short to allow the sorbents to obtain its optimum adsorption capacity. Therefore, to get a more reliable CO₂ capacity in regard to true application environments, another 20 cycles adsorption / desorption operation was setup after then. The adsorption and desorption time were both changed from 100 minutes to 10 minutes. Figure 23 presents the first and second cycle of CO₂ adsorption / desorption for 10 minutes contact time.

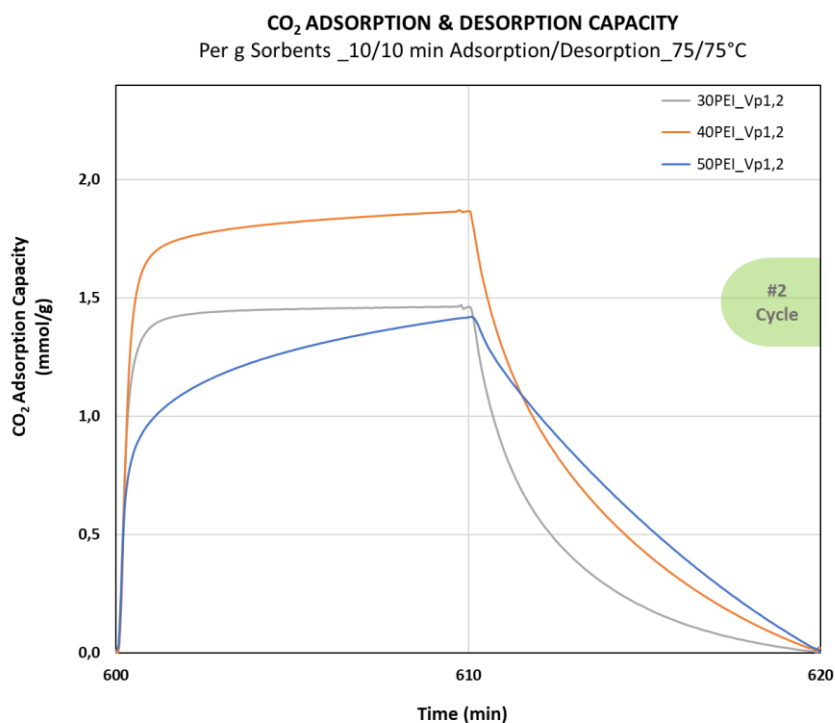
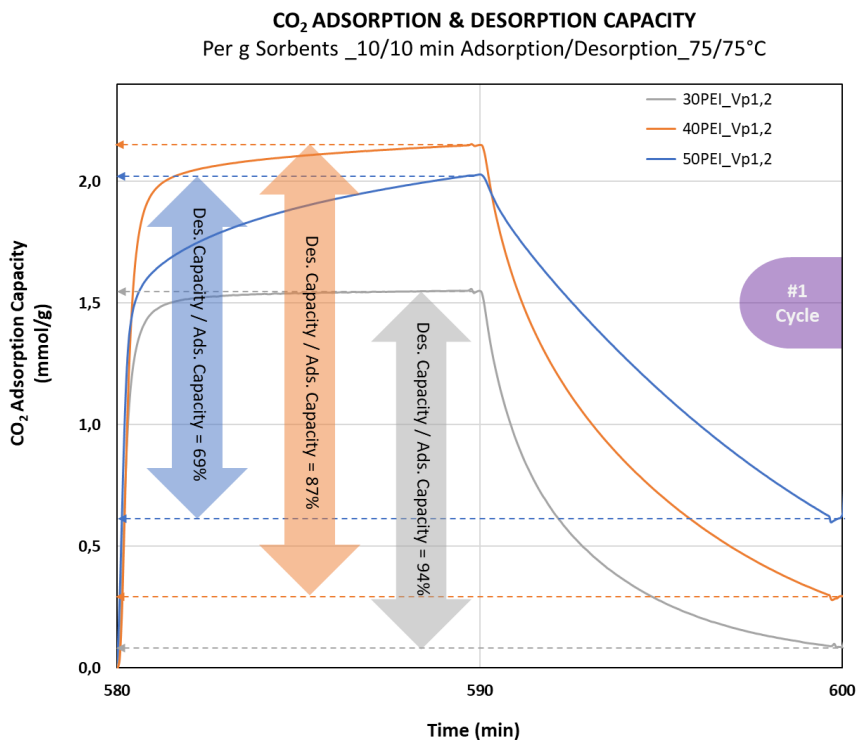


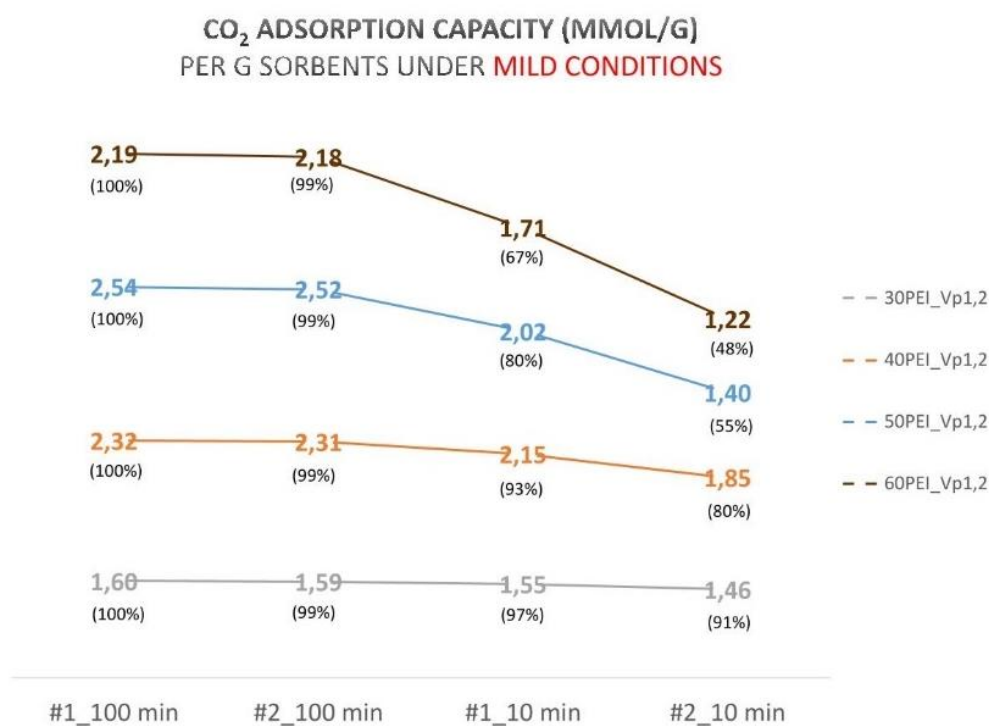
Figure 23: CO₂ uptake of the first (top) and second (bottom) cycle during 10 min contact time of PEI-SiO₂-Vp1.2

Different from the CO₂ capture performed with longer contact time, it is clear that all samples can not be regenerated completely in 10 minutes after CO₂ adsorption, as shown the #1 cycle

5. RESULT AND DISCUSSION

curve in Figure 23. The desorption capacity could reach at 94%, 87% and 69% of the adsorption capacity to samples of 30PEI_SiO₂_Vp1.2, 40PEI_SiO₂_Vp1.2, and 50PEI_SiO₂_Vp1.2, respectively. In other words, not all loaded PEI could react with CO₂ in a short time and be functionalized as it supposed to be. Since the second cycle, the balance was occurred between adsorption and desorption same as long contact time, because it only needed 10 minutes for regenerating the actual occupied active sites of the sorbents. Therefore, the CO₂ capacity obtained from the #2 cycle provided the ‘Practical Capacity’ of each sorbent.

Obviously, the SiO₂ impregnated with different PEI amounts have significant differences in terms of both CO₂ optimal and actual absorption capacity. Figure 24 shows the CO₂ adsorption capacities of the first two cycles with different duration. PEI loading in a range of 30 to 60 wt.% in PEI_SiO₂_Vp1.2 samples.



**CO₂ ADSORPTION CAPACITY (MMOL/G)
PER G PEI UNDER MILD CONDITIONS**

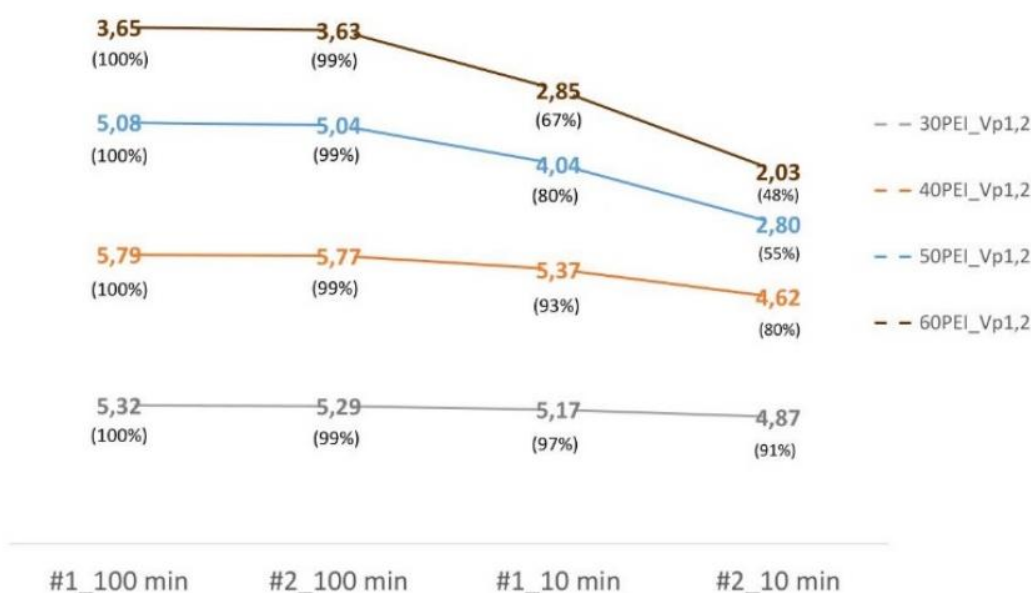


Figure 24: CO₂ uptake per gram sorbents (top) and per gram PEI (bottom) from first two cycles in different contact time of PEI_SiO₂_Vp1.2

From Figure 24 it is found that the CO₂ adsorption optimum capacity of PEI_SiO₂_Vp1.2 increases from 1.59 to 2.54 mmol/g sorbents as PEI loading increases from 30 to 50 wt.%, but there is a sharp capacity reduction on 60PEI_SiO₂_Vp1.2 to 2.19 mmol/g sorbents which was less than 40PEI_SiO₂_Vp1.2 with 2.32 mmol/g sorbents. Same trend was shown on the CO₂ adsorption practical capacities but 40PEI_SiO₂_Vp1.2 had the best CO₂ uptake of 1.85 mmol/g.

The CO₂ adsorption optimum and practical capacity calculated as per unit PEI mass gave a similar trend on change with amine mass ratio of adsorbents, except that the 40PEI_SiO₂_Vp1.2 performed best among all adsorbents at 5.77 mmol/g PEI of the optimum CO₂ capacity, whereas 30PEI_SiO₂_Vp1.2 contributed the highest practical CO₂ capacity at 4.87 mmol/g PEI. As calculation, the practical capacity was 91%, 80%, 55% and 48% of the optimum capacity, respectively, for adsorbent impregnated to 30, 40, 50 and 60 wt.% PEI amounts.

5. RESULT AND DISCUSSION

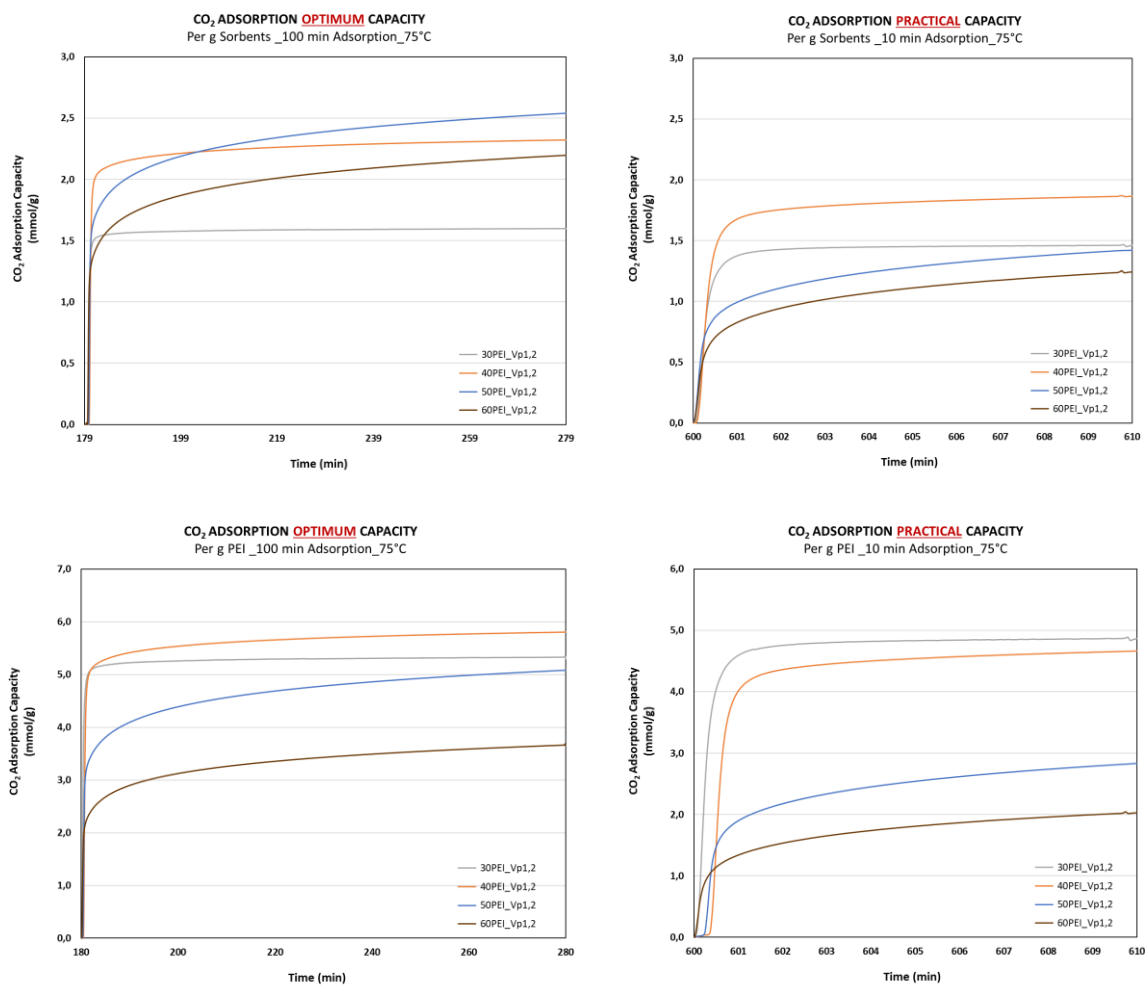


Figure 25: Adsorption performance of PEI_SiO₂_Vp1.2 with optimum and practical CO₂ capacities per gram sorbents (top) and per gram PEI (bottom)

Figure 25 explicitly shows the change in CO₂ uptake of different PEI_SiO₂_Vp1.2 adsorbents over time in a given contact duration. Combined with the physical properties studies of PEI impregnated sorbents (see Table 19), the larger leftover pore volume of sorbents, the better practical CO₂ capacity per PEI it has due to a fast-kinetic reaction between amine and CO₂ as well as good gas distribution in the pore of adsorbents. A summary of CO₂ adsorption capacities and stability of PEI_SiO₂_Vp1.2 is given in Figure 26 and Figure 27, respectively.

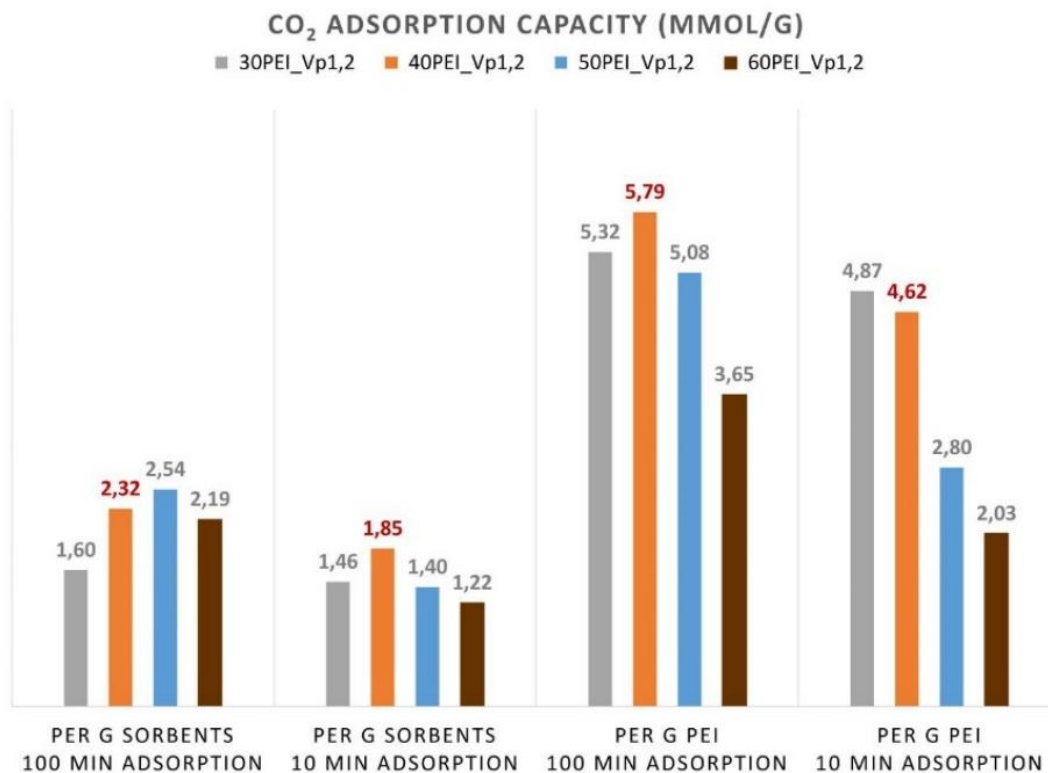


Figure 26: Comparison of the CO₂ adsorption capacity of different PEI_SiO₂_Vp1.2 samples under mild operation conditions

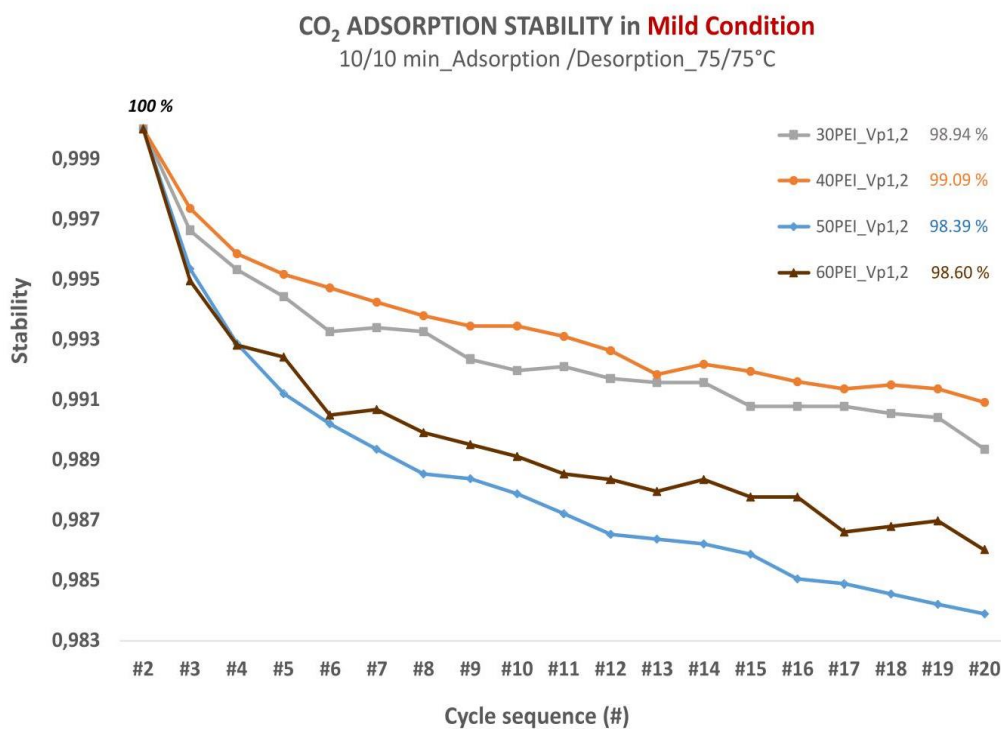


Figure 27: Comparison of the stability of different PEI_SiO₂_Vp1.2 samples under mild operation conditions

5.2.2. CO₂ uptake and stability of PEI_Vp1.5 silica samples

For a comparison purpose on the studies of CO₂ capture performances with different pore volume, same PEI loading was impregnated into PEI_SiO₂_Vp1.5 samples which varied from 30 to 50 wt.%. Based on the TGA results of PEI_SiO₂_Vp1.2, 60PEI_SiO₂ was excluded due to its poor CO₂ capture performance both on CO₂ optimum and practical capacity as well as the stability results. Figure 28 shows the experimental curves presented in regard to the weight change with time of the PEI_Vp1.5 silica samples under mild conditions.

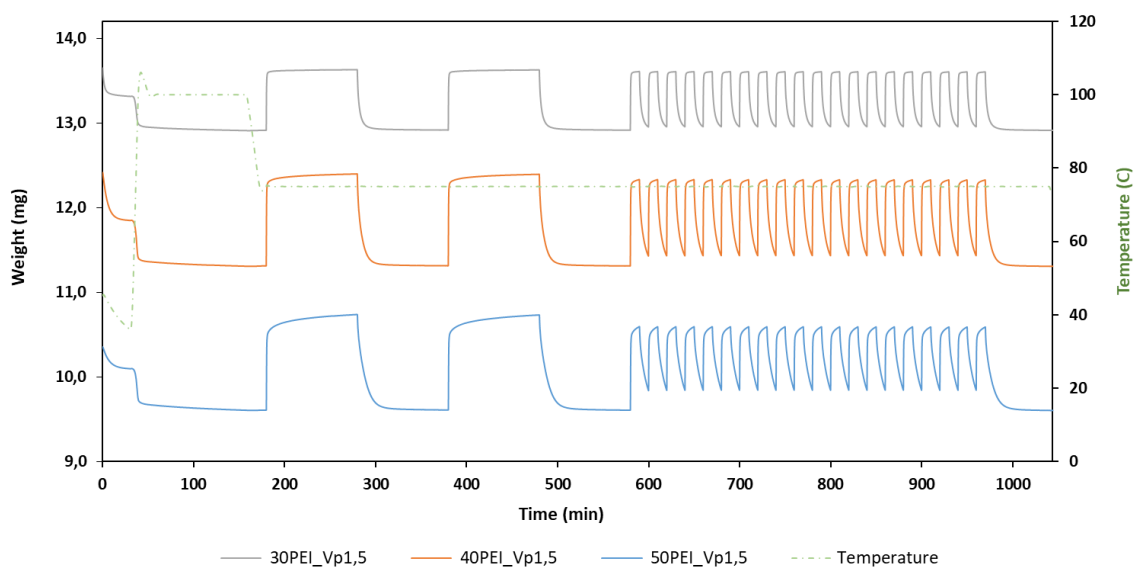


Figure 28: CO₂ capture performance analysis of PEI_SiO₂_Vp1.5 under mild conditions

Operation condition of the CO₂ capture performance analysis on PEI_SiO₂_Vp1.5 were exactly same as which implemented with PEI_SiO₂_Vp1.2 sorbents. Here below Table 11, Table 12 and Table 13 shown detailed CO₂ uptake and stability change in such '2 + 20' cycles of adsorption / desorption.

Table 11: CO₂ uptake and stability of 30PEI_Vp1.5 in mild adsorption / desorption condition

Samples: 30 wt.% PEI-modified mesoporous silica with pore volume at 1.5 cm³/g

Cycle sequence (#)	Ads./Des. Time (min)	Ads./Des. Temperature (°C)	CO ₂ adsorption capacity		Stability (%)
			mmol/g Sorbents	mmol/g PEI	
1	100 / 100	75 / 75	1.484	4.948	-
2			1.474	4.913	-
1	10 / 10	75 / 75	1.436	4.786	-
2			1.351	4.504	100.00
3			1.347	4.490	99.68
4			1.345	4.483	99.54
5			1.344	4.480	99.46
6			1.343	4.477	99.40
7			1.342	4.473	99.31
8			1.342	4.473	99.31
9			1.341	4.472	99.28
10			1.341	4.470	99.23
11			1.340	4.468	99.20
12			1.340	4.467	99.18
13			1.340	4.465	99.14
14			1.340	4.466	99.15
15			1.339	4.464	99.11
16			1.338	4.461	99.04
17			1.338	4.461	99.04
18			1.338	4.460	99.03
19			1.338	4.460	99.01
20			1.337	4.457	98.95

5. RESULT AND DISCUSSION

Table 12: CO₂ uptake and stability of 40PEI_Vp1.5 in mild adsorption / desorption condition

Samples: 40 wt.% PEI-modified mesoporous silica with pore volume at 1.5 cm³/g

Cycle sequence (#)	Ads./Des. Time (min)	Ads./Des. Temperature (°C)	CO ₂ adsorption capacity		Stability (%)
			mmol/g Sorbents	mmol/g PEI	
1	100 / 100	75 / 75	2.182	5.454	-
2			2.169	5,424	-
1	10 / 10	75 / 75	2.047	5.118	-
2			1.799	4.497	100.00
3			1.794	4.485	99.73
4			1.792	4.479	99.60
5			1.790	4.475	99.51
6			1.789	4.473	99.45
7			1.789	4.471	99.42
8			1.788	4.469	99.36
9			1.787	4.468	99.34
10			1.787	4.466	99.31
11			1.786	4.465	99.27
12			1.786	4.465	99.29
13			1.785	4.463	99.24
14			1.785	4.462	99.21
15			1.785	4.462	99.22
16			1.785	4.462	99.21
17			1.785	4.462	99.21
18			1.784	4.460	99.16
19			1.784	4.459	99.14
20			1.783	4.457	99.10

Table 13: CO₂ uptake and stability of 50PEI_Vp1.5 in mild adsorption / desorption condition

Samples: 50 wt.% PEI-modified mesoporous silica with pore volume at 1.5 cm³/g

Cycle sequence (#)	Ads./Des. Time (min)	Ads./Des. Temperature (°C)	CO ₂ adsorption capacity		Stability (%)
			mmol/g Sorbents	mmol/g PEI	
1	100 / 100	75 / 75	2.310	4.619	-
2			2.296	4.593	-
1	10 / 10	75 / 75	2.017	4.035	-
2			1.524	3.048	100.00
3			1.519	3.039	99.70
4			1.518	3.035	99.58
5			1.516	3.032	99.46
6			1.515	3.031	99.44
7			1.515	3.030	99.41
8			1.514	3.028	99.34
9			1.514	3.027	99.32
10			1.513	3.027	99.30
11			1.512	3.025	99.23
12			1.512	3.024	99.22
13			1.512	3.024	99.22
14			1.511	3.023	99.18
15			1.511	3.022	99.15
16			1.511	3.021	99.13
17			1.511	3.021	99.13
18			1.510	3.020	99.09
19			1.510	3.019	99.06
20			1.510	3.019	99.06

5. RESULT AND DISCUSSION

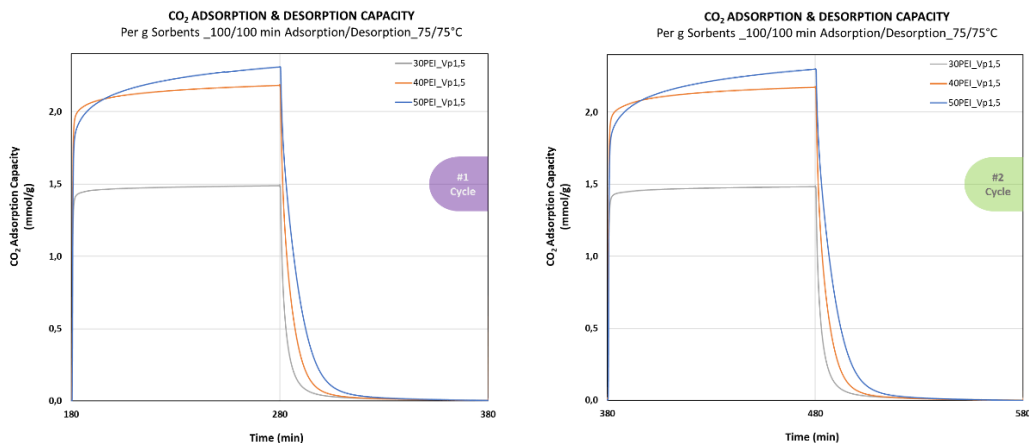
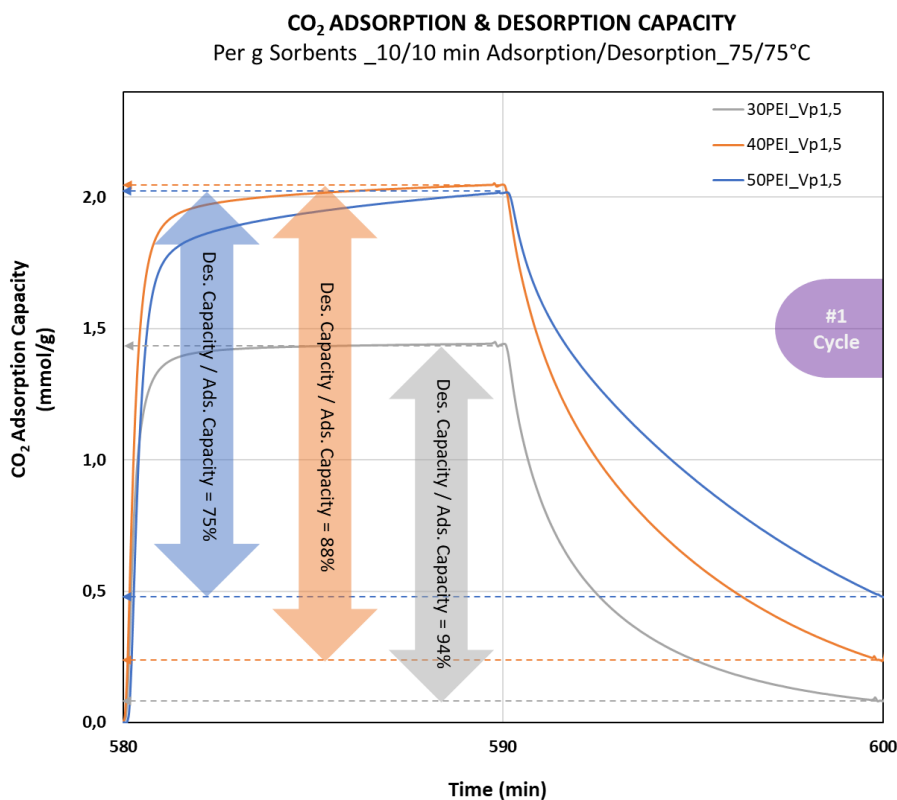


Figure 29: CO₂ uptake of the first (left) and second (right) cycle during 100 min contact time of PEI_SiO₂_Vp1.5

CO₂ adsorption and desorption uptake shown in Figure 29 also demonstrated an equilibrium CO₂ adsorption of different PEI_SiO₂_Vp1.5 samples and a fully regeneration after 100 minutes desorption. Same principle used for PEI_SiO₂_Vp1.2, the final optimum CO₂ capacity was determined for each sample by #2 adsorption/desorption run in 100 minutes, i.e. data in red shown in above datasheets.



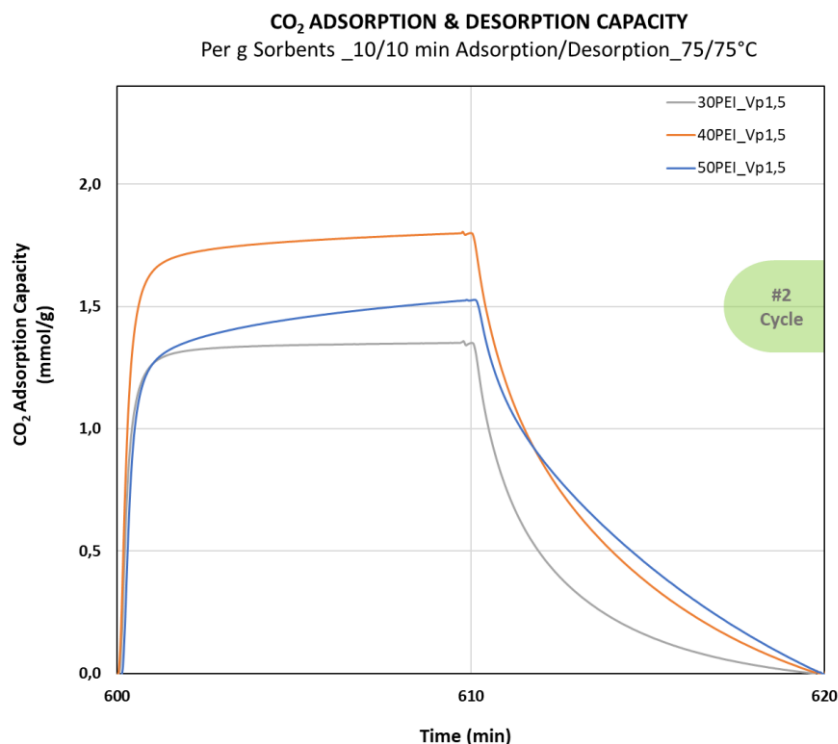


Figure 30: CO₂ uptake of the first (top) and second (bottom) cycle during 10 min contact time of PEI_SiO₂_Vp1.5

The first cycle of 20 cycles operating during 10 minutes per each adsorption / desorption shown an incomplete desorption phenomenon (see Figure 30) as same as PEI_SiO₂_Vp1.2 samples. The desorption capacity could reach at 94%, 88% and 75% of the adsorption capacity to samples of 30PEI_SiO₂_Vp1.5, 40PEI_SiO₂_Vp1.5, and 50PEI_SiO₂_Vp1.5, respectively. Compared the ratio to corresponding PEI_SiO₂_Vp1.2, there was no obvious differences on 30PEI_SiO₂ and 40PEI_SiO₂, but a 6% increasing on 50PEI_SiO₂ in regard to the regeneration degree. Due to a larger pore volume of silica supports, more pore volume available after PEI impregnation in turn to a better gas distribution during adsorption and desorption process which further led to a faster kinetics on 50PEI_SiO₂ with a better regeneration performance.

Figure 31 shows the CO₂ adsorption capacities of the first two cycles with different duration. PEI loading in a range of 30 to 50 wt.% in PEI_SiO₂_Vp1.5 samples. The CO₂ adsorption optimum capacity of PEI_SiO₂_Vp1.5 increases from 1.47 to 2.30 mmol/g sorbents as PEI loading increases from 30 to 50 wt.%. Regarding to the CO₂ adsorption practical capacities, 40PEI_SiO₂_Vp1.5 presented the best CO₂ uptake of 1.80 mmol/g sorbents.

5. RESULT AND DISCUSSION

Regarding the CO₂ adsorption optimum and practical capacity calculated as per unit PEI, the 40PEI_SiO₂_Vp1.5 was outstanding with 5.42 mmol/g PEI of the optimum CO₂ capacity, whereas shown a practical CO₂ capacity at 4.50 mmol/g PEI same as the 30PEI_SiO₂_Vp1.5. As calculation, the practical capacity was 91%, 82% and 66% of the optimum capacity, respectively, for adsorbent impregnated to 30, 40 and 50 wt.% PEI amounts.

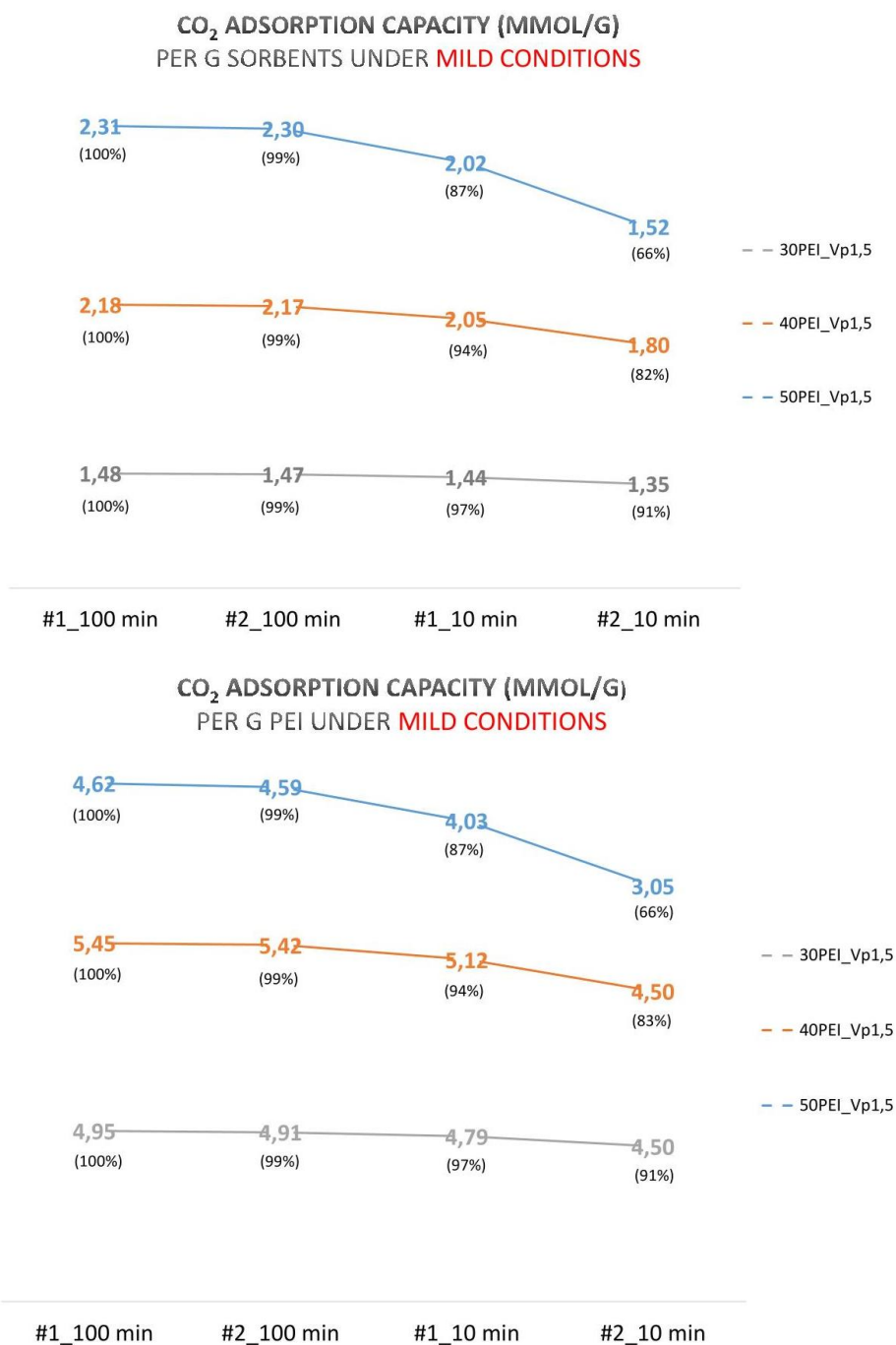


Figure 31: CO₂ uptake per gram sorbents (top) and per gram PEI (bottom) from first two cycles in different contact time of PEI_SiO₂_Vp1.2

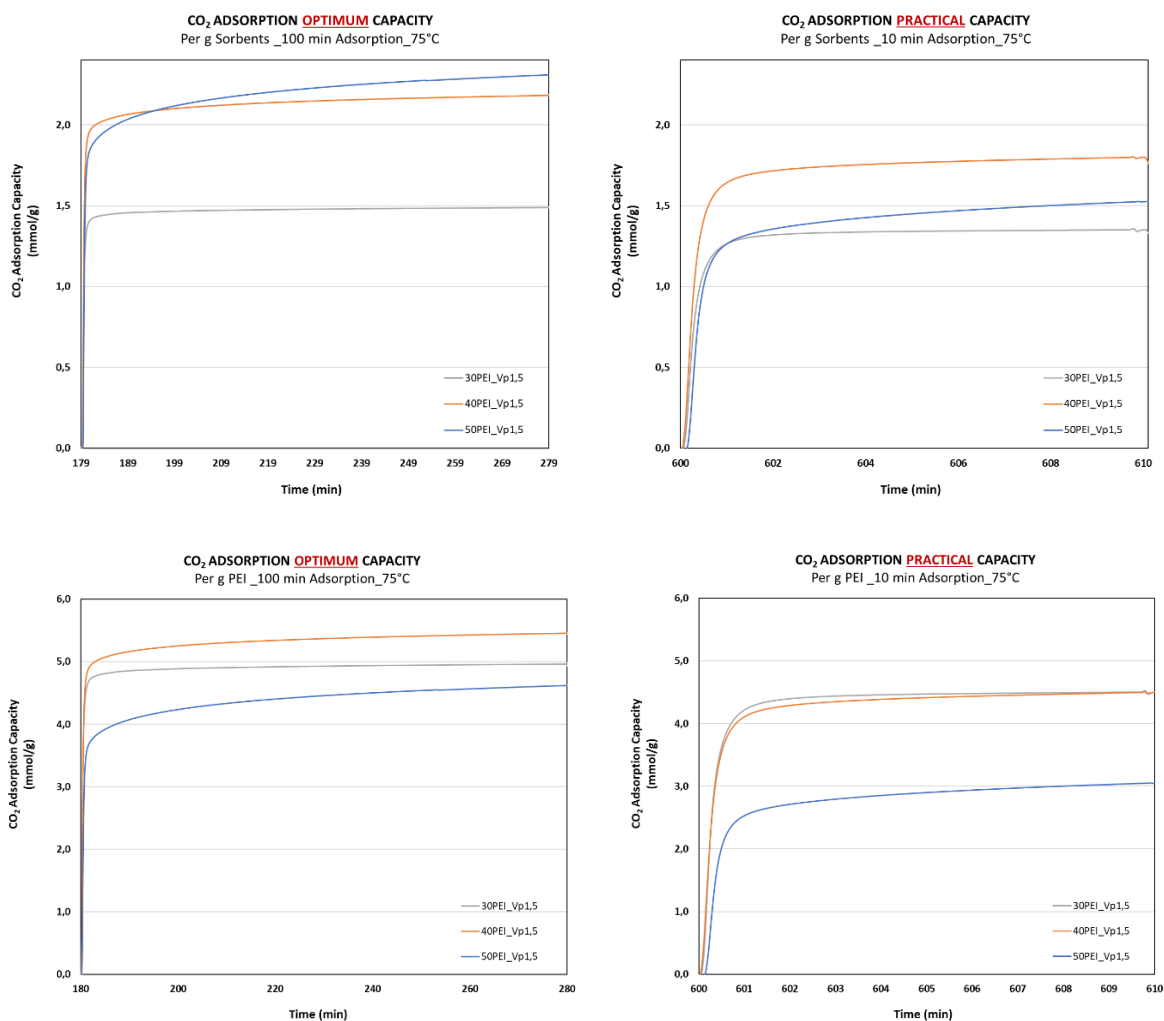


Figure 32: Adsorption performance of PEI_SiO₂_Vp1.5 with optimum and practical CO₂ capacities per gram sorbents (top) and per gram PEI (bottom)

Figure 32 explicitly shows the change in CO₂ uptake of different PEI_SiO₂_Vp1.5 adsorbents over time in a given contact duration. To be noticed that the CO₂ practical capacity on 50PEI_SiO₂_Vp1.5 was increased due to a better regeneration as discussed above. Meanwhile, 40PEI cached up to the same level as 30PEI with large pore volume supports, where it was slightly lower than 30PEI with small pore volume supports. That was contributed by more leftover space in the pore which helped on fast-kinetics reaction. A summary of CO₂ adsorption capacities and stability of PEI_SiO₂_Vp1.2 is given in Figure 33 and Figure 34, respectively.

5. RESULT AND DISCUSSION

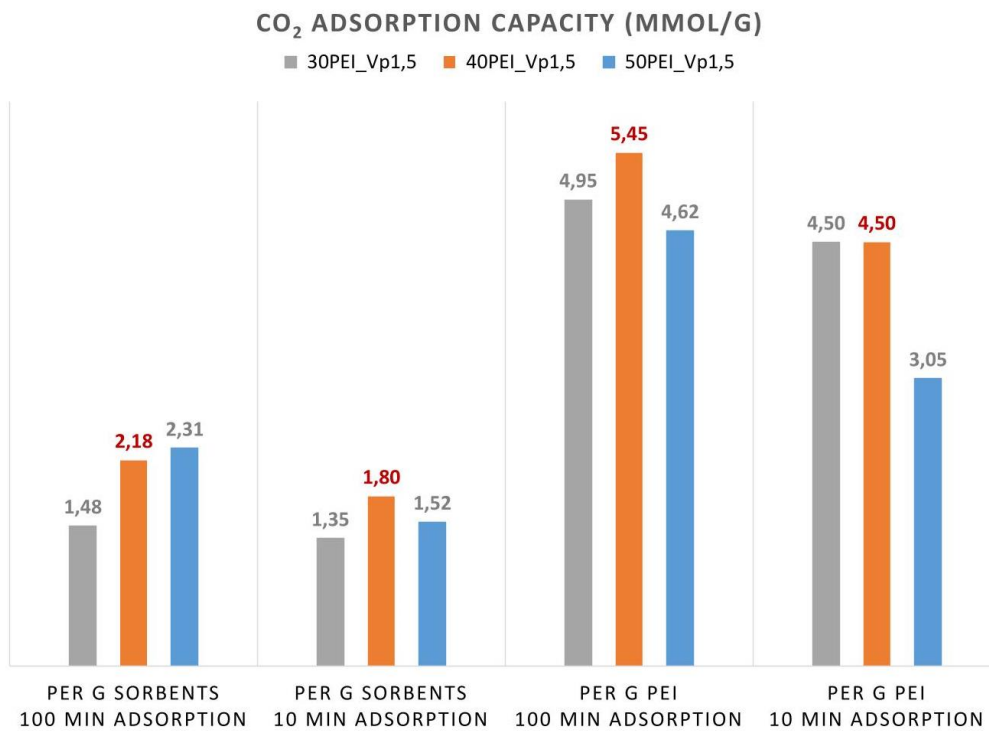


Figure 33: Comparison of the CO₂ adsorption capacity of different PEI_SiO₂_Vp1.5 samples under mild operation conditions

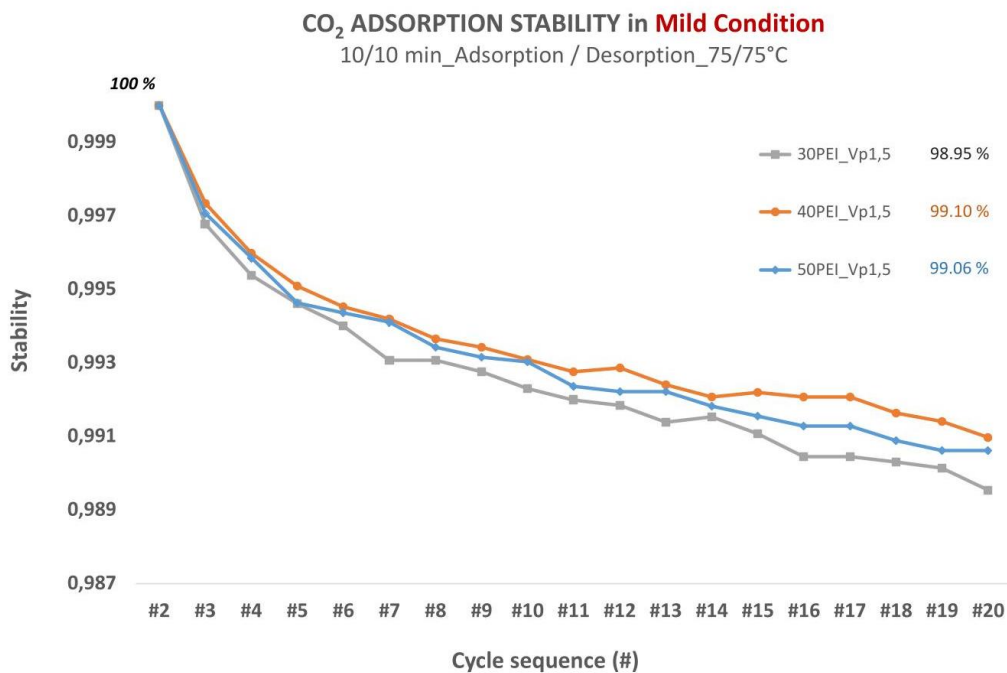


Figure 34: Comparison of the stability of different PEI_SiO₂_Vp1.5 samples under mild operation conditions

5.2.3. CO₂ uptake and stability of PEI_Vp1.5 silica samples in harsh condition

Low energy consumption is a vital target in CO₂ capture process, in a short, the adsorbed CO₂ should be desorbed easily, meanwhile the a fairly cyclic stability of the adsorbents used for the CO₂ adsorption / desorption technology is very important from practical application considerations. Normally, a loss of CO₂ capture capacity to different extents in the cyclic CO₂ adsorption / desorption runs is inevitably, one of reasons is the amine degradation closely related to the operation temperature and gas atmosphere. For this thesis study, two different operation conditions were chosen as described in Table 6. As shown in Table 14, PEI_SiO₂ sorbents synthesized in this study demonstrated a high CO₂ practical capture and high stability in 19 cycle runs under mild conditions. To further investigate their stability, PEI_SiO₂_Vp1.5 sorbents were tested again under harsh condition, i.e., high desorption temperature at 120 °C during longer gas residence time, see Figure 35. CO₂ capture performance were given with cycles in below Table 15, Table 16 and Table 17.

Table 14: Summary of the CO₂ capture practical performance with different PEI_SiO₂ sorbents under mild operation conditions in this thesis studies

	Ads./Des. Time	Ads./Des. Temp.	Stability after 19 cycles	CO ₂ adsorption practical capacity (mmol/g)	
	(min)	(°C)	(%)	Per sorbents	Per PEI
30PEI_Vp1.2	10/10	75/75	98.94	1.46	4.86
40PEI_Vp1.2	10/10	75/75	99.09	1.85	5.37
50PEI_Vp1.2	10/10	75/75	98.39	1.40	4.48
30PEI_Vp1.5	10/10	75/75	98.95	4.87	4.50
40PEI_Vp1.5	10/10	75/75	99.10	4.62	4.50
50PEI_Vp1.5	10/10	75/75	99.06	2.80	3.05

5. RESULT AND DISCUSSION

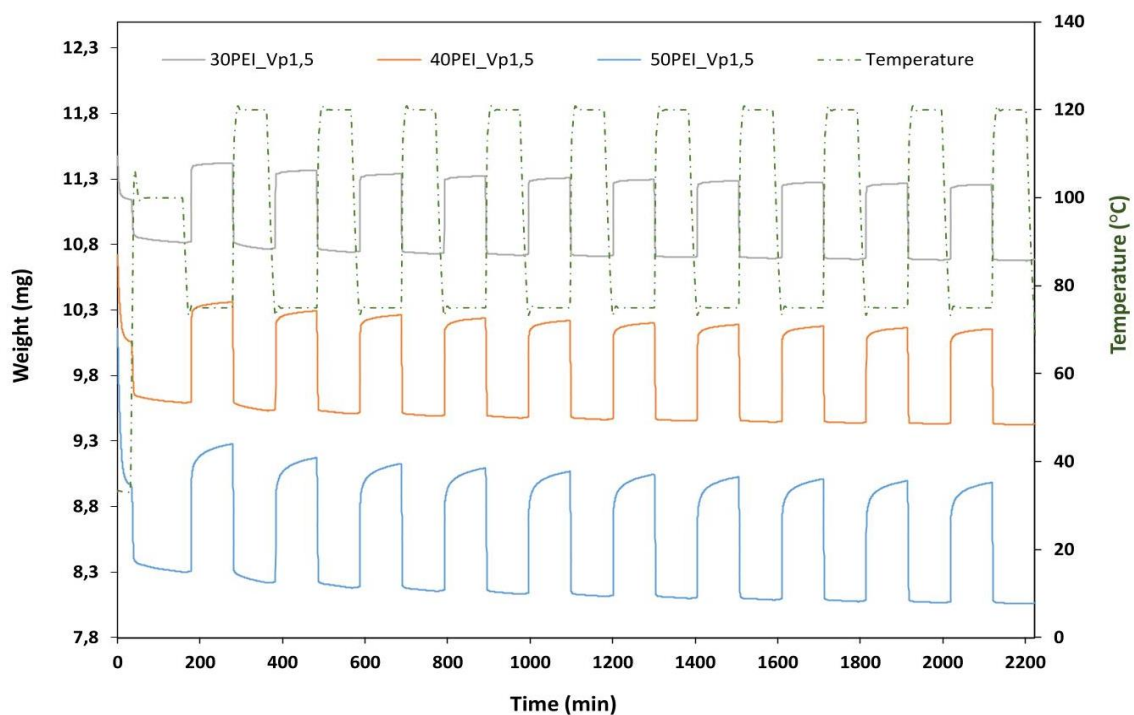


Figure 35: CO₂ capture performance analysis of PEI_SiO₂_Vp1.5 under harsh conditions

Table 15: CO₂ uptake and stability of 30PEI_Vp1.5 in hash adsorption / desorption condition

Samples: 30 wt.% PEI-modified mesoporous silica with pore volume at 1.5 cm³/g

Cycle sequence (#)	Ads./Des. Time (min)	Ads./Des. Temperature (°C)	CO ₂ adsorption capacity		Stability (%)
			mmol/g Sorbents	mmol/g PEI	
1			1.484	4.948	-
2			1.459	4.864	100.00
3			1.450	4.833	99.35
4			1.442	4.807	98.82
5			1.431	4.869	98.04
6	100 / 100	75 / 120	1.426	4.752	97.70
7			1.414	4.714	96.91
8			1.411	4.704	96.70
9			1.407	4.689	96.39
10			1.398	4.659	95.78

Table 16: CO₂ uptake and stability of 40PEI_Vp1.5 in hash adsorption / desorption condition

Samples: 40 wt.% PEI-modified mesoporous silica with pore volume at 1.5 cm³/g

Cycle sequence (#)	Ads./Des. Time (min)	Ads./Des. Temperature (°C)	CO ₂ adsorption capacity		Stability (%)
			mmol/g Sorbents	mmol/g PEI	
1			2.182	5.454	-
2			2.148	5.370	100.00
3			2.129	5.323	99.12
4			2.112	5.279	98.31
5	100 / 100	75 / 120	2.100	5.251	97.79
6			2.084	5.209	97.00
7			2.077	5.193	96.71
8			2.067	5.168	96.25
9			2.055	5.137	95.67
10			2.049	5.123	95.41

Table 17: CO₂ uptake and stability of 50PEI_Vp1.5 in hash adsorption / desorption condition

Samples: 50 wt.% PEI-modified mesoporous silica with pore volume at 1.5 cm³/g

Cycle sequence (#)	Ads./Des. Time (min)	Ads./Des. Temperature (°C)	CO ₂ adsorption capacity		Stability (%)
			mmol/g Sorbents	mmol/g PEI	
1			2.310	4.619	-
2			2.237	4.475	100.00
3			2.198	4.397	98.26
4			2.184	4.368	97.63
5	100 / 100	75 / 120	2.168	4.336	96.91
6			2.162	4.324	96.64
7			2.148	4.296	96.00
8			3.143	4.285	95.78
9			2.138	4.276	95.56
10			2.120	4.260	95.21

Same as stability study operated under mild operation conditions and experiences from experimental operation, the first cycle was usually not included in the stability study with consideration of machine interference on data reliability. Table 18 gives the summary of optimum capacity and stability after 9 cycles CO₂ adsorption / desorption operation achieved by different PEI_SiO₂ sorbents.

Table 18: Summary of the CO₂ capture optimum performance with different PEI_SiO₂ sorbents under harsh operation conditions in this thesis studies

	Ads./Des. Time	Ads./Des. Temp.	Stability after 9 cycles	CO ₂ adsorption capacity (mmol/g)	
	(min)	(°C)	(%)	Per sorbents	Per PEI
30PEI_Vp1.5	100/100	75/120	95.78	1.46	4.86
40PEI_Vp1.5	100/100	75/120	95.41	2.15	5.37
50PEI_Vp1.5	100/100	75/120	95.21	2.24	4.48

Figure 36 shows the trends of stability reduction with cycle. Both 30PEI and 40PEI silica adsorbents appeared approximately a linear decrease and reached 95.78 % and 95.41 respectively. Although the CO₂ uptake of 50PEI silica adsorbents was less competitive than other two sorbents, its stability after 9 cycle runs under harsh operation conditions resulted at 95.21%, which was almost identical to the other two sorbents. In general, cycle stability is decreased with high desorption temperature from 99% to 95% compared with value gotten under mild conditions. It makes sense as the high temperature will accelerate the amine degradations during long-term CO₂ adsorption / desorption operations. Especially, the amines do not provide the strong interaction with the supporting surface via physical impregnation, which shall lead to poor cycling stability when PEI_SiO₂ exposed under high temperature.

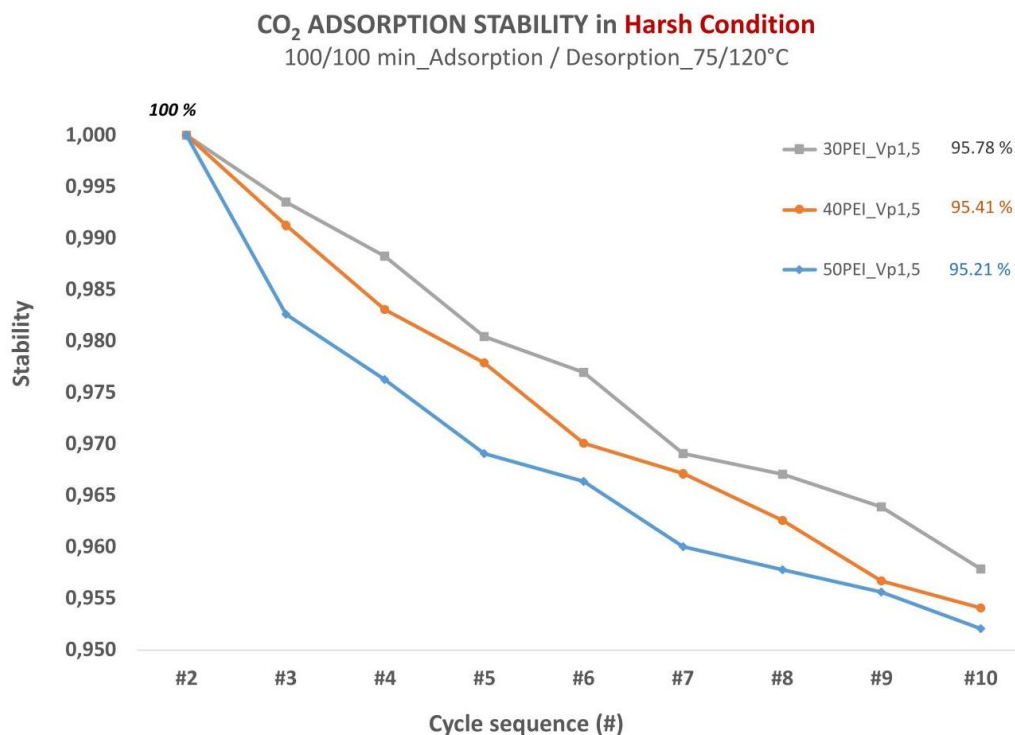


Figure 36: Comparison of the stability of different PEI_SiO₂_Vp1.5 samples under harsh operation conditions

5.3. CO₂ uptake correction as per actual PEI loading

According to the TGA test results, the CO₂ adsorption performances showed a good performance and increasing trend as amine concentration increased as per unit gram of sorbents. However, the data shown based on unit gram PEI provides an interesting and more reliable reference to evaluate the CO₂ capture performance of solid sorbents from economical perspective. Therefore, an accuracy on amine loading amounts is need.

5.3.1. Physical properties and Morphology of PEI-modified mesoporous silica

Table 19 provides the physical properties including the surface area, pore volume and pore size of silica samples after impregnated by PEI to target amine concentration. Both surface area and pore volume of PEI-modified SiO₂ shows a reduction trend as amine weight percentage increases, meanwhile the pore size of samples increased due to a pore expansion slightly with amine loading into the support sorbents. In theory, PEI (branched, Mw=600) used for wet impregnation has a density of 1,05 g/ml at 25 °C, which allowed a maximum PEI weight

5. RESULT AND DISCUSSION

percentage of 56% and 60% to SiO₂_Vp1.2 and SiO₂_Vp1.5, respectively. therefore, it is not surprising that 60PEI_SiO₂_Vp1.2 showed a nearly zero leftover pore volume and larger pore size than non-modified support materials as probably a pore broken happened because of an exceeded mass impregnation,

Table 19: Physical properties of PEI-modified mesoporous silica samples

	Surface arer_{BET} <i>(m²/g)</i>	Pore volume <i>(cm³/g)</i>	Pore size <i>(nm)</i>
SiO ₂ _Vp1.2	672	1.24	5.8
30wt.%PEI_SiO ₂ _Vp1.2	274	0.51	4.6
40wt.%PEI_SiO ₂ _Vp1.2	146	0.29	4.7
50wt.%PEI_SiO ₂ _Vp1.2	109	0.22	5.0
60wt.%PEI_SiO ₂ _Vp1.2	13	0.04	7.2
SiO ₂ _Vp1.5	707	1.47	6.6
30wt.%PEI_SiO ₂ _Vp1.5	285	0.62	5.3
40wt.%PEI_SiO ₂ _Vp1.5	157	0.36	5.5
50wt.%PEI_SiO ₂ _Vp1.5	100	0.24	5.9

Besides the physical properties check, morphology studies of PEI-modified silica samples were also implemented to assist evaluation the amine loading accuracy conducted by SEM. Figure 37 shows the morphology of the silica samples with pore volume of 1.5 cm³/g in each stages: (i) after templates removal, (ii) after PEI impregnation and (iii) after CO₂ adsorption / desorption experiments. There is almost no obvious morphological change from the images, in other words, it is difficult to evaluate the mass change of samples quantitatively from the shape modification.

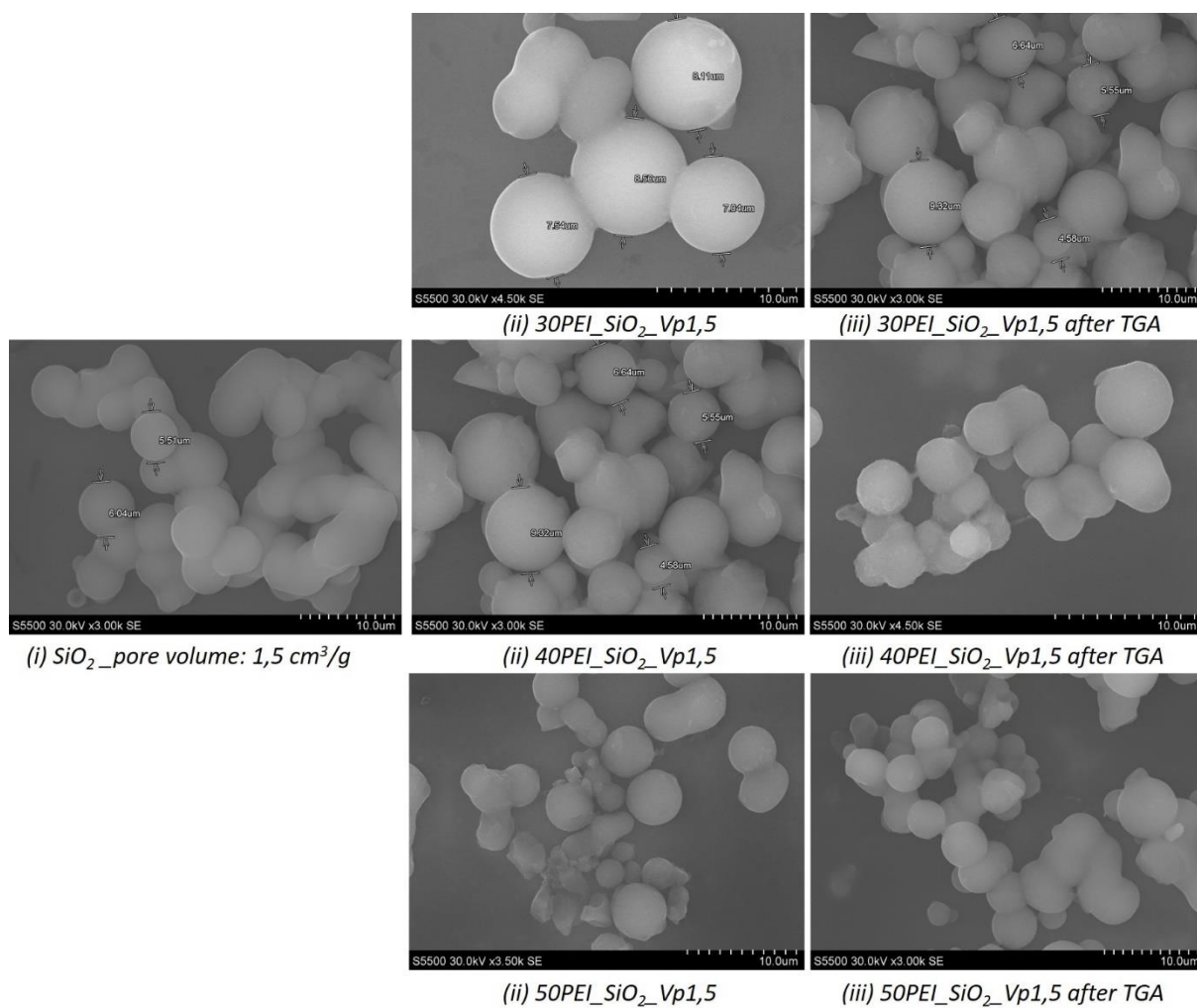


Figure 37: An example of SEM images of silica sorbents in different stage

5.3.2. Amine decomposition and remove at high temperature

As reported the amine can be decomposed and removed as volatiles at high temperatures (Xu et al., 2003), so in addition to CO_2 adsorption performance analysis, the amine loading was measured by the weight loss in the process of heating the composite to $600 \text{ }^\circ\text{C}$ after adsorption / desorption procedure by TGA in this thesis research as shown in Figure 38.

5. RESULT AND DISCUSSION

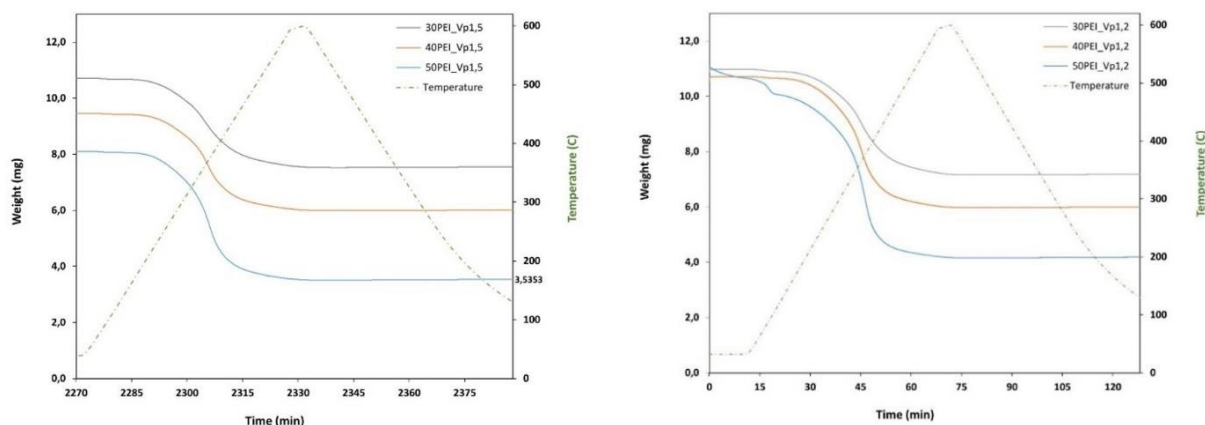


Figure 38: PEI decomposition experiments carried on different PEI-modified SiO₂ samples

According to the mass change of each sample, the actual PEI loading concentration has been calculated and summarized in Table 20. Based on actual amine weight percentages, relevant CO₂ capacity as per unit PEI was obtained as well. Table 21 and Table 22 summarized the updated optimum and practical CO₂ capacity of different amine functionalized mesoporous silica materials. Observations of the difference between theoretical and investigated PEI weight contents indicated that the physical impregnation of PEI procedure could be influenced by several infacts for example the operation temperature, stirring ratio, mixing time, drying process, human error and etc. Although all negative effects can be avoided through experimental optimization, the procedure of PEI contents check enhanced the reliability of experimental results both on the determination of the actual amine load and subsequent CO₂ capture performance research of amine functionalized silica materials.

Table 20: Summary of amine loading correction to PEI-modified SiO₂ samples

PEI-modified mesoporous silica samples	Initial sample weight (g)	Final sample weight (g)	Δ mass = Init. – Final weight (g)	PEI loading = Δ mass / Int. weight (wt. %)
30PEI_Vp1.2	10.9710	7.1863	3.7847	34
40PEI_Vp1.2	10.5657	6.0000	4.5657	43
50PEI_Vp1.2	11.0510	4.1848	6.8662	62
30PEI_Vp1.5	10.7140	7.5476	3.1664	30
40PEI_Vp1.5	9.4584	6.0110	3.4474	36
50PEI_Vp1.5	8.1010	3.5355	4.5655	56

Table 21: Updated CO₂ optimum capacities of PEI-modified SiO₂ samples

PEI-modified mesoporous silica samples	Theoretical PEI loading (wt.%)	Investigated PEI loading (wt.%)	CO ₂ adsorption OPTIMUM capacity (mmol/g PEI)	
			TGA	Correction
			30PEI_Vp1.2_75°C	30
40PEI_Vp1.2_75°C	40	43	5.77	5.37
50PEI_Vp1.2_75°C	50	62	5.04	4.06
30PEI_Vp1.5_75°C	30	30	4.91	4.91
40PEI_Vp1.5_75°C	40	36	5.42	6.02
50PEI_Vp1.5_75°C	50	56	4.59	4.10
30PEI_Vp1.5_120°C	30	30	4.86	4.86
40PEI_Vp1.5_120°C	40	36	5.37	5.97
50PEI_Vp1.5_120°C	50	56	4.48	4.00

Table 22: Updated CO₂ practical capacities of PEI-modified SiO₂ samples

PEI-modified mesoporous silica samples	Theoretical PEI loading (wt.%)	Investigated PEI loading (wt.%)	CO ₂ adsorption PRACTICAL capacity (mmol/g PEI)	
			TGA	Correction
			30PEI_Vp1.2	30
40PEI_Vp1.2	40	43	4.62	4.30
50PEI_Vp1.2	50	62	2.80	2.26
30PEI_Vp1.5	30	30	4.50	4.91
40PEI_Vp1.5	40	36	4.50	5.00
50PEI_Vp1.5	50	56	3.05	2.72

5.4. CO₂ capture performances comparison between different samples

5.4.1. CO₂ adsorption performance of PEI_SiO₂ samples with different mesoporous structure

Figure 39 shows the CO₂ adsorption optimum capacity as per unit amine of different PEI_SiO₂ samples and desorption temperature. It is found that the PEI_SiO₂ with 40 wt.% amine loading

presented the highest CO₂ capacity in both large and small pore volume of support mesoporous silica supports. The CO₂ adsorption optimum capacity of 40PEI_SiO₂_Vp1.2 and 40PEI_SiO₂_Vp1.5 was 5.37 and 6.02 mmol/g PEI, respectively. With the change of porosity from 1.2 to 1.5 cm³/g of mesoporous silica sorbents, the CO₂ optimum capacity increases by 12%. Even if it was operated for a long-term in a harsh condition with high desorption temperature, the optimum capacity was maintained with slight change within an acceptable range compared with its performance under the mild operating conditions.

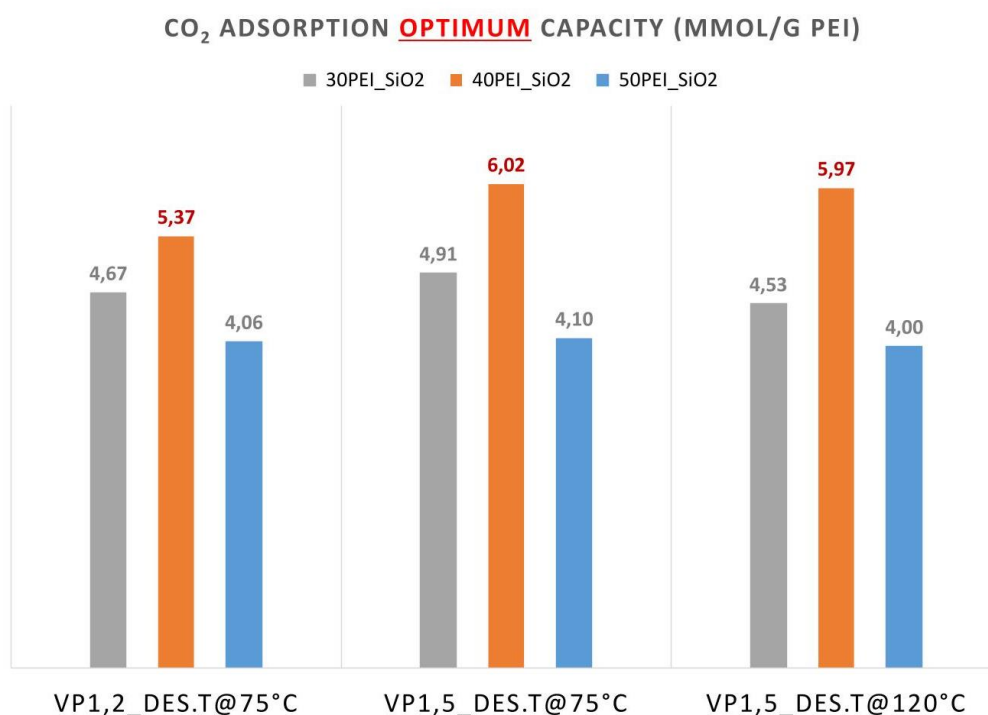


Figure 39: CO₂ optimum adsorption capacity of PEI_SiO₂ samples under different operating conditions

Refer to Figure 40, the practical CO₂ capacity and stability was illustrated, PEI_SiO₂ with 30 wt.% amine loading demonstrated a strong competitive performance nearly same as the 40 wt.% PEI_SiO₂ both within small and large porosity of silica supports. Same as the optimal capacity, With the change of porosity from 1.2 to 1.5 cm³/g of mesoporous silica sorbents, the CO₂ practical capacity increases by 14% and 16% for 30PEI_SiO₂ and 40PEI_SiO₂, respectively.

The stability study was carried out both under mild and harsh conditions with different contact time and desorption temperature. It is found that the PEI_SiO₂ with different porosity and amine loading contents all have a very high stability around 99% and 95% after adsorption / desorption

cycle operation under mild conditions and harsh conditions, respectively. There are no significant differences among them, even if the PEI_SiO₂ with 40 wt.% amine loading shown a slight advantage than others.

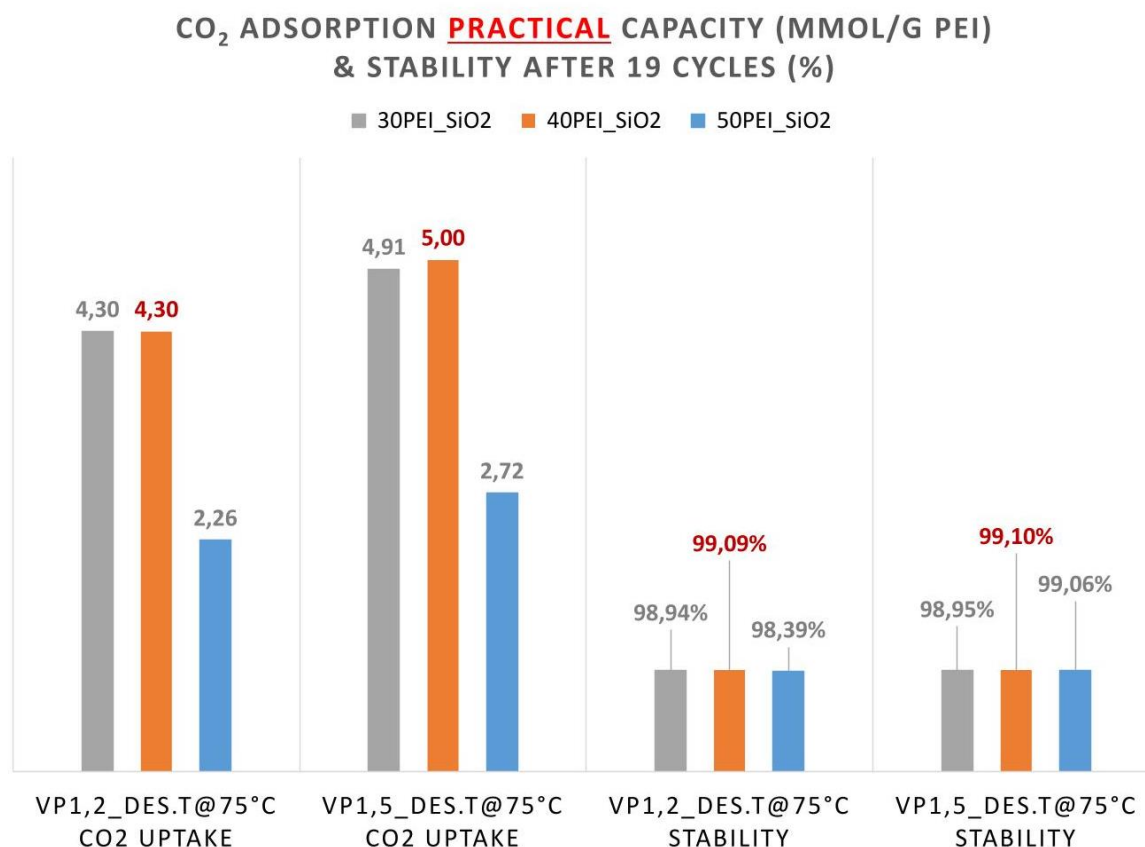


Figure 40: CO₂ practical adsorption capacity and cycle stability of PEI_SiO₂ samples with different porosity under mild conditions

5.4.2. CO₂ adsorption performance of 40PEI_SiO₂ samples compared with previous master study work

A comparison analysis on cycle stability was carried out between mesoporous silica synthesized in this thesis study and other mesoporous amine modified silica chosen from previous thesis study implemented by Siyu Wang in 2019 (Wang, 2019). As given in Table 23, the CO₂ adsorption and desorption operating conditions (including adsorption/desorption gas composition, adsorption temperature and cycle duration) were setup same, except the desorption temperature: 120 °C for this thesis study and 100 °C using in her research.

5. RESULT AND DISCUSSION

Table 23: CO₂ capture performance compared with other study for 40PEI_SiO₂ adsorbents

Samples (a): 40 wt.% PEI-modified mesoporous SiO₂_Vp1,5 (corrected with PEI loading check)

Cycle sequence (#)	Ads./Des. Time (min)	Ads./Des. Temperature (°C)	CO ₂ adsorption capacity		Stability (%)
			mmol/g Sorbents	mmol/g PEI	
1			2.182	6.060	-
2			2.148	5.967	100.00
3			2.129	5.914	99.12
4			2.112	5.866	98.31
5	100 / 100	75 / 120	2.100	5.834	97.79
6			2.084	5.788	97.00
7			2.077	5.770	96.71
8			2.067	5.742	96.25
9			2.055	5.708	95.67
10			2.049	5.692	95.41

Samples (b): 40 wt.% PEI-modified mesoporous silica from previous thesis studies in 2019

Notes:

1. Data was unavailable from original source. For comparison purpose with this thesis study, it was calculated from CO₂ uptake per g sorbents divided by PEI weight percentage.
2. Data were unavailable from original source.

Cycle sequence (#)	Ads./Des. Time (min)	Ads./Des. Temperature (°C)	CO ₂ adsorption capacity		Stability (%)
			mmol/g Sorbents	mmol/g PEI ¹	
1			n/a ²	n/a ²	-
2			1.770	4.425	100.00
3			1.718	4.288	96.89
4			1.650	4.125	93.22
5	100 / 100	75 / 100	1.630	4.075	92.09
6			1.603	4.008	90.56
7			1.576	3.940	89.04
8			1.567	3.918	88.53
9			1.533	3.833	86.61
10			1.512	3.780	85.42

Table 24: Summary of the CO₂ capture optimum performance between 40PEI_SiO₂ sorbents from this thesis studies and previous master study

	Ads./Des. Time	Ads./Des. Temp.	Stability after 9 cycles	CO ₂ adsorption capacity (mmol/g)	
	(min)	(°C)	(%)	Per sorbents	Per PEI
40PEI_Vp1.5	100/100	75/120	95.41	2.15	5.97
40PEI/20-25 Si (750 °C)	100/100	75/100	85.42	1.77	4.43

Table 24 gives the comparison of optimum capacity and stability after 9 cycles CO₂ adsorption / desorption operation achieved by different 40PEI_SiO₂ sorbents. Figure 41 shows the trends of their stability reduction with cycle. Obviously, the samples synthesized in this thesis study have much better CO₂ adsorption capacity and cycle stability, compared with previous student's work. The main reason could be due to a poor structure of solid sorbents, as shown in Table 25, which led to a serious amine loss by both leaching during impregnation and degradation in adsorption and desorption cycle runs.

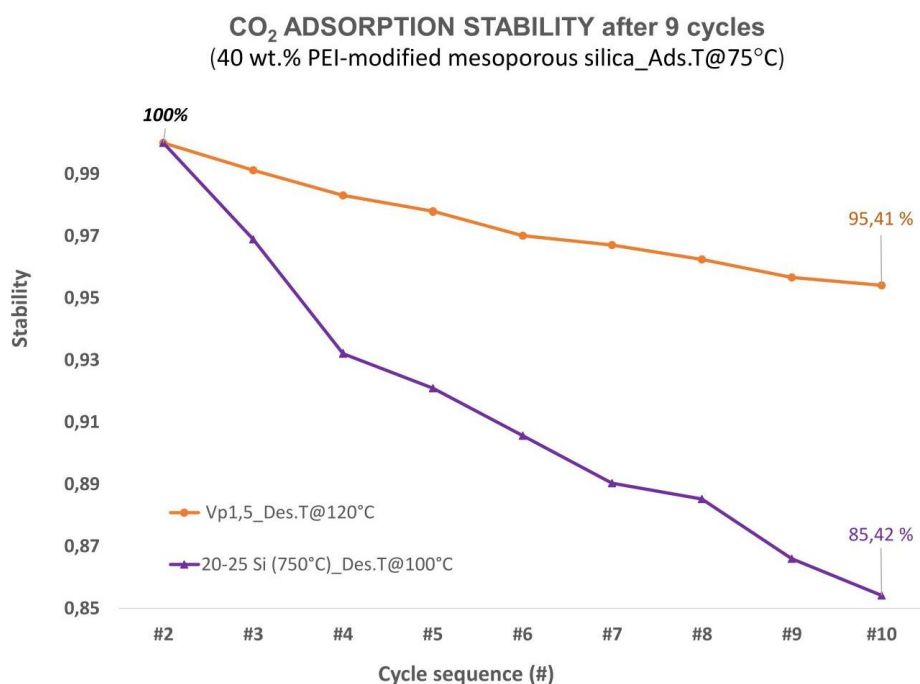


Figure 41: Comparison of the stability of 40PEI_SiO₂ samples with previous thesis study

Table 25: Physical properties of two 40 wt.% loaded silica materials

	Surface area_{BET} <i>(m²/g)</i>	Pore volume <i>(cm³/g)</i>	Pore size <i>(nm)</i>
40PEI_Vp1.5	707	1.47	6.6
40PEI/20-25 Si (750 °C)	137	0.51	13.7

6. CONCLUSION

Mesoporous silica sorbents were prepared at different synthesis conditions and studied by nitrogen adsorption / desorption and SEM techniques. The expected mesoporous silica materials of high surface area and large pore volume with narrow distribution were obtained by tuning the initial gel composition and operation condition. The optimal composition of solution was setup with a molar ratio of TEOS: 1, P123: 0.044, CTAB: 0.122, HCl: 2.67, EtOH: 9.5 and H₂O: 116, in two step aging procedure at 80 °C during 5 hours and 130 °C during 12 hours. According to characterization results, the surface area, pore volume, pore size of optimal silica sorbents synthesized in this study were 700 m²/g, 1.5 cm³/g and 7 nm. These mesoporous silica particles presented a rigid spherical morphology with sizes from 4 to 10 μm. Two mesoporous silica particles with pore volume of 1.2 and 1.5 cm³/g were chosen as the support material for amine functionalization and further utilized as adsorbent in the CO₂ capture process application.

By physical impregnation, the mesoporous silica samples with different porosity were functionalized by PEI, and the loading amount of amine varied from 30 to 60 wt.% of total sorbents. Through customized TGA procedure, the '2 + 20 cycle' mode was used for the first time to test the CO₂ optimum and practical adsorption capacity as well as the cycle stability of PEI modified mesoporous silica materials under mild conditions, which was applied in a dry adsorption gas within 5 vol.% CO₂ and sorbents' regeneration in pure N₂.

The silica sorbents with 40 wt.% PEI loading presented the highest CO₂ capacity among different PEI modified silica materials, and high porosity of silica support sorbents provided a positive impact on increasing the CO₂ uptake as well as better cycle stability. The best performance shown in this thesis study of PEI-modified mesoporous silica was 6.02 mmol/g PEI as optimum capacity and 5 mmol/g PEI as practical capacity, while the cycle stability was 99.1 % and 95.4 % under mild and harsh condition, respectively. Study taken on the comparison

6. CONCLUSION

with previous thesis work results shown a huge improvement of CO₂ capacity and cycle stability obtained by adsorbents synthesized in this thesis research.

A PEI loading check program was added after CO₂ adsorption / desorption runs to determine actual amine impregnation amount in the tested adsorbents, which was helpful on the correction of CO₂ capacity and in turns to a reliable database for further economic research on amine-modified silica sorbents in the application of CO₂ capture process.

7. FUTURE WORK

Due to COVID-19 pandemic, the parallel loading capacity of the laboratory has dropped a lot compared to usual, so many expected experiments and research works cannot be implemented in this thesis study with such time limitation. By combining the previous theoretical research and experiments results from this thesis study, research on the application of amine modified mesoporous silica sorbents in CO₂ capture process could have the following directions for the future work:

- Using pure CO₂ instead of pure N₂ as the stripping gas for a thorough regeneration to solving the potential problems both on N₂ availability and contaminant of final CO₂ products by a mixture of N₂.
- Testing with an inlet gas mixture closed to real industrial conditions. The inlet gas condition chosen for most of solid sorbents in the application of CO₂ capture was a dry mixture of CO₂ and N₂ as a simulation of flue gas from post-combustion process. The effect of other gas components and water contents in the actual flue gas on the solid sorbents shall be conducted in the further laboratory research for a comprehensive study on amine-modified silica sorbents as well.
- Optimizing amine functionality and modification methods on solid support sorbents. The type of amine chosen for silica sorbents functionalization and how to impregnate it with those solid sorbents is a vital effects on CO₂ adsorption / desorption performance for the CO₂ capture process by solid sorbents, especially on the balance between energy consumption and CO₂ capacity accepted by industrial application in a feasible and economic way.



BIBLIOGRAPHY

- ABD, A. A. & NAJI, S. Z. 2020. Comparison study of activators performance for MDEA solution of acid gases capturing from natural gas: Simulation-based on a real plant. *Environmental Technology & Innovation*, 17, 100562.
- ABD, A. A., NAJI, S. Z., HASHIM, A. S. & OTHMAN, M. R. 2020. Carbon dioxide removal through physical adsorption using carbonaceous and non-carbonaceous adsorbents: a review. *Journal of Environmental Chemical Engineering*, 104142.
- AGUDELO, N. A., ESCOBAR, S., TEJADA, J. C. & LÓPEZ, B. L. 2020. Understanding of the formation of mesocellular-like silica foam particles of nano size and its chemical surface to immobilization of *Thermomyces lanuginosus* lipase. *Microporous and Mesoporous Materials*, 294, 109948.
- AHMED, S., RAMLI, A., YUSUP, S. & FAROOQ, M. 2017. Adsorption behavior of tetraethylenepentamine-functionalized Si-MCM-41 for CO₂ adsorption. *Chemical engineering research and design*, 122, 33-42.
- ANBIA, M., HOSEINI, V. & MANDEGARZAD, S. 2012. Synthesis and characterization of nanocomposite MCM-48-PEHA-DEA and its application as CO₂ adsorbent. *Korean Journal of Chemical Engineering*, 29, 1776-1781.
- ASSOCIATION, I. E. 2015. Key trends in CO₂ emissions. *Excerpt from: CO₂ Emissions from Fuel Combustion*.
- AZMI, A. & AZIZ, M. 2019. Mesoporous adsorbent for CO₂ capture application under mild condition: A review. *Journal of Environmental Chemical Engineering*, 7, 103022.
- BEN-MANSOUR, R., HABIB, M., BAMIDELE, O., BASHA, M., QASEM, N., PEEDIKAKKAL, A., LAOUI, T. & ALI, M. 2016. Carbon capture by physical adsorption: materials, experimental investigations and numerical modeling and simulations—a review. *Applied Energy*, 161, 225-255.
- BILALIS, P., KATSIKIANNPOULOS, D., AVGEROPOULOS, A. & SAKELLARIOU, G. 2014. Non-covalent functionalization of carbon nanotubes with polymers. *Rsc Advances*, 4, 2911-2934.
- CAPLOW, M. 1968. Kinetics of carbamate formation and breakdown. *Journal of the American Chemical Society*, 90, 6795-6803.
- CASKEY, S. R., WONG-FOY, A. G. & MATZGER, A. J. 2008. Dramatic tuning of carbon dioxide uptake via metal substitution in a coordination polymer with cylindrical pores. *Journal of the American Chemical Society*, 130, 10870-10871.
- CHANGE, W. G. I. O. T. I. P. O. C. 2005. *Carbon dioxide capture and storage*, Cambridge University Press.
- CHEN, C. & BHATTACHARJEE, S. 2017. Trimodal nanoporous silica as a support for amine-based CO₂ adsorbents: Improvement in adsorption capacity and kinetics. *Applied Surface Science*, 396, 1515-1519.

- CHEN, H., LIANG, Z., YANG, X., ZHANG, Z. & ZHANG, Z. 2016. Experimental Investigation of CO₂ Capture Capacity: Exploring Mesoporous Silica SBA-15 Material Impregnated with Monoethanolamine and Diethanolamine. *Energy & Fuels*, 30, 9554-9562.
- CHESTER, A. W. & DEROUANE, E. G. 2009. *Zeolite characterization and catalysis*, Springer.
- CHOI, S., DRESE, J. H. & JONES, C. W. 2009. Adsorbent materials for carbon dioxide capture from large anthropogenic point sources. *ChemSusChem: Chemistry & Sustainability Energy & Materials*, 2, 796-854.
- CHOI, W., MIN, K., KIM, C., KO, Y. S., JEON, J. W., SEO, H., PARK, Y.-K. & CHOI, M. 2016. Epoxide-functionalization of polyethyleneimine for synthesis of stable carbon dioxide adsorbent in temperature swing adsorption. *Nature communications*, 7, 1-8.
- CHOWDHURY, S. & BALASUBRAMANIAN, R. 2016. Holey graphene frameworks for highly selective post-combustion carbon capture. *Scientific reports*, 6, 1-10.
- CINKE, M., LI, J., BAUSCHLICHER JR, C. W., RICCA, A. & MEYYAPPAN, M. 2003. CO₂ adsorption in single-walled carbon nanotubes. *Chemical physics letters*, 376, 761-766.
- D'ALESSANDRO, D. M., SMIT, B. & LONG, J. R. 2010. Carbon dioxide capture: prospects for new materials. *Angewandte Chemie International Edition*, 49, 6058-6082.
- DANKS, A. E., HALL, S. R. & SCHNEPP, Z. 2016. The evolution of 'sol-gel' chemistry as a technique for materials synthesis. *Materials Horizons*, 3, 91-112.
- DAVRAN-CANDAN, T. 2014. DFT modeling of CO₂ interaction with various aqueous amine structures. *The Journal of Physical Chemistry A*, 118, 4582-4590.
- DE CONINCK, H., STEPHENS, J. C. & METZ, B. 2009. Global learning on carbon capture and storage: A call for strong international cooperation on CCS demonstration. *Energy Policy*, 37, 2161-2165.
- DEMESSENCE, A., D'ALESSANDRO, D. M., FOO, M. L. & LONG, J. R. 2009. Strong CO₂ binding in a water-stable, triazolate-bridged metal-organic framework functionalized with ethylenediamine. *Journal of the American Chemical Society*, 131, 8784-8786.
- DEROUANE, E. G. 1998. Zeolites as solid solvents. *Journal of Molecular Catalysis A: Chemical*, 134, 29-45.
- FISHER, J. C. & GRAY, M. 2015. Cyclic Stability Testing of Aminated-Silica Solid Sorbent for Post-Combustion CO₂ Capture. *ChemSusChem*, 8, 452-455.
- FOLEY, H. C. 1995. Carbogenic molecular sieves: synthesis, properties and applications. *Microporous Materials*, 4, 407-433.
- GALARNEAU, A., CAMBON, H., DI RENZO, F. & FAJULA, F. 2001. True microporosity and surface area of mesoporous SBA-15 silicas as a function of synthesis temperature. *Langmuir*, 17, 8328-8335.
- GRAY, M., CHAMPAGNE, K., FAUTH, D., BALTRUS, J. & PENNLIN, H. 2008. Performance of immobilized tertiary amine solid sorbents for the capture of carbon dioxide. *International Journal of Greenhouse Gas Control*, 2, 3-8.
- HARLICK, P. J. & SAYARI, A. 2006. Applications of pore-expanded mesoporous silicas. 3. Triamine silane grafting for enhanced CO₂ adsorption. *Industrial & Engineering Chemistry Research*, 45, 3248-3255.

-
- HU, X. E., LIU, L., LUO, X., XIAO, G., SHIKO, E., ZHANG, R., FAN, X., ZHOU, Y., LIU, Y. & ZENG, Z. 2020. A review of N-functionalized solid adsorbents for post-combustion CO₂ capture. *Applied Energy*, 260, 114244.
- HU, Z., KHURANA, M., SEAH, Y. H., ZHANG, M., GUO, Z. & ZHAO, D. 2015. Ionized Zr-MOFs for highly efficient post-combustion CO₂ capture. *Chemical Engineering Science*, 124, 61-69.
- INSTRUMENTS, N. 2021. Scanning Electron Microscopy. <https://www.nanoscience.com/nanoscience-instruments>.
- KAPDI, S., VIJAY, V., RAJESH, S. & PRASAD, R. 2005. Biogas scrubbing, compression and storage: perspective and prospectus in Indian context. *Renewable energy*, 30, 1195-1202.
- KIM, H. R., YOON, T.-U., KIM, S.-I., AN, J., BAE, Y.-S. & LEE, C. Y. 2017. Beyond pristine MOFs: carbon dioxide capture by metal-organic frameworks (MOFs)-derived porous carbon materials. *RSC advances*, 7, 1266-1270.
- KRUK, M., JARONIEC, M., KO, C. H. & RYOO, R. 2000. Characterization of the porous structure of SBA-15. *Chemistry of materials*, 12, 1961-1968.
- KUMAR, S., MALIK, M. & PUROHIT, R. 2017. Synthesis methods of mesoporous silica materials. *Materials Today: Proceedings*, 4, 350-357.
- LEE, H. & YAVUZ, C. T. 2016. Increasing mesoporosity by a silica hard template in a covalent organic polymer for enhanced amine loading and CO₂ capture capacity. *Microporous and Mesoporous Materials*, 229, 44-50.
- LEE, S.-Y. & PARK, S.-J. 2015. A review on solid adsorbents for carbon dioxide capture. *Journal of Industrial and Engineering Chemistry*, 23, 1-11.
- LI, G., XIAO, P., XU, D. & WEBLEY, P. A. 2011. Dual mode roll-up effect in multicomponent non-isothermal adsorption processes with multilayered bed packing. *Chemical engineering science*, 66, 1825-1834.
- LIU, X., LI, L., DU, Y., GUO, Z., ONG, T. T., CHEN, Y., NG, S. C. & YANG, Y. 2009. Synthesis of large pore-diameter SBA-15 mesostructured spherical silica and its application in ultra-high-performance liquid chromatography. *Journal of Chromatography A*, 1216, 7767-7773.
- LLEWELLYN, P. L., BOURRELLY, S., SERRE, C., VIMONT, A., DATURI, M., HAMON, L., DE WEIRELD, G., CHANG, J.-S., HONG, D.-Y. & KYU HWANG, Y. 2008. High uptakes of CO₂ and CH₄ in mesoporous metal-organic frameworks mil-100 and mil-101. *Langmuir*, 24, 7245-7250.
- LOZANO-CASTELLÓ, D., CAZORLA-AMORÓS, D., LINARES-SOLANO, A. & QUINN, D. 2002. Activated carbon monoliths for methane storage: influence of binder. *Carbon*, 40, 2817-2825.
- MA, Y., QI, L., MA, J., WU, Y., LIU, O. & CHENG, H. 2003. Large-pore mesoporous silica spheres: synthesis and application in HPLC. *Colloids and Surfaces A: Physicochemical and Engineering Aspects*, 229, 1-8.
- MELÉNDEZ-ORTIZ, H. I., PUENTE-URBINA, B., CASTRUITA-DE LEON, G., MATA-PADILLA, J. M. & GARCÍA-URIOSTEGUI, L. 2016. Synthesis of spherical SBA-15 mesoporous silica. Influence of reaction conditions on the structural order and stability. *Ceramics International*, 42, 7564-7570.

- MINJU, N., NAIR, B. N., MOHAMED, A. P. & ANANTHAKUMAR, S. 2017. Surface engineered silica mesospheres—A promising adsorbent for CO₂ capture. *Separation and Purification Technology*, 181, 192-200.
- MODAK, A. & JANA, S. 2019. Advancement in porous adsorbents for post-combustion CO₂ capture. *Microporous and Mesoporous Materials*, 276, 107-132.
- NAJI, S. Z. & ABD, A. A. 2019. Sensitivity analysis of using diethanolamine instead of methyl diethanolamine solution for GASCO'S Habshan acid gases removal plant. *Frontiers in Energy*, 13, 317-324.
- OOI, Z. L., TAN, P. Y., TAN, L. S. & YEAP, S. P. 2020. Amine-based solvent for CO₂ absorption and its impact on carbon steel corrosion: A perspective review. *Chinese Journal of Chemical Engineering*, 28, 1357-1367.
- PASSÉ-COUTRIN, N., JEANNE-ROSE, V. & OUENSANGA, A. 2005. Textural analysis for better correlation of the char yield of pyrolysed lignocellulosic materials. *Fuel*, 84, 2131-2134.
- PLANT, D., MAURIN, G., DEROCHE, I. & LLEWELLYN, P. 2007. Investigation of CO₂ adsorption in Faujasite systems: Grand Canonical Monte Carlo and molecular dynamics simulations based on a new derived Na⁺-CO₂ force field. *Microporous and mesoporous materials*, 99, 70-78.
- QUANG, D. V., DINDI, A. & ABU-ZAHRA, M. R. 2017. One-step process using CO₂ for the preparation of amino-functionalized mesoporous silica for CO₂ capture application. *ACS Sustainable Chemistry & Engineering*, 5, 3170-3178.
- SAMANTA, A., ZHAO, A., SHIMIZU, G. K., SARKAR, P. & GUPTA, R. 2012. Post-combustion CO₂ capture using solid sorbents: a review. *Industrial & Engineering Chemistry Research*, 51, 1438-1463.
- SANZ-PÉREZ, E., ARENCIBIA, A., SANZ, R. & CALLEJA, G. 2016a. New developments on carbon dioxide capture using amine-impregnated silicas. *Adsorption*, 22, 609-619.
- SANZ-PÉREZ, E. S., MURDOCK, C. R., DIDAS, S. A. & JONES, C. W. 2016b. Direct capture of CO₂ from ambient air. *Chemical reviews*, 116, 11840-11876.
- SARTORI, G. & SAVAGE, D. W. 1983. Sterically hindered amines for carbon dioxide removal from gases. *Industrial & Engineering Chemistry Fundamentals*, 22, 239-249.
- SATYAPAL, S., FILBURN, T., TRELA, J. & STRANGE, J. 2001. Performance and properties of a solid amine sorbent for carbon dioxide removal in space life support applications. *Energy & Fuels*, 15, 250-255.
- SEO, M.-K. & PARK, S.-J. 2010. Influence of air-oxidation on electric double layer capacitances of multi-walled carbon nanotube electrodes. *Current Applied Physics*, 10, 241-244.
- SILVESTRE-ALBERO, J., WAHBY, A., SEPÚLVEDA-ESCRIBANO, A., MARTÍNEZ-ESCANDELL, M., KANEKO, K. & RODRÍGUEZ-REINOSO, F. 2011. Ultrahigh CO₂ adsorption capacity on carbon molecular sieves at room temperature. *Chemical Communications*, 47, 6840-6842.
- SIRIWARDANE, R. V., SHEN, M.-S. & FISHER, E. P. 2003. Adsorption of CO₂, N₂, and O₂ on Natural Zeolites. *Energy & fuels*, 17, 571-576.

-
- SIRIWARDANE, R. V., SHEN, M.-S., FISHER, E. P. & POSTON, J. A. 2001. Adsorption of CO₂ on molecular sieves and activated carbon. *Energy & Fuels*, 15, 279-284.
- SU, F., LU, C. & CHEN, H.-S. 2011. Adsorption, desorption, and thermodynamic studies of CO₂ with high-amine-loaded multiwalled carbon nanotubes. *Langmuir*, 27, 8090-8098.
- SUBAGYONO, D. J., LIANG, Z., KNOWLES, G. P. & CHAFFEE, A. L. 2011. Amine modified mesocellular siliceous foam (MCF) as a sorbent for CO₂. *Chemical Engineering Research and Design*, 89, 1647-1657.
- TARKA JR, T. J., CIFERNO, J. P. & FAUTH, D. J. CO₂ capture systems utilizing amine enhanced solid sorbents. ABSTRACTS OF PAPERS OF THE AMERICAN CHEMICAL SOCIETY, 2006. AMER CHEMICAL SOC 1155 16TH ST, NW, WASHINGTON, DC 20036 USA.
- TONG, L., YUE, T., ZUO, P., ZHANG, X., WANG, C., GAO, J. & WANG, K. 2017. Effect of characteristics of KI-impregnated activated carbon and flue gas components on Hg⁰ removal. *Fuel*, 197, 1-7.
- TREWYN, B. G., SLOWING, I. I., GIRI, S., CHEN, H.-T. & LIN, V. S.-Y. 2007. Synthesis and functionalization of a mesoporous silica nanoparticle based on the sol-gel process and applications in controlled release. *Accounts of chemical research*, 40, 846-853.
- VARGHESE, A. M. & KARANIKOLOS, G. N. 2020. CO₂ capture adsorbents functionalized by amine-bearing polymers: A review. *International Journal of Greenhouse Gas Control*, 96, 103005.
- VERDEGAAL, W. M., WANG, K., SCULLEY, J. P., WRIEDT, M. & ZHOU, H. C. 2016. Evaluation of Metal-Organic Frameworks and Porous Polymer Networks for CO₂-Capture Applications. *ChemSusChem*, 9, 636-643.
- WALTERS, M. S., EDGAR, T. F. & ROCHELLE, G. T. 2016. Regulatory control of amine scrubbing for CO₂ capture from power plants. *Industrial & Engineering Chemistry Research*, 55, 4646-4657.
- WANG, J., HUANG, L., YANG, R., ZHANG, Z., WU, J., GAO, Y., WANG, Q., O'HARE, D. & ZHONG, Z. 2014. Recent advances in solid sorbents for CO₂ capture and new development trends. *Energy & Environmental Science*, 7, 3478-3518.
- WANG, S. 2019. *SYNTHESIS OF LOW-TEMPERATURE SORBENTS FOR CO₂ CAPTURE*. Master NTNU.
- WANG, Y., ZHOU, Y., LIU, C. & ZHOU, L. 2008. Comparative studies of CO₂ and CH₄ sorption on activated carbon in presence of water. *Colloids and Surfaces A: Physicochemical and Engineering Aspects*, 322, 14-18.
- WEBB, P. A. & ORR, C. 1997. *Analytical methods in fine particle technology*, Micromeritics Instrument Corporation.
- XU, J., SHI, J., CUI, H., YAN, N. & LIU, Y. 2018. Preparation of nitrogen doped carbon from tree leaves as efficient CO₂ adsorbent. *Chemical Physics Letters*, 711, 107-112.
- XU, X., SONG, C., ANDRESEN, J. M., MILLER, B. G. & SCARONI, A. W. 2003. Preparation and characterization of novel CO₂ "molecular basket" adsorbents based on polymer-modified mesoporous molecular sieve MCM-41. *Microporous and mesoporous materials*, 62, 29-45.

- XU, X., SONG, C., ANDRESEN, J. M., MILLER, B. G. & SCARONI, A. W. 2004. Adsorption separation of CO₂ from simulated flue gas mixtures by novel CO₂ "molecular basket" adsorbents. *International journal of environmental technology and management*, 4, 32-52.
- YAMADA, H., MATSUZAKI, Y., OKABE, H., SHIMIZU, S. & FUJIOKA, Y. 2011. Quantum chemical analysis of carbon dioxide absorption into aqueous solutions of moderately hindered amines. *Energy Procedia*, 4, 133-139.
- ZHANG, H.-B., WANG, J.-W., YAN, Q., ZHENG, W.-G., CHEN, C. & YU, Z.-Z. 2011. Vacuum-assisted synthesis of graphene from thermal exfoliation and reduction of graphite oxide. *Journal of Materials Chemistry*, 21, 5392-5397.
- ZHANG, J., SINGH, R. & WEBLEY, P. A. 2008. Alkali and alkaline-earth cation exchanged chabazite zeolites for adsorption based CO₂ capture. *Microporous and Mesoporous Materials*, 111, 478-487.
- ZHANG, W., LIU, H., SUN, C., DRAGE, T. C. & SNAPE, C. E. 2014. Performance of polyethyleneimine–silica adsorbent for post-combustion CO₂ capture in a bubbling fluidized bed. *Chemical Engineering Journal*, 251, 293-303.
- ZHAO, X., CUI, Q., WANG, B., YAN, X., SINGH, S., ZHANG, F., GAO, X. & LI, Y. 2018. Recent progress of amine modified sorbents for capturing CO₂ from flue gas. *Chinese Journal of Chemical Engineering*, 26, 2292-2302.

APPENDIX

HSE RISK ASSESSMENT



ID	33436	Status	Date
Risk Area	Risikovurdering: Helse, miljø og sikkerhet (HMS)	Created	12.06.2019
Created by	Yun Liu	Assessment started	03.07.2019
Responsible	Yun Liu	Measures decided	
		Closed	

Risk Assessment:**CAT_Master student_2019_Yun Liu**

Valid from-to date:

6/12/2019 - 6/12/2022

Location:

K5-321, K5-441, K5-425, K5-447, chemical hall D

Goal / purpose

Synthesis, characterization and test of solid sorbents for low temperature CO2 capture

Background

The synthesis, characterization and test of N doped silica spheres integrated with PEI.

The polymer spheres will be synthesis by polymerization with inverse emulsion technology. The polymerization and carbonation conditions, hard templates and reactant precursors, PEI molecular loading will be studied with aiming of controlling the size and shape of spheres, porosity, pore size distribution, integration of PEI and silica surfaces. The capacity, kinetics, stability of solid will be studied at both dry and wet conditions.

Description and limitations



Silica spheres are fabricated by using resorcinol and formaldehyde as carbon precursors, colloidal nano-particle as silica source. Other chemicals used also includes span80, paraffin oil. Formaldehyde is toxic chemical. But it will be only used inside of the fume cabinet. Temperature is around 80 °C at atmosphere pressure. Synthesis procedures are done at Lab-321. Acetone for cleaning.

Calcination of silica spheres is done at Chemical hall D
Temperature is 500-700°C using air as inlet gas.

Impregnation is done at Lab-321 under ventilation.
PEI is used to impregnate into silica spheres.
Methanol is used in the impregnation process.
Temperature is 35 °C under atmospheric pressure.

TGA is done at Lab-441 and BET is done at Lab-425.
S(T)EM is done at Nano lab.

April-Mai 2020 - preventive measures towards Covid-situation:

1) Switch off procedure for MY SET-UP (No fixed setup for my lab work, but heating plates with magnetic mixer will be used during synthesis)

- Synthesis will be executed in lab K5-321
- Switch off the power of apparatus
- Leave the chemicals in the fume hood

2) Risk related to shortage of personnel in the labs:
- No special risks

3) Safety measures related to spread of covid-19 infection

- Avoid touching the face
- Disinfection before and after with ethanol on all surfaces I will in contact with (door knob – card reader with code panel – common equipment (BET 3000 and TGA-TA) keyboard – mouse – screen – desk)
- Keep 2m distance from colleagues
- Use nitrile gloves when touching shared lab set-ups and equipment
- Wash hands as often as possible

Prerequisites, assumptions and simplifications

For the synthesis of silica spheres, the stirring reactor is placed in the fume hood. The SDS of the chemicals involved in the project are presented in Attachments.
New SDS will be uploaded if using new chemicals

Attachments

SDS Formaldehyde Solution-2019.pdf
SDS Polyethylenimine-2019.pdf
SDS Resorcinol-CASNO-108-46-3.pdf
SDS Acetone.pdf
SDS Colloidal silica.pdf
SDS Span_80.pdf
SDS Methanol.pdf
SDS Paraffin_oil.pdf
SDS TEOS.pdf

References

[Ingen registreringer]

Summary, result and final evaluation


The summary presents an overview of hazards and incidents, in addition to risk result for each consequence area.

Hazard:	Hazardous chemicals used for adsorbent's synthesis and implegnation			
Incident:	Spillage of formaldehyde			
Consequence area:	Helse	Risk before measures:	Risiko after measures:	
	Ytre miljø	Risk before measures:	Risiko after measures:	
Incident:	Spillage of resorcinol			
Consequence area:	Helse	Risk before measures:	Risiko after measures:	
	Ytre miljø	Risk before measures:	Risiko after measures:	
Incident:	Spillage of PEI			
Consequence area:	Helse	Risk before measures:	Risiko after measures:	
	Ytre miljø	Risk before measures:	Risiko after measures:	
Incident:	Spillage of methanol			
Consequence area:	Helse	Risk before measures:	Risiko after measures:	
	Ytre miljø	Risk before measures:	Risiko after measures:	
Incident:	Spillage of TEOS			
Consequence area:	Helse	Risk before measures:	Risiko after measures:	
	Ytre miljø	Risk before measures:	Risiko after measures:	



Hazard: Cleaning and waste handling

Incident: Inhale or spill acetone on skin

Consequence area: Helse Risk before measures:  Risiko after measures: 

Hazard: Instruments (apparatus, reactors) manipulation

Incident: Skin burns when operating calcination oven

Consequence area: Helse Risk before measures:  Risiko after measures: 

Incident: Frostbite when manipulation the liquid nitrogen during the utilization of BET instrumen

Consequence area: Helse Risk before measures:  Risiko after measures: 

Hazard: Pressurized gas manipulation

Incident: Large leak of CO₂, O₂ or N₂

Consequence area: Helse Risk before measures:  Risiko after measures: 

Hazard: Working in the lab under covid-situation

Incident: Personnel infection caused by covid-19

Consequence area: Helse Risk before measures:  Risiko after measures: 

Final evaluation

Organizational units and people involved

A risk assessment may apply to one or more organizational units, and involve several people. These are listed below.

Organizational units which this risk assessment applies to

- Institutt for kjemisk prosesssteknologi

Participants

De Chen
Estelle Marie M. Vanhaecke
Ainara Moral Larrasoana
Anne Hoff
Kumar Ranjan Rout

Readers

[Ingen registreringer]

Others involved/stakeholders

[Ingen registreringer]

The following accept criteria have been decided for the risk area Risikovurdering: Helse, miljø og sikkerhet (HMS):

Helse



Materielle verdier



Omdømme



Ytre miljø



Overview of existing relevant measures which have been taken into account

The table below presents existing measures which have been taken into account when assessing the likelihood and consequence of relevant incidents.

Hazard	Incident	Measures taken into account
Hazardous chemicals used for adsorbent's synthesis and impregnation	Spillage of formaldehyde	SDS
	Spillage of formaldehyde	Local exhaust
	Spillage of formaldehyde	Fume hood
	Spillage of formaldehyde	Personal measures
	Spillage of formaldehyde	Personal measures
	Spillage of formaldehyde	Fume hood
	Spillage of formaldehyde	Local exhaust
	Spillage of formaldehyde	SDS
	Spillage of resorcinol	Personal measures
	Spillage of resorcinol	Fume hood
	Spillage of resorcinol	Local exhaust
	Spillage of resorcinol	SDS
	Spillage of PEI	Personal measures
	Spillage of PEI	Fume hood
	Spillage of PEI	Local exhaust
	Spillage of PEI	SDS
	Spillage of methanol	Personal measures
	Spillage of methanol	Fume hood
	Spillage of methanol	Local exhaust
	Spillage of methanol	SDS
Spillage of TEOS	Personal measures	
Spillage of TEOS	Fume hood	
Spillage of TEOS	Local exhaust	
Spillage of TEOS	SDS	
Cleaning and waste handling	Inhale or spill acetone on skin	Personal measures
	Inhale or spill acetone on skin	Personal measures
Instruments (apparatus, reactors) manipulation	Skin burns when operating calcination oven	Personal measures
	Skin burns when operating calcination oven	Procedures
	Skin burns when operating calcination oven	Previous risk assessment for instruments/methods
	Skin burns when operating calcination oven	Apparatus card



Instruments (apparatus, reactors) manipulation	Frostbite when manipulation the liquid nitrogen during the utilization of BET instrumen	Personal measures
	Frostbite when manipulation the liquid nitrogen during the utilization of BET instrumen	Instrument/method training
	Frostbite when manipulation the liquid nitrogen during the utilization of BET instrumen	Procedures
	Frostbite when manipulation the liquid nitrogen during the utilization of BET instrumen	Previous risk assessment for instruments/methods
Pressurized gas manipulation	Large leak of CO ₂ , O ₂ or N ₂	Personal measures
	Large leak of CO ₂ , O ₂ or N ₂	Fume hood
	Large leak of CO ₂ , O ₂ or N ₂	Local exhaust
	Large leak of CO ₂ , O ₂ or N ₂	SDS
	Large leak of CO ₂ , O ₂ or N ₂	Instrument/method training
	Large leak of CO ₂ , O ₂ or N ₂	Gas detection
	Large leak of CO ₂ , O ₂ or N ₂	Procedures
Working in the lab under covid-situation	Personnel infection caused by covid-19	Personal measures
	Personnel infection caused by covid-19	Nitrile gloves
	Personnel infection caused by covid-19	NTNU guidelines for laboratory work
	Personnel infection caused by covid-19	NTNU guidelines for laboratory work

Existing relevant measures with descriptions:**Personal measures**

Safety goggles
Lab coat
Safety goggles
Gas mask (6075)

Fume hood

[Ingen registreringer]

Local exhaust

[Ingen registreringer]

SDS

[Ingen registreringer]

Instrument/method training

[Ingen registreringer]

Gas detection

Where it is installed

Procedures

Operation procedure
Instrument manual



Ergonomic measures

[Ingen registreringer]

Previous risk assessment for instruments/methods

[Ingen registreringer]

Apparatus card

[Ingen registreringer]

Gas trolley

[Ingen registreringer]

Nitrile gloves

[Ingen registreringer]

NTNU guidelines for laboratory work

[Ingen registreringer]

Risk analysis with evaluation of likelihood and consequence

This part of the report presents detailed documentation of hazards, incidents and causes which have been evaluated. A summary of hazards and associated incidents is listed at the beginning.

The following hazards and incidents has been evaluated in this risk assessment:

- **Hazardous chemicals used for adsorbent's synthesis and implegnation**
 - Spillage of formaldehyde
 - Spillage of resorcinol
 - Spillage of PEI
 - Spillage of methanol
 - Spillage of TEOS
- **Cleaning and waste handling**
 - Inhale or spill acetone on skin
- **Instruments (apparatus, reactors) manipulation**
 - Skin burns when operating calcination oven
 - Frostbite when manipulation the liquid nitrogen during the utilization of BET instrumen
- **Pressurized gas manipulation**
 - Large leak of CO₂, O₂ or N₂
- **Working in the lab under covid-situation**
 - Personnel infection caused by covid-19

Detailed view of hazards and incidents:**Hazard: Hazardous chemicals used for adsorbent's synthesis and impregnation**

Hazardous chemicals involved in synthesis: formaldehyde, resorcinol;
Hazardous chemicals involved in Impregnation: PEI, methanol.

Incident: Spillage of formaldehyde

Solution spill or beaker broken

Likelihood of the incident (common to all consequence areas): **Less likely (2)**

Kommentar:

Use of gloves, labcoat and fume hood

Consequence area: Helse

Assessed consequence: **Large (3)**

Comment: Formaldehyde:

H226 Flammable liquid and vapour.
H301 + H311 + H331 Toxic if swallowed, in contact with skin or if inhaled.
H314 Causes severe skin burns and eye damage.
H317 May cause an allergic skin reaction.
H335 May cause respiratory irritation.
H341 Suspected of causing genetic defects.
H350 May cause cancer.
H370 Causes damage to organs

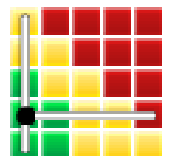
Risk:

**Consequence area: Ytre miljø**

Assessed consequence: **Small (1)**

Comment: [Ingen registreringer]

Risk:



Incident: Spillage of resorcinol

Solution spill or beaker broken

Likelihood of the incident (common to all consequence areas): **Less likely (2)**

Kommentar:

Use of gloves, labcoat and fume hood

Consequence area: Helse

Assessed consequence: **Large (3)**

Comment: H302 Harmful if swallowed.
H315 Causes skin irritation.
H317 May cause an allergic skin reaction.
H319 Causes serious eye irritation.
H370 Causes damage to organs (Central nervous system, Blood, Respiratory system) if swallowed.
H410 Very toxic to aquatic life with long lasting effects.

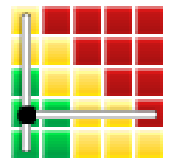
Risk:

**Consequence area: Ytre miljø**

Assessed consequence: **Small (1)**

Comment: [Ingen registreringer]

Risk:

**Incident: Spillage of PEI**

Solution spill or beaker broken

Likelihood of the incident (common to all consequence areas): **Less likely (2)**

Kommentar:

Use of gloves, labcoat and fume hood

Consequence area: Helse

Assessed consequence: **Large (3)**

Comment: Hazard statement(s)
H302 Harmful if swallowed.
H317 May cause an allergic skin reaction.
H319 Causes serious eye irritation.
H411 Toxic to aquatic life with long lasting effects.

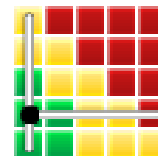
Risk:



**Consequence area: Ytre miljø**

Assessed consequence: **Small (1)**

Comment: [Ingen registreringer]

Risk:**Incident: Spillage of methanol**

Solution spill or beaker broken

Likelihood of the incident (common to all consequence areas): **Less likely (2)**

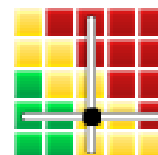
Kommentar:

Use of gloves, labcoat and fume hood

Consequence area: Helse

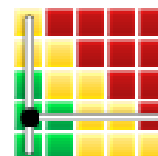
Assessed consequence: **Large (3)**

Comment: Hazard statement(s)
H225 Highly flammable liquid and vapour.
H301 + H311 + H331 Toxic if swallowed, in contact with skin or if inhaled.
H370 Causes damage to organs

Risk:**Consequence area: Ytre miljø**

Assessed consequence: **Small (1)**

Comment: [Ingen registreringer]

Risk:

**Incident: Spillage of TEOS**

Solution spill or beaker broken

Likelihood of the incident (common to all consequence areas): **Less likely (2)**

Kommentar:

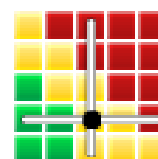
Use of gloves, labcoat and fume hood

Consequence area: Helse

Assessed consequence: **Large (3)**

Comment: H226 Flammable liquid and vapour.
H319 Causes serious eye irritation.
H332 Harmful if inhaled.
H335 May cause respiratory irritation

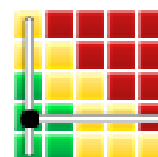
Risk:

**Consequence area: Ytre miljø**

Assessed consequence: **Small (1)**

Comment: [Ingen registreringer]

Risk:



**Hazard: Cleaning and waste handling**

Incident: Inhale or spill acetone on skin

Likelihood of the incident (common to all consequence areas): **Less likely (2)**

Kommentar:

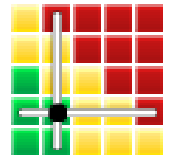
Work in fume hood, change gloves if spillage or use Barrier gloves that are resistant to acetone

Consequence area: Helse

Assessed consequence: **Medium (2)**

Comment: H225 Highly flammable liquid and vapour.
H319 Causes serious eye irritation.
H336 May cause drowsiness or dizziness

Risk:



Hazard: Instruments (apparatus, reactors) manipulation

Incident: Skin burns when operating calcination oven

Likelihood of the incident (common to all consequence areas): **Unlikely (1)**

Kommentar:

Heat protecting gloves
Screen for reading the temperature value
Instrument training

Consequence area: Helse

Assessed consequence: **Medium (2)**

Comment: The calcination is realized at elevated temperatures and in order to avoid skin burns the temperature should be read on the screen or to use heat protecting gloves resistant to a limited temperature value

Risk:



Incident: Frostbite when manipulation the liquid nitrogen during the utilization of BET instrumen

Likelihood of the incident (common to all consequence areas): **Unlikely (1)**

Kommentar:

Personal protective equipments

Consequence area: Helse

Assessed consequence: **Large (3)**

Comment: Skin burns if there is a direct contact of liquid nitrogen with the skin or the unprotected skin is near the nitrogen container

Risk:





Hazard: Pressurized gas manipulation

Incident: Large leak of CO2, O2 or N2

Likelihood of the incident (common to all consequence areas): **Less likely (2)**

Kommentar:

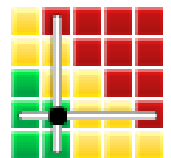
Personal protective equipments, gas detector, fume hood

Consequence area: Helse

Assessed consequence: **Medium (2)**

Comment: If a large gas leak occurs, especially in a limited room space, the person in contact can suffer a suffocation

Risk:





Hazard: Working in the lab under covid-situation

Incident: Personnel infection caused by covid-19

Likelihood of the incident (common to all consequence areas): **Less likely (2)**

Kommentar:

Strict guidelines for lab work, personal protective equipment

Consequence area: Helse

Assessed consequence: **Large (3)**

Comment: covid-19 is a virus which is highly infectious and highly lethal

Risk:





Overview of risk mitigating measures which have been decided:

Below is an overview of risk mitigating measures, which are intended to contribute towards minimizing the likelihood and/or consequence of incidents:

Overview of risk mitigating measures which have been decided, with description:



Detailed view of assessed risk for each hazard/incident before and after mitigating measures